Heat and Moisture Transfer in a Bed of Gypsum Boards

A Thesis Submitted to the College of

Graduate Studies and Research

in Partial Fulfillment of the Requirements

for the Degree of

Master of Science

in the Department of Mechanical Engineering

University of Saskatchewan

Saskatoon

By

Christopher Michael James

© Copyright Christopher Michael James, April 2009. All rights reserved.

Permission to Use

In presenting this thesis in partial fulfilment of the requirements for a Postgraduate degree from the University of Saskatchewan, I agree that the Libraries of this University may make it freely available for inspection. I further agree that permission for copying of this thesis in any manner, in whole or in part, for scholarly purposes may be granted by the professor who supervised my thesis work or, in his absence, by the Head of the Department or the Dean of the College in which my thesis work was done. It is understood that any copying or publication or use of this thesis or parts thereof for financial gain shall not be allowed without my written permission. It is also understood that due recognition shall be given to me and to the University of Saskatchewan in any scholarly use which may be made of any material in my thesis.

Requests for permission to copy or to make other use of material in this thesis in whole or part should be addressed to:

Head of the Department of Mechanical Engineering

University of Saskatchewan

Saskatoon, Saskatchewan S7N 5A9

Abstract

Several recent projects in building science have examined the hygric performance of building materials. Most building materials adsorb from and desorb water vapour to their environments. This phenomenon could be used to help control relative humidity fluctuations in buildings, experienced during periods of moisture production such as cooking, washing or bathing. They could also be used to reduce the need for mechanical ventilation and air conditioning to remove excess moisture. To understand how a building material responds to transient changes in relative humidity, testing is required.

This thesis outlines the testing performed on gypsum board, a common wall and ceiling finishing material used inside buildings. The effect of paint coatings on the gypsum boards and heat and mass transfer coefficients of the air passing over the gypsum bed was tested. The data produced from these experiments was used to validate several numerical models through an International Energy Agency/Energy Conservation in Buildings and Community Systems (IEA/ECBCS), Annex 41: Whole Building Heat, Air and Moisture Response. The validated models are important for simulating the process of adsorption and desorption in building materials to predict failure in the building envelope and expected indoor air conditions.

A sensitivity analysis is also presented which examines the effects of the sorption isotherm and vapour permeability of the gypsum and paints as well as the heat and mass transfer coefficients the boards are exposed to. The sensitivity range used was determined from the tests performed on the gypsum boards and paints which were also performed during the work of Annex 41.

The results of this thesis produced a high quality data which can also be used to validate future numerical models. All information required for validation of future models is available such as dimensions of test section, test conditions, material properties and the experimental data.

The results show that when designing for passive humidity control in buildings using gypsum boards, the most influential factor is the type of coating or paint applied to the surface. The sensitivity analysis showed that material properties such as vapour permeability and the sorption isotherms, for the expected temperature range, should be well known for increased accuracy of the simulation. The material properties were determined from inter-laboratory testing at 14 different institutions to achieve confident values.

The effect of increasing the heat and mass transfer coefficients, over the range of coefficients studied in this thesis, showed negligible differences in the results. The simulated results had very good agreement between the models and were mostly within experimental uncertainty of the measurements.

Acknowledgements

I want to thank my supervisor, Professor Carey J. Simonson for his expertise, support, patience and for providing me with many great experiences. My gratitude goes to the members of Annex 41, especially the researchers who provided the numerical simulations; without whose work, this research would not have been possible. I would also like to thank to my committee members (Professor Ike Ogoucha and Professor David Torvi) for their input to make this thesis a success. I give many thanks to Mr. Dave Deutscher for his technical support and knowledge over the years.

I thank my wife, Christine, for her patience and editing through this journey and to my children, Alandra and Indira, who accepted my absence to complete this work. I thank my parents, Dean and Cheryl, for supporting me during this thesis work and throughout my childhood.

Dedication

I dedicate this work to my wife Christine and children Alandra, Indira and Alister.

Table of Contents

List of Tables

List of Figures

Nomenclature/Abbreviations

1-D	one dimensional
2-D	two dimensional
ASHRAE	American Society of Heating Refrigeration and Air Conditioning Engineers
ASTM	American Society for Testing and Materials
CFD	Computational Fluid Dynamics
ECBCS	Energy Conservation in Buildings and Community System
EPD	Effective Penetration Depth
EU	European Union
h	heat transfer coefficient
HAM	heat, air and moisture
HAMSTAD	Heat air and Moisture Standards Development
hm	mass transfer coefficient
HVAC	heating ventilating and air conditioning
IEA	International Energy Agency
ISO	International Standards Organisation
MBV	moisture buffer value
Re	Reynolds number
RH	relative humidity
σ	standard deviation
Δt	length of time for cycle
T	temperature
t	student-t distribution
TMT	Transient Moisture and Temperature
U	mass change from moisture accumulation/loss
WDR	Wind Driven Rain
WMZ	Well Mixed Zonal
x	axial distance along gypsum bed
$X_{endofcycle}$	value of RH or U for the end of the cycle
$X_{beginningofcycle}$	value of RH or U for the beginning of the cycle
ΔX	calculated change in variable (RH or U) for the cycle
y	depth in gypsum bed

Chapter 1

Introduction

Engineers are continually examining and improving the design of building structures to improve indoor air quality and decrease the energy used for their heating, ventilating and air-conditioning (HVAC) systems. Many moisture and temperature problems can occur from poor design. Researchers have been studying many topics related to building performance. Examples include toxic emissions from building materials [Wang *et al.* 2007, Gupta et al. 2006, Neuner and Seidel 2006], damage to building materials due to moisture movement or condensation [Lucas *et al.* 2002] including corrosion, degrading strength and cracking [Roels *et al.* 2005], mould growth [Nielsen *et al.* 2004, Pasanen *et al.* 2000, Clarke *et al.* 1999] and increased heat loss from high moisture contents [Ochs *et al.* 2007]. Building research is crucial because, as a society, we spend a large portion of our lives inside buildings and they account for a large portion of global energy use. Energy used to control the indoor air quality of a building account for much of the overall energy that a building uses. Passive (i.e. no active operation) methods can be utilized for temperature and relative humidity control to ultimately reduce the size of HVAC equipment.

Most finishing materials used in buildings are hygroscopic, which means they readily adsorb and retain moisture. The materials include furniture, window coverings,

floors, ceilings and walls. They adsorb water vapor during periods of high space relative humidity experienced during cooking, bathing, washing and any other process that introduces moisture into the building. The moisture diffuses into the building material or furnishing and is stored until the relative humidity of the space is at a level low enough to allow for the stored moisture to transfer back to the space. This is known as moisture buffering and can be an effective method to help reduce the size of HVAC equipment. The HVAC equipment can be reduced because one of its functions in humid climates is to remove moisture from the air and improve the indoor air quality.

The use of interior hygroscopic materials to buffer fluctuations in room air moisture content has led to the definition of moisture buffering value (MBV). The MBV is a material property used to compare the dynamic performance of building materials to cyclic moisture loading [Rode and Grau, 2008, Osanyintola and Simonson, 2006, Roels and Janssen, 2006, Peuhkuri and Rode, 2005]. It has also been presented in other studies that the use of hygroscopic materials can improve indoor air quality [Simonson *et al.* 2002].

Large international studies have been taken on to determine the heat, air and moisture transfer in buildings, such as International Energy Agency/Energy Conservation in Buildings and Community Systems (IEA/ECBCS) Annex 41 – Whole Building Heat, Air and Moisture Response. IEA/ECBCS Annex 41 aims to investigate the key issues facing the building industry, which are human comfort, energy efficiency, durability, and sustainability. This Annex is expected to lead to increased knowledge of indoor comfort, longer service life for buildings and reduced energy use. Four subtasks were selected to focus the group contributions for the Annex [Woloszyn and Rode, 2008, Roels, 2008, Kumaran and Sanders, 2008, Holm, 2008] one of which examined

how building materials store and release moisture to provide a moisture buffering to the indoor space humidity and improving numerical modeling.

1.1 Determining Hygric Performance Through Experiments

Researchers and engineers can determine how a material adsorbs and desorbs moisture with its surroundings through experiments. Heat and moisture experiments can be used to determine processes which are unknown for a specific building material. These experiments also are used to develop material property information that can be used by engineers to calculate more global building phenomena. Many moisture properties are determined by using international standards, ISO, ASTM, ASHRAE, etc.. A well controlled experiment can provide data to help describe how a material will react to changes in temperature and moisture content in relation to building design. Often, experiments are performed on components rather than whole systems (i.e., testing of wall constructions versus whole building systems) to reduce the number of factors which could affect the results. This thesis presents experimental results of heat and moisture transfer in gypsum boards. Gypsum boards are hygroscopic materials commonly used in walls and ceilings of buildings.

1.2 Determining Hygric Performance Through Modeling

Another method of examining the design and performance of a building is the use of computer models. Much work has been done to develop models that solve the heat, air and moisture (HAM) transfer in buildings and their components. These HAM models can be powerful tools for building researchers. Parameters such as weather conditions, indoor air requirements and material properties can be changed quite easily

to determine the performance of the entire building for different operating conditions and climates. To model a whole building without knowing how each of its components will perform can result in inaccurate results which may lead to building inefficiencies. It is necessary to accurately simulate the heat and moisture transfer in building materials, furniture and other finishes before pursuing a whole or even partial building simulation to predict the global moisture and energy performance of a building subject to its local climatic conditions. The HAM models developed can help determine if there will be shortcomings in the building design, predict conditions for potential mould growth, excessive heat loss or other unwanted conditions in the building space. Numerical models will need to be compared to analytical models or experimental data to ensure that they are performing calculations correctly and accurately predicting the response they are modeling. Another method for increasing confidence in the results is to compare the results of a simulation with the results of other numerical models and examine the consistency of the results. Using logical assumptions for a very well defined case study will allow for comparisons between models. A process like this can also help determine strengths or limitations of the models.

Many models that were developed for the study of heat and moisture transfer in materials are diffusive models. A diffusive model predicts the moisture and temperature changes to a medium based on the boundary conditions applied. The diffusion of heat, water vapor and liquid through the medium is calculated based upon material properties such as porosity, thermal conductivity, density and permeability.

Another type of tool gaining popularity in HAM modeling is Computational Fluid Dynamics (CFD), which is a very useful method for the modeler. It is mainly applicable to spatial and time flows of fluids, like the air in a building space. The

application of CFD in HAM studies can permit better boundary conditions to be used for the diffusive model or the diffusive model can be directly incorporated into the CFD model [Blocken *et al.* 2007 and Steeman *et al.* 2008].

1.3 Comparison of Numerical Models and Experiments

As computer models become more common in building research and design and as numerical HAM models improve, there is a great need for experimental data that can be used to validate these models. Experiments can help determine where simplifications in the code can be made to reduce computational times without sacrificing accuracy. The experimental data generated act as benchmarks to which the models can be compared.

Often, models are validated using analytical solutions or comparison with other numerical models because of lack of published experimental data. An example of this is the benchmark study by Hagentoft *et al.* [2004] in which the use of five cases which had an analytical or numerical solution were used for model validation.

This thesis presents experimental results for one-dimensional heat and moisture transfer in gypsum boards subject to a step change in the convective boundary condition. The experiments were performed to address the gap in the research relating to model validation studies using actual experimental measurements. The experimental results are compared to ten different models as a validation exercise as part of the IEA/ECBCS Annex 41. Comparing the results of the numerical and experimental data serves a dual purpose: validating the numerical models and confirming the experiments. The experimental data which were generated for this research were intended to be one - dimensional diffusive heat and moisture transfer. However it is impossible eliminate all

other minor transport and multidimensional effects. Comparison of the results of the one-dimensional diffusive models to the experimental data would reveal the importance of the multidimensional effects, such as heat and moisture loss. The comparison can also help to identify if systematic errors, possibly from improper calibration, have been eliminated and all experimental uncertainties accounted for.

1.4 Gypsum Boards, Acrylic and Latex Paints

Gypsum board, often referred to as drywall, wallboard or plasterboard, is a popular finishing material for indoor walls and ceilings in buildings. It has many attractive qualities such as sound dampening, fire resistance and ease of installation. It is manufactured mainly from gypsum, a common mineral found in sedimentary rock in a crystalline form called calcium sulfate dihydrate ($CaSO_4 \cdot 2H_2O$). The gypsum rock is mined, crushed into a fine powder and dried to remove chemically bonded water. This dried powder is then used as the base for gypsum boards and gypsum plaster, a product used to patch cracks and fill joints on gypsum wall. The base is mixed with water and other additives to form a slurry which is placed between sheets of paper. The slurry re-crystallizes and reverts to its original rock state forming the drywall boards. The boards are then cut into manageable sizes and dried before being shipped to suppliers.

Due to their porous nature and hygroscopic properties, gypsum boards have been identified as a finishing material that could buffer the relative humidity of interior spaces and is thus, the material of focus in this thesis. To obtain accurate material properties for the gypsum boards (GYPROC A ABA-board) supplied by GYPROC BPB™, Belgium, round-robin testing was performed with various institutions measuring the water vapor permeability and sorption isotherms [Roels 2008a]. Three main test series

were performed using uncoated gypsum board, acrylic painted gypsum boards and latex painted gypsum board respectively. Random samples of the gypsum boards, both uncoated and with the acrylic and latex coats, were sent to the 14 different partners for testing.

Water vapor permeability testing was done by each of the partners using existing facilities, which are all described in Roels [2008a]. Three test conditions were used for the measurement of water vapor permeability using standard EN ISO 12572:2001 with relative humidity gradients of 50, 43 and 7% across the samples at a temperature of 23 ±0.5°C. These gradients were generated using saturated aqueous salt solutions. Sorption testing was also carried by the 14 testing partners. The isotherms were generated at 23 ± 1°C for relative humidities of 33, 53, 80 and 94% using the aqueous salt solutions. The process of measuring the sorption isotherm can be found in the work by Roels [2008a].

After installation, gypsum boards are often painted for aesthetic reasons. The applications of two paint types are examined in this thesis namely acrylic and latex. Each type of paint was applied to the surface of a gypsum board to test their effect on moisture transport. Acrylic paint is water vapor permeable, while latex paint has a very high resistance to moisture transfer. Both paints were supplied by BOSS Paints, nv Bossuyt, Belgium. The acrylic finishing paint is a Decomat (BOSS Paints) type and is light blue in color. The latex paint is Bolatex (BOSS Paints) and is light yellow in color.

1.5 Literature Review

Many studies have been done on building materials and how they react to heat and moisture transfer. The use of numerical studies has increased dramatically in recent

years due to significant increase in computing power. Many researchers have used or developed numerical models to study heat and moisture effects on buildings or building material performance [Qin *et al.* 2005, Kalagasidis *et al.* 2006, Janssen *et al.* 2006, Mendes *et al.* 2002]. These studies provide useful information regarding the effects that heat and moisture have on building materials. These numerical models are based on empirical correlations and governing mathematical equations and thus require validation either through the use of experimental benchmark testing [Belarbi *et al.* 2007, Syed *et al.* 2005, Dalgliesh and Surry, 2003, Talukdar *et al.* 2007] or analytical solutions the latter of which are often difficult to find. The focus of the literature search will be on the validation of numerical models as well as experimental methods.

1.5.1 Heat and Mass Transfer Models

Many models have been developed to study heat, air and moisture (HAM) transfer in buildings and building materials. These models, which range from commercially available packages to user-developed codes, can be used for a variety of tasks, such as studying moisture degradation of building materials [Roels *et al.* 2006], volatile organic compounds (VOC) emissions [Hu *et al.* 2007], determining how a building envelope performs in various climates [Lucas *et al.* 2002, Hirano *et al.* 2006] and, more recently, how building materials can be used to passively control the indoor temperature and humidity [Rode *et al.* 2008]. In some cases, two different models are used to more accurately solve problems. For example, the use of a fluid modeling package to determine boundary conditions for a model that calculates heat and moisture transfer within a material has been a recent improvement to modeling building material interactions with the interior or exterior space.

HAM models have also been used to predict the degradation of building materials due to moisture infiltration and repeated loading conditions [Roels *et al.* 2005]. When a material becomes saturated with water, swelling will cause a decrease in both the stiffness and strength. This often causes cracks to form, especially in the case of concrete structures, which accelerate infiltration of both water vapor and liquid water causing further damage to the area. The model of Roels *et al.* [2005] used a coupled discrete-continuum approach to solve the fracture mechanics of a concrete wall. The continuum model examined the movement of moisture through the porous structure by liquid moisture uptake and diffusion through the medium. The discrete model used for the fracture mechanics simulations can use a large finite element mesh structure to solve for stresses. One important consideration, as reported by Roels, is that varying widths and connectivity of cracks can greatly influence permeability and infiltration of moisture, thus resulting in numerical instabilities when simulating the moisture content of the crack. To overcome this, the cracks are modeled as displacement continuities. A 1-D discrete model of liquid flow in the crack is combined with the finite element model that solves the unsaturated liquid flow in the un-cracked matrix [Roels *et al.* 2006]. Two examples are presented in Roels *et al.* [2006] that highlight uptake of moisture in a crack and the resulting damage done from the degradation once a load is applied. It is important to mention that the moisture uptake model has been validated by experimental measurements of the free water uptake using X-ray radiography on a naturally-fractured brick sample [Roels *et al.* 2003]. As mentioned, validation of numerical models is important to ensure accurate simulation results and a better understanding of the events.

Blocken *et al.* [2007] presented the use of a CFD-HAM model to study the effect of wind driven rain (WDR) on a building façade. One of the shortfalls of 1-D HAM

models is that they generally incorporate boundary condition in a simplified way. Boundary conditions are typically modeled by using constant average heat and mass transfer coefficients between the air and the porous media. In the case of WDR, the boundary conditions are complex algorithms that incorporate wind speed and direction, rainfall distribution which are some of the factors. In the study by Blocken *et al.* [2007], a catch ratio relationship was developed that uses six basic influencing parameters of: building geometry, position on the building façade, reference wind speed, reference wind direction, horizontal rainfall intensity and horizontal raindrop-size distribution. The catch ratio represents the rain fall intensity on a building surface relative to a horizontal surface. These factors are spatial and time dependent and lead to the use of CFD.

The CFD model used by Blocken *et al.* [2007] generated a catch ratio chart which is a multi-dimensional function of wind speed and horizontal rainfall intensity which are unique for specific locations on the building façade and for a given wind direction. The modeling approach was applied to a two-layer porous wall for two different rain events. The CFD-assisted results indicate when the exterior surface becomes saturated and runoff occurs better than the use of semi-empirical WDR relationships, previously used for boundary conditions. This CFD-assisted approach has been implemented in HAM software for studying WDR, but it is noted that this research is not complete and there is a need for validation studies to establish high quality databases in order to validate other models in the future.

Abuku *et al.* [2008] studied the WDR load on a small tower made with brick walls. The simulations were performed for a 4 x 4 x 10 m tower placed in a cold and humid climate. The hygrothermal behavior of the brick wall was then considered as moisture penetrated, causing an increase in relative humidity in the interior space. This

increase in moisture content was analyzed for its impact on mould growth. The simulations determined that WDR can have a significant impact on increased mould growth on the interior walls. Further analysis was presented showing the effects of WDR on the increase of indoor relative humidity and, in turn, an increase in energy costs associated with heating the interior air. The authors recommend that the numerical results be validated to come to a better understanding of the performance of brick walls under WDR loading. This model also presented some initial steps into whole building modeling of heat air and moisture performance.

Steeman *et al.* [2008] presented a comparison of CFD and well-mixed zonal (WMZ) modeling of the indoor air and wall interactions in a building. Well-mixed zonal gas models use uniform properties and are commonly used in HAM modeling. The CFD model incorporated time and spatial variation in temperature and moisture content, while the WMZ model used uniform properties throughout the space. Improvement to the well-mixed model was also investigated from comparison to the CFD results. Both the CFD and WMZ model were used in conjunction with the same effective penetration depth (EPD) model to compare results. The penetration depth is the thickness of the surface layer where hygric interaction with the air and material occur for periodic boundary conditions. Simulations were run using test cases involving a small room (3.1 x 3.1 x 2.5 m) with a supply air inlet and exhaust air outlet. Three test cases were examined: an isothermal test with hygrothermal wall interaction (moisture uptake, storage and release) and non-isothermal cases with hygrothermal wall interactions and non-isothermal cases without hygrothermal wall interactions. The air inlet was located in the top center of one wall in the room and the outlet was located on the bottom center of the opposite wall (symmetrically). The results of the study showed

that the WMZ model predicts the average indoor relative humidity with good accuracy. CFD models can improve the estimation of the heat and mass transfer coefficients as WMZ models typically use free stream conditions as the surface boundary conditions. There was good agreement between the WMZ boundary conditions and the average of the local CFD boundary conditions over the entire wall. This indicates that it is not always necessary to use a fully coupled CFD-EPD model as the computing "cost" is much greater with that configuration than with average boundary conditions. One only needs to determine the heat and mass transfer coefficients for the space and use them in the well mixed zone models. CFD-EPD models give good results for studies focused on local heat and moisture transfer, while the WMZ is accurate enough for modeling the global indoor conditions.

1.5.2 Benchmarking and Validating Numerical Models

As shown in many of the papers discussed in section 1.5.1, there is a need for validation data from experimental studies to confirm the research being conducted by numerical models. The following review describes studies that have completed experiments that can be and have been used for validation.

Experiments have been designed to research various transport phenomena and provide benchmark data for validating numerical models. Ampofo and Karayiannis [2003] designed an experimental rig to study low level turbulence natural convection in a square cavity created by two isothermal walls. The temperatures of the hot and cold walls were controlled to 50 and 10°C, respectively. The 2-dimensional fluid temperature and velocity distributions were measured simultaneously using a very small thermocouple and a laser doppler anemometer. The experimental results were in good

agreement with two numerical simulations that have been developed for studying a similar flow field. The data tables of velocity and temperature are provided as benchmark data for comparison with CFD codes, with a recommendation that similar boundary conditions be used during validation. While this study did not examine heat and moisture transfer in building materials, it provided a high quality data for numerical model validation of 2-dimensional fluid flows.

Cunningham [1990] compared analytical and numerical solutions with experimental results obtained for 1 m^2 flat roof samples placed between two climate chambers. The experiments tested the use of vapor barriers and roof claddings at different steady state operating conditions on the interior and exterior sides of the roof specimen. Comparisons were shown for the mean roof assembly moisture content from the experimental, numerical and analytical results. The results of the numerical model and the experimental results agreed quite closely. The numerical model results showed fine details, such as small fluctuations from the experiment, while the analytical model only matched the overall trend of the experimental data.

Belarbi *et al.* [2007] validated 1-D and 2-D models which studied non-isothermal moisture migration in porous building materials. The models were validated with experiments on lime-cement mortar (1-D model) and sandstone (2-D model). For the 1-D model validation, lime cement mortar samples 100 mm long and 62 mm in diameter, along with thermocouples embedded axially in the matrix, were exposed to convective conditions of 20°C and 65% RH on one side and 40°C and 82% RH on the other. Before testing, the samples were either initially soaked in water or oven dried at 60°C for several days. After each week of the four week test, one soaked and one oven dried sample was removed and cut into slices to be weighed, dried and weighed again to

determine the moisture content. The experimental results were similar to the numerical results for weeks 2, 3 and 4 of testing.

The experiment to validate the 2-D model in which one half of the face of a large block of sandstone was exposed to circulated air at 20°C and 65% RH and the other half of the face was exposed to circulated air at 20°C and 90% RH for 4 weeks. All other sides of the sample were sealed. The specimen was initially saturated by storing it in water for 7 days. After four weeks of exposure the specimen was divided into 70 equal parts, weighed, dried at 105°C for 24 hours and weighed again to determine the 2-D moisture distribution. Good agreement was found between the predicted and measured results. For both the 1-D and 2-D cases, the models were validated using the experimental data obtained. The authors intend to use these validated models by integrating them into a whole building heat air and moisture transfer program to determine the performance of the building envelope when exposed to the environment.

A study by Hagentoft *et al.* [2004] provides five numerical benchmark cases for the validation of simulation models which investigated 1-D heat, air and moisture transfer. These cases were developed as part of the HAMSTAD (heat, air and moisture standards development) project initiated by the European Union (EU). The five benchmark cases are:

1. An insulated roof consisting of insulation and concrete where the dry thermal conductivity of the insulation was 50 times larger than that of the concrete. Simulation results were presented for the moisture content in the two layers for a one year period.
2. A lightweight homogeneous wall under isothermal conditions and initially in equilibrium with the surrounding ambient air. The wall was suddenly exposed to a

different relative humidity in the surroundings and the moisture change was simulated for 1000 hours.

3. A lightweight homogeneous wall exposed to exfiltration (20 days) and infiltration (80 days) with a humidity gradient of 10% RH across the wall. Moisture content and temperature were presented for the midpoint of the wall.
4. A two-layered wall exposed to a variety of external and internal climatic loads. The wall is representative of a wall with a hygroscopic finish. Many moisture and temperature profiles were presented for surface moisture content and temperature as well as for distributions across the wall during four days of simulation.
5. A three layered wall for studying moisture redistribution inside the wall with capillary active interior insulation. The three layers are brick (365mm), mortar (15mm) and insulating material (40mm). The initial temperature and moisture content are constant over the whole wall. The wall is suddenly exposed to a change in temperature and relative humidity on both sides of the wall. Results of the moisture distribution through the wall after 60 days of simulation are presented.

The results of the quantitative analysis of the different models showed very good agreement between them. The unique part of the data presented by Hagentoft *et al.* [2004] is that they included numerical data from eight different numerical models to "add confidence" and showed the range of expected agreement between numerical data. The benchmark cases will serve as a reference for validating existing and future models.

Talukdar *et al.* [2007] reported experimental data for benchmarking 1-D transient heat and moisture transfer models of hygroscopic building materials. Experimental results obtained from testing of cellulose insulation and spruce plywood were presented

from work done with the transient moisture transfer facility (TMT) at the University of Saskatchewan. The TMT is a small scale wind tunnel that can provide fully-developed laminar or turbulent airflow at a controlled temperature and humidity over a building material. Testing on the spruce plywood examined three cases: a single step change in relative humidity, different Reynolds numbers in the air flow channel above the plywood and a 12 day cyclical test with a step change in relative humidity every two days. Results were compared to a numerical model to validate the model and increase confidence in the control of the experiment. Since the experiments were intended to measure 1-D diffusive heat and moisture transport, it was important to see good agreement between the model and experimental data to ensure that other minor experimental effects such as multidimensional transport areas did not overly affect the results. Relative humidity and temperature were measured at two depths inside the spruce plywood to determine the moisture and heat penetration. The results for the numerical model and the experiments agreed very well for the three cases examined thus validating the model.

The cellulose insulation results were presented by Talukdar *et al.* [2007] for the following cases: a step change in relative humidity air passed over the top of the cellulose bed, different air flow rates and a wetting and drying test using 70% and 15% RH air over a span of two days. Similar to the spruce plywood tests, the relative humidity and temperature were monitored at different depths in the cellulose bed. The numerical results also agreed quite well with the experimental results which validated the model for a different building material.

A sensitivity study was presented by Talukdar *et al.* [2007] for the results of the spruce plywood simulations due to differences in material properties. Variations of

±10% in the sorption isotherm, thermal conductivity, water vapor permeability and heat of adsorption of the building material properties were studied. The results were presented for the expected change in relative humidity and temperature from a ±10% change in the material properties. The simulated and measured results were further compared to analytical solutions, available from Incropera & Dewitt [2002]. The analytical solutions were modified to account for moisture storage in the material. The results of the modified analytical comparisons add even more confidence to the results of the numerical solution.

The results from Talukdar *et al.* [2007] provide very solid benchmarking data that can be used to validate 1-D models studying diffusive heat and mass transport in porous building materials.

Li *et al.* [2008] presented another HAM tool to be used in building envelope analysis. The tool was developed to assess the hygrothermal performance of different wood-frame wall constructions in North America. The key characteristics of the program are extensive material libraries, the ability to calculate multi-dimensional and transient coupling of heat and mass transfer, different modes of heat transfer (both latent and sensible). The model was tested against the five HAMSTAD project benchmark cases by Hagentoft *et al.* [2004]. The results, generated using the HAM tool, were quite comparable with other institutions' models from Hagentoft *et al.* [2004]. The model was also validated by comparing its results with some full scale experimental test results. In total, 12 pairs of walls, representing building practices in Canada, were constructed and tested in a large environmental chamber. Temperature and relative humidity were measured at different locations in the wall with the loading and testing taking place over

284 days. The agreement between the transient moisture transport measured and simulated was quite good.

Vera *et al.* [2007] examined moisture transport between two rooms, stacked one above the other separated by a small horizontal opening that represents a staircase or ventilation shaft. The rooms were temperature controlled by using a 1000 W heater, located at the door, controlled by a thermostat in each room. Each room had an air intake located above the door and an exhaust located on the opposite wall from the intake at the bottom. Each inlet and outlet was controlled. A rectangular opening, between the two rooms, representing 12.3% of the floor area, allowed for heat, air and moisture transport between the spaces, by natural buoyancy or active ventilation. A moisture source was introduced in one of the two rooms for 10 hours, followed by 14 hours without moisture production. The rooms were constructed in a large environmental chamber with test conditions controlled to -4.7 ± 0.2°C and 68 ± 4% RH. The inlet conditions for ventilation were 18ºC and 38% RH, ventilation rates of 0.3, 0.5 and 0.75 air changes per hour were examined. The moisture source was located at different positions in the room during testing as well. The temperature of the rooms were controlled using the thermostat and electric heater to control the temperature of the rooms between 17 and 23°C with a difference in temperature between the rooms ranging from 3 to -3.5°C; positive temperature represents the upper floor being warmer than the lower. Three cases for the combination of ventilation strategies and moisture source locations were analyzed in the paper:

1. Moisture source (107 ± 1 g/h) located in bottom room with active ventilation intake in top room and exhaust in bottom room.

2. Same as Case 1, with moisture source (113 ± 1 g/h and 130 ± 1 g/h) located in top room.
3. Moisture source (107 ± 1 g/h) located in bottom room with separate active ventilation in both the top and bottom rooms.

From the experimental testing, three initial conclusions were drawn. Natural buoyancy, from the moisture source on the bottom level, causes moisture to migrate from the bottom level to the top level even when forced air movement is in the downward direction. When the moisture source was located on the top level and net air flow was in the downward direction the moisture migrated more to the bottom level. A colder upper floor promotes the transport of moisture between the two rooms regardless of ventilation strategies. From the experimental aspect, there were large variations in humidity ratio measured at different locations in both rooms, more notably when the upper level was warmer than the bottom. The author also concludes that there is a need for simulation work to compliment the experimental study shown in the paper.

The study by Vera *et al.* [2007] was one of many experimental studies examined in part for the IEA/ECBCS Annex 41.

1.6 Research Objectives and Scope of Thesis

The objective of this research was to perform testing on gypsum boards using facilities at the University of Saskatchewan (discussed in Section 2.1). Testing was carried out to determine the transient heat and moisture transfer response of the gypsum boards from a step change in relative humidity at an isothermal temperature. The experiments were well controlled and examined moisture loading and unloading times, laminar and turbulent air flow above the samples and the effect of two surface coatings,

namely acrylic and latex paint applied to the top of the gypsum sheet. The data from these tests will be used as benchmark data to validate numerical models simulating transient heat and moisture transfer in gypsum boards. The testing was performed as part of a commitment to the IEA/ECBCS Annex 41 as a common exercise to validate heat, air and moisture models. The results of the models will be presented, compared with each other and to the experimental results. This comparison should also add confidence to the experimental data, if the results are similar. A sensitivity study will be presented to show the influence of material properties, convective mass transfer coefficients and hysteresis. The results should identify the most influential properties that require consideration when modeling heat and moisture transfer in gypsum boards.

In this thesis, the scope of the experimental works was limited to isothermal tests on a bed of gypsum boards, which were three layers thick and stacked tightly together to represent a homogeneous gypsum sheet. The relative humidity and temperature were measured at the interfaces between the gypsum sheets. The effects of adsorption and desorption time length, convective mass transfer coefficient and surface coatings on moisture transfer were examined.

1.7 Overview of the Thesis

This thesis is divided into six chapters. Chapter 1 contains the introduction, literature survey, objectives and overview of the thesis. Chapter 2 describes the experimental test facilities including instrumentation, materials and properties. The second chapter also presents an examination of repeatability, 1-D assumption of heat and moisture transfer and other simplifications found from testing. Chapter 3 covers the results of the five tests performed on the gypsum beds. Chapter 4 includes a summary of

comparisons between the experimental results and the numerical model results. Chapter 5 presents the results of the sensitivity study including results from a hysteresis study and fine tuning of material properties to achieve optimal results. Chapter 6 provides conclusions and recommendations.

Chapter 2

Experimental Facilities

The experiments performed in this thesis were carried out using the transient moisture transfer (TMT) facility housed at the University of Saskatchewan. The TMT (Figure 2.1) has been used to measure heat and moisture transfer in other building materials such as cellulose insulation and spruce plywood [Talukdar *et al.* 2007].

Three gypsum boards were initially conditioned between 30 and 35% RH at 23°C. The boards were assembled in a tray, tightly stacked together. Testing consisted of exposing the gypsum bed to an air flow conditioned to approximately 70% RH and 23°C for a period of 8 or 24 hours and then a step change that decreased the relative humidity to 30% for another 8 or 24 hours. The temperature of the air passing above the boards was kept constant at a temperature of approximately 23°C for all tests. The relative humidities selected for the step change were chosen to have a difference large enough to see detail in the measured and simulated hygric performance in the gypsum bed.

The initial conditions were achieved by holding the gypsum boards in a chamber controlled at 30-35% RH and 23°C until the boards were in equilibrium. Another method used to condition the bed was by passing air above the gypsum bed that was at 30% RH and 23°C until the bed was in equilibrium.

The relative humidity and temperature of the air flow was measured before and after the gypsum bed using Vaisala HMP333 capacitive humidity sensors and resistance temperature devices with post calibration uncertainties of ±1% RH and ±0.1°C, respectively. The air flow was measured using a tapered orifice plate and a Validyne DP103 differential pressure transducer with an uncertainty of ±1% of the full scale reading, giving a total uncertainty of ±6% in the mass flow rate of air and ±8% in the Reynolds number. The measured boundary conditions of each test were provided to the participants and are summarized in Section 2.1. The relative humidity and temperature were measured at 6 locations in the gypsum bed distributed at depths of 12.5 and 25 mm. The relative humidity in between sheets was measured with Honeywell HIH 3610 capacitive sensors that have an uncertainty of ±2% RH and the temperature was measured using T- type thermocouples with an uncertainty of ±0.1°C. The horizontal and vertical positions of the sensors are provided in Figure 2.2. These small sensors are located at the interface between the gypsum boards. To minimize the effects of the sensor and leads, they were placed in small grooves, machined in the upper surface of the middle and bottom gypsum boards shown in Figure 2.3. In addition, 6 nylon screws (3 mm in diameter) were used to hold the gypsum bed together and minimize air gaps between the boards, also shown in Figure 2.3. The nylon screws and the edges of the gypsum boards in the bed were covered with aluminum tape to minimize moisture transfer in these areas.

As shown in Figure 2.1, moisture accumulation was measured for the bed using Interface load cells with an uncertainty of ±2 g.

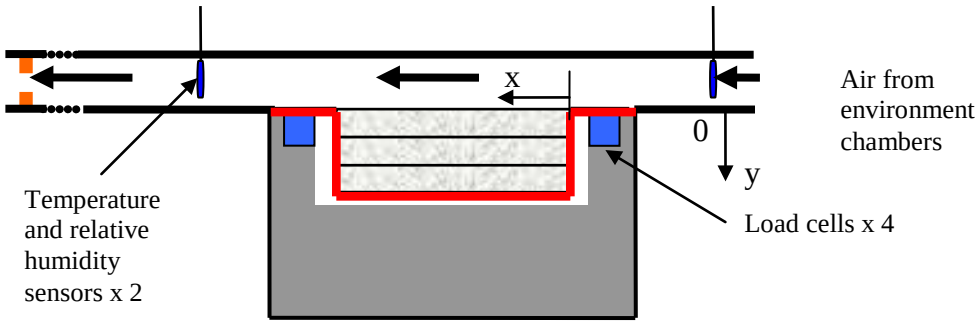

Figure 2.1: Schematic representation of the gypsum bed in the test section of the wind tunnel.

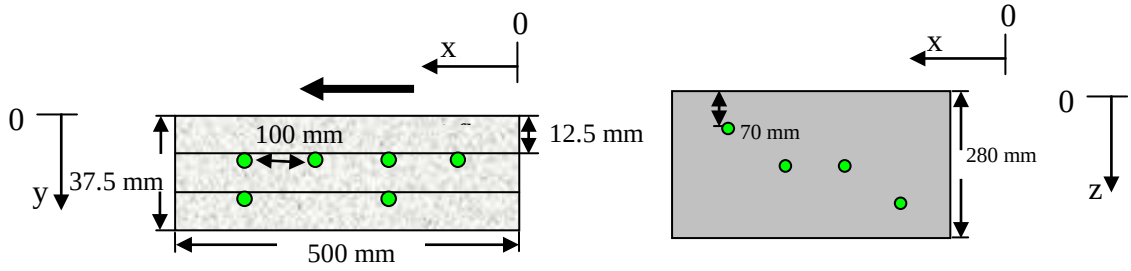

(a) (b)

Figure 2.2: Side view (a) and top view (b) of the gypsum bed with locations of the humidity and temperature measurements shown.

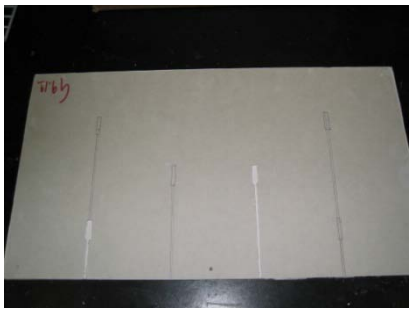

(a)

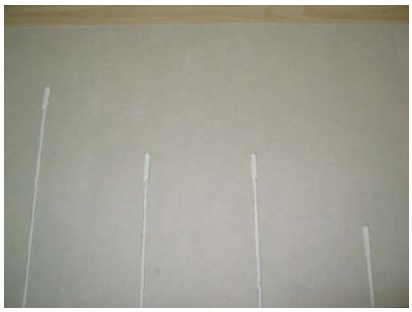

(b)

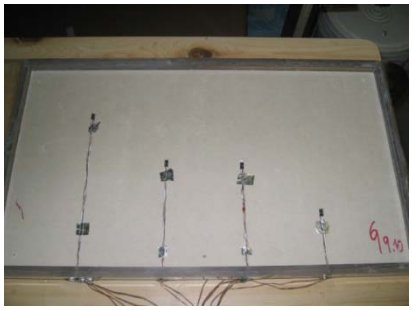

(c)

(d)

Figure 2.3: Gypsum boards showing the machined grooves to hold sensors and the nylon screws used to hold the bed together. (a) bottom board, (b) middle board, (c) middle board with sensors in place, (d) bed assembled with six nylon screws.

A separate test was conducted to determine the convective mass transfer coefficient of the TMT facility [Iskra and Simonson, 2007]. This experiment passed air at known relative humidity and temperature over a tray of water in the test section. As this controlled air flows over the free surface of the water, the mass of the water tray decreased due to evaporation. The temperature and relative humidity entering and leaving the test section were measured to determine the vapor density of the air flowing above the water. The temperature of the water was also measured to determine the water vapor density of the air at the surface of the water. The convective mass transfer coefficient of the facility was determined from measurements in the TMT facility and then used to calculate the Sherwood number. Based on the concept that the Sherwood number is equivalent to the Nusselt number, the convective heat transfer coefficient was determined. The uncertainties in the convective heat and mass transfer coefficients were found to be ±10% [Iskra and Simonson, 2007]. The convective heat and mass transfer coefficients are provided in Section 2.4.

2.1 Calibration of Sensors

The following section introduces the different instrumentation used for measurement of the heat and mass transfer in the gypsum bed. Each sensor was calibrated to determine the bias uncertainty.

The temperature sensors used in the study were either T-type thermocouples, used to measure planar temperatures between the boards and the air temperature at the orifice plate or platinum resistance temperature devices, in the Vaisala sensors, used to measure the bulk air properties entering and leaving the test section. All temperature devices were calibrated against an aluminum dry block temperature calibrator with a

bias uncertainty of ±0.01°C. The sensors were calibrated between temperatures of 15 and 30°C. Sensors were left in the dry block calibrator for each temperature set point for 30 minutes.

The Vaisala and Honeywell relative humidity sensors used in the study were capacitive type sensors that measured either the planar relative humidity or the bulk air relative humidity entering and leaving the test section. The sensors were calibrated using a humidity generator with a bias uncertainty of ±0.5%RH. Sensors were calibrated over the range of 10 to 90%RH at 10% intervals. The sensors recorded readings for at least 30 minutes at each set point.

The Validyne pressure transducer used to measure the pressure drop at the orifice plate, to in turn calculate air flow rate, was calibrated against a pressure generator with a bias uncertainty of ±0.025% of the reading. The pressure transducer was calibrated from 0 to 5 inches of water at intervals of 0.5 inches of water.

The Interface load cells used to measure the moisture accumulation in the gypsum bed were calibrated against calibration weights added to the loaded gypsum bed. This approach was taken as the study is only interested in the increase or decrease in mass of the gypsum bed. The calibration weights had a very small uncertainty, but the measurements from the load cells were not as repeatable as expected. The uncertainty in the measurements was determined to be ±2 g from these fluctuations.

2.2 Test Data Provided to the Participants

A total of five tests were conducted using the TMT facility and the gypsum boards. The effect of cycle length (8 or 24 hour), Reynolds number (2000 or 5000) and coatings on the top layer of the gypsum bed (uncoated, acrylic paint coated and latex

paint coated) were examined. As was mentioned in Section 2.0, the initial conditions were attained by exposing the gypsum boards, either separately or in a bed, to air controlled to approximately 30% RH and 23ºC, see Figure 2.4 for the schematic representation.

Table 2.1 shows all tests performed and the various conditions examined. The convective moisture and heat transfer coefficients are provided in Tables 2.2 and 2.3. For a complete listing of material (gypsum and paint) properties (density, specific heat, thermal conductivity, vapor permeability and sorption) provided to the participants, see Appendix A. Certain material properties, vapor permeability and sorption, were developed from inter-laboratory testing [Roels 2008a] consisting of random samples of the material sent to participating institutions around the world listed in Appendix A. The same gypsum boards and paint were used for the material testing and the experiments of this thesis.

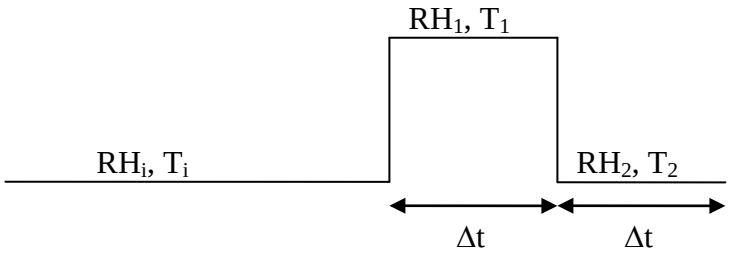

Figure 2.4: Schematic representation of relative humidity and temperature initial and testing conditions.

Table 2.1: All tests performed with initial conditions, flow rate and air conditions.

Test	Material	Re number	Initial conditions		Air flow conditions (average of upstream and downstream sensors)		
			T_i (ºC)	RH_i(%)	$T_{1,2}$ (ºC)	$RH_{1,2}$ (%)	Time (hours) Δt
Case 1	All 3 gypsum sheets uncoated	2000	23.3	30	23.8	71.9	24
					22.5	29.6	24
Case 2	All 3 gypsum sheets uncoated	2000	23.7	32.1	23.6	71.2	8
					23.6	31.9	8
Case 3	All 3 gypsum sheets uncoated	5000	22.7	31.6	23.2	71.4	24
					23.2	30.9	24
Case 4	Acrylic coated sheet on top 2 uncoated sheets	2000	24	34.6	23.2	72.2	24
					23.2	30.8	24
Case 5	Latex coated sheet on top 2 uncoated sheets	2000	24.1	31.4	23.4	70.9	24
					23.4	31.2	24

Table 2.2: Surface moisture transfer coefficients for all cases.

Test	Total surface transfer coefficient (kg/(m^2-s-Pa)) for **paint included in surface transfer coefficient**	Surface transfer coefficient (kg/(m^2-s-Pa)) for **paint as a separate porous layer**
1	2.41e-8	
2	2.41e-8	
3	3.22e-8	
4	1.18e-9	2.41e-8
5	7.31e-11	2.41e-8

The surface moisture transfer coefficients were calculated to include a resistance due to the paint layer when applicable and are dependent on the flow rate of air.

Table 2.3: Convective heat transfer coefficients for all cases.

Test	Heat transfer coefficient ($W/(m^2 K)$) for all steps	Reynolds Number
1	3.45	2000
2	3.45	2000
3	4.61	5000
4	3.45	2000
5	3.45	2000

2.3 1-Dimensional Heat and Mass Transfer

The heat and mass transfer in the gypsum bed was expected to be 1-Dimensional. This expectation was supported by the measurements of temperature and humidity in a 2-Dimensional plane at 12.5 and 25 mm. The results showed that the measured temperature and humidity tended to be 1-Dimensional. The measured relative humidity for the case when there was no coating on the gypsum is shown in Figure 2.5; the results show a measured difference of less than 2% RH for humidity sensors at the same depth in the bed. The convective coefficients are expected to change due to the developing heat and mass transfer boundary layers which will result in higher convective coefficients at the leading edge compared to the trailing edge of the gypsum bed. The effects of two dimensional heat and mass transfer will be more pronounced for the uncoated gypsum board due to a lower resistance to heat and mass transfer at the surface compared to the coated boards. The relative humidity at a depth of y = 12.5 mm and y = 25 mm along the bed at different times in a test is presented in Figure 2.6. The measured temperature at all locations in the gypsum for the uncoated case had a variation of less than 0.2°C due to the isothermal testing and 1-Dimensional heat transfer and are not presented graphically.

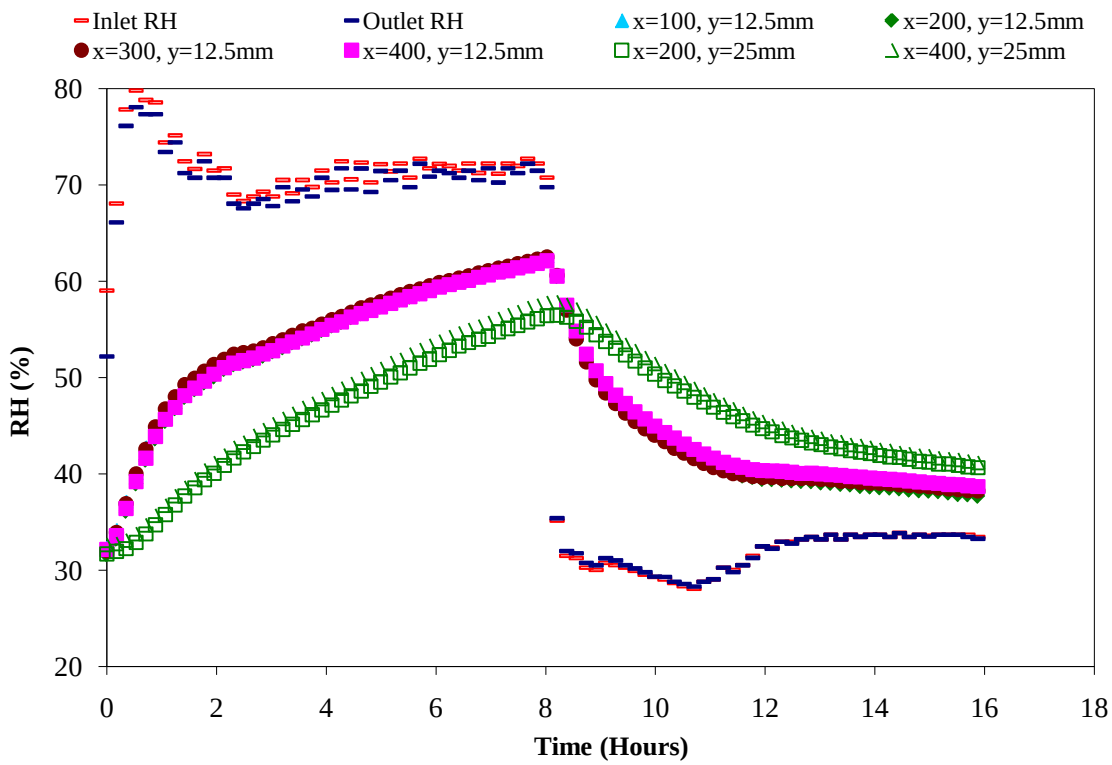

Figure 2.5: All relative humidity measurements in the gypsum bed. Note the small differences in the planes of y = 12.5 and y = 25 mm.

(a)

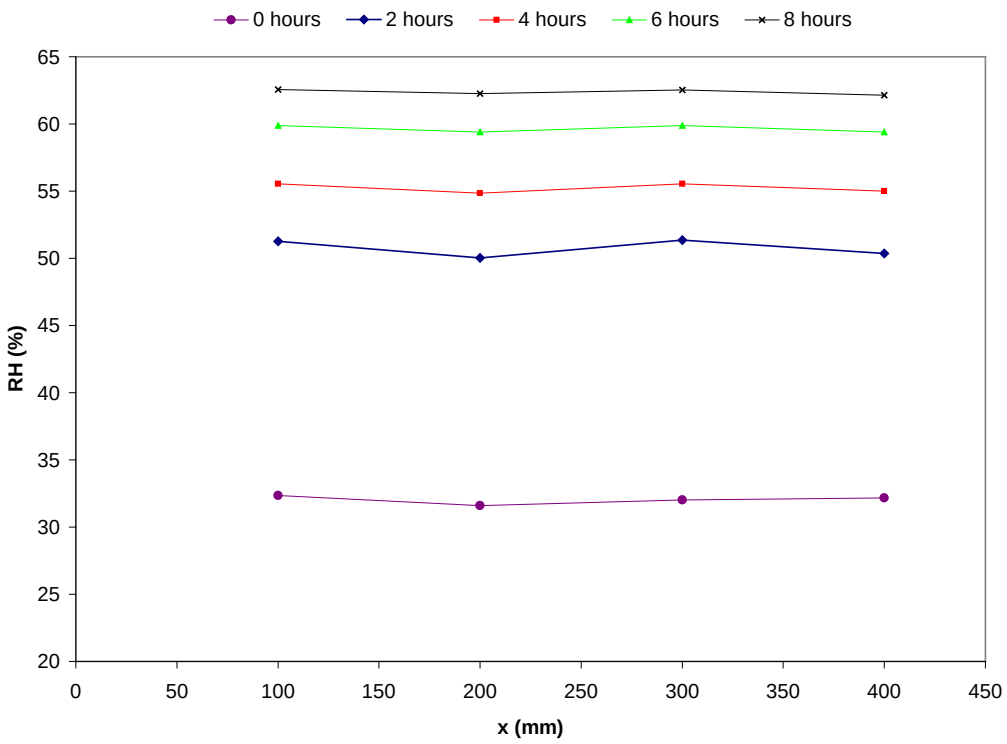

(b)

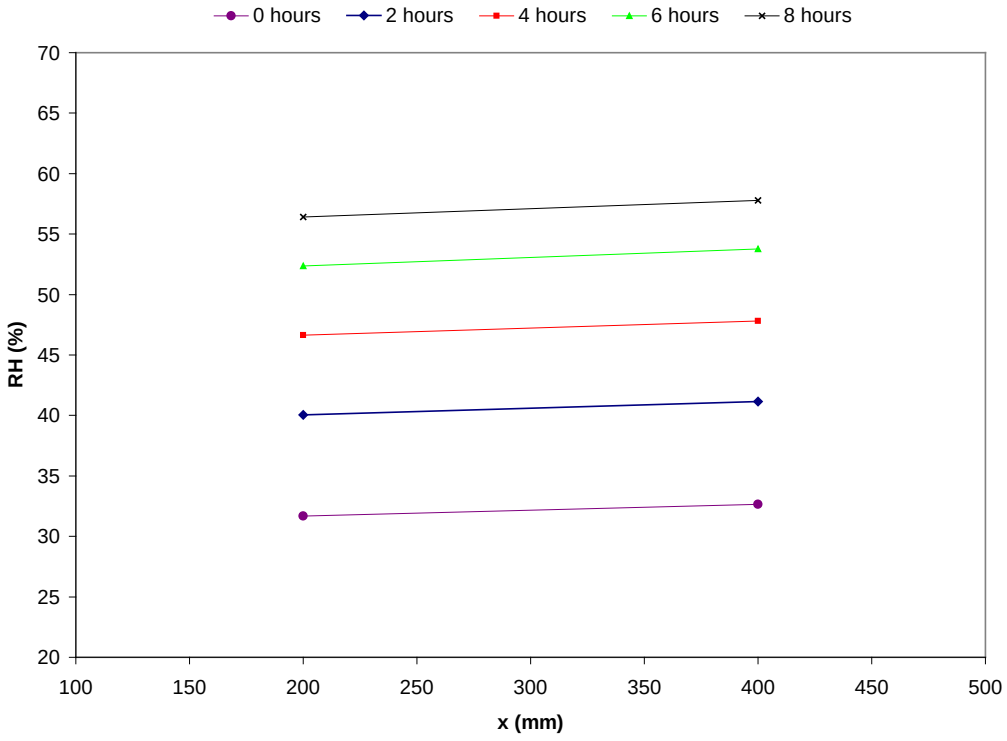

Figure 2.6: Relative humidity along x-axis from leading edge at different times at depths of (a) y = 12.5 mm and (b) y = 25 mm in the gypsum bed.

The comparison of relative humidity measured at the same depth throughout the test show very little difference in measured relative humidity at increasing distances from the leading edge of the gypsum bed. Due to the minute differences, the assumption of 1-Dimensional heat and mass transfer is valid and average heat and mass transfer convective coefficients can be used for simulation.

The differences in the planar relative humidity measurements were more significant when the gypsum had a coating of either acrylic or latex paint. To present this difference, relative humidity measurements in an acrylic coated gypsum test are shown in Figure 2.7. The largest difference between the in-plane measurements was found to be approximately 3% RH.

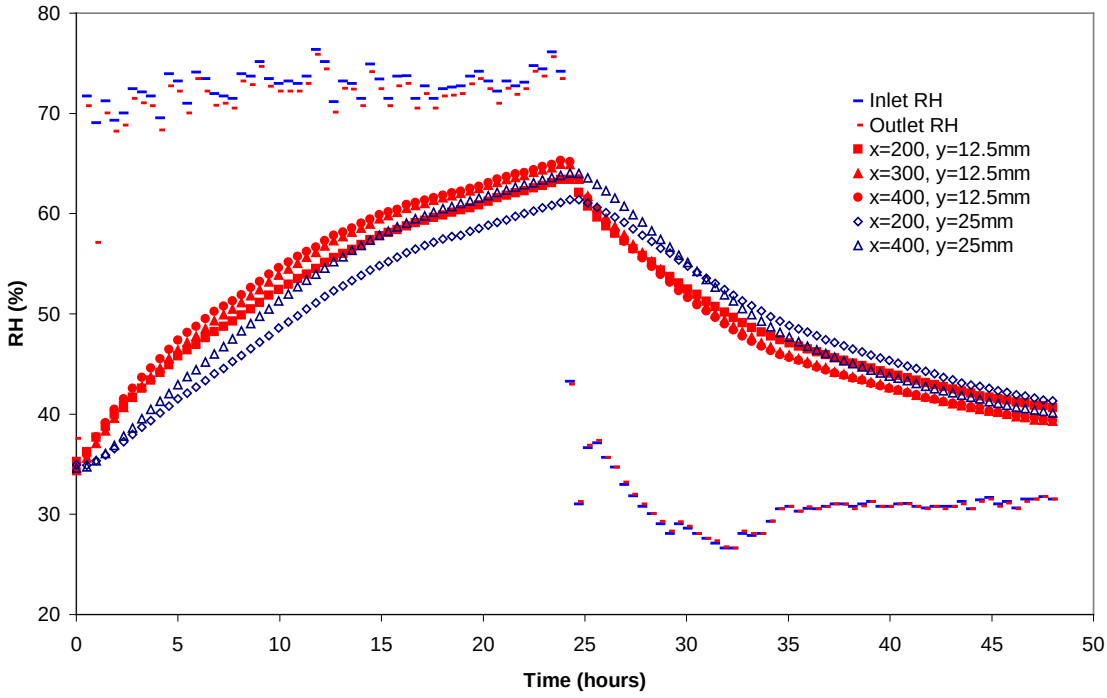

Figure 2.7: All relative humidity measurements within the gypsum bed for the test with acrylic coating on the top sheet of gypsum.

The possible reason of the larger difference in measured relative humidity results for the coated case was inconsistency in the paint layer thickness causing a larger resistance to moisture transfer in certain areas along the bed. The relative humidity measurements taken at a depth of 12.5 and 25 mm in the gypsum bed along the direction of flow is presented in Figure 2.8. Note that there is a noticeable maximum measured at a distance of 300 mm along the gypsum bed at y = 12.5 mm, possibly indicating that the paint layer is thinner at this section and moisture penetration is less impeded by the acrylic paint.

(a)

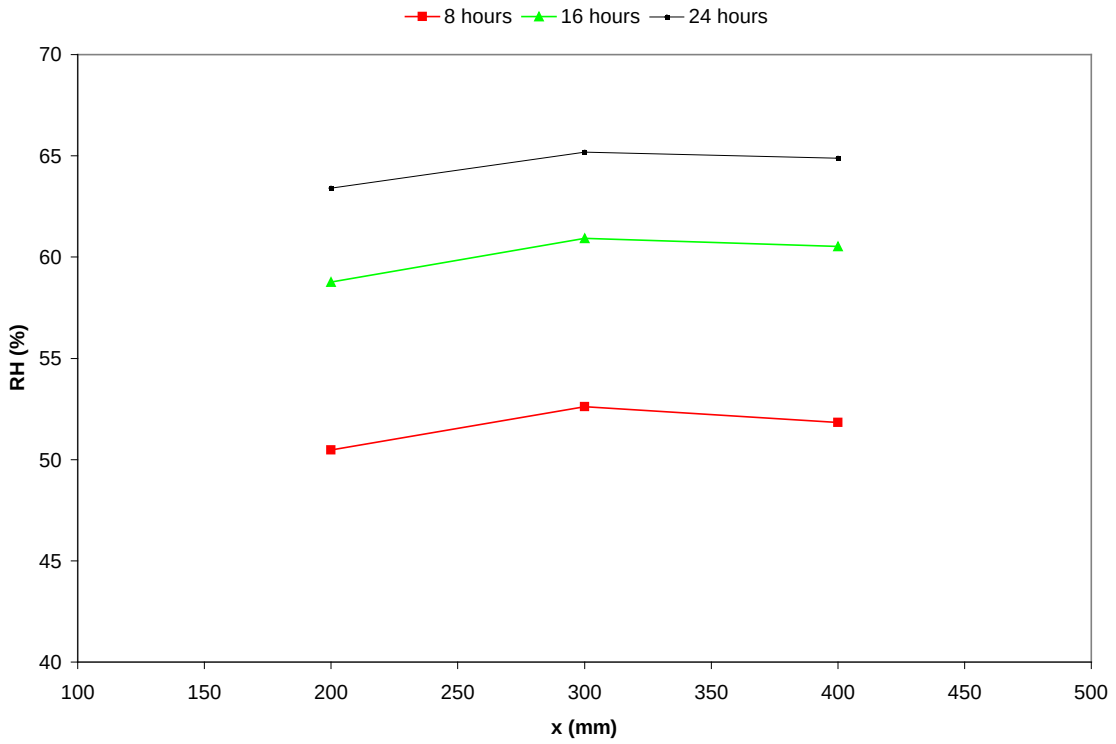

(b)

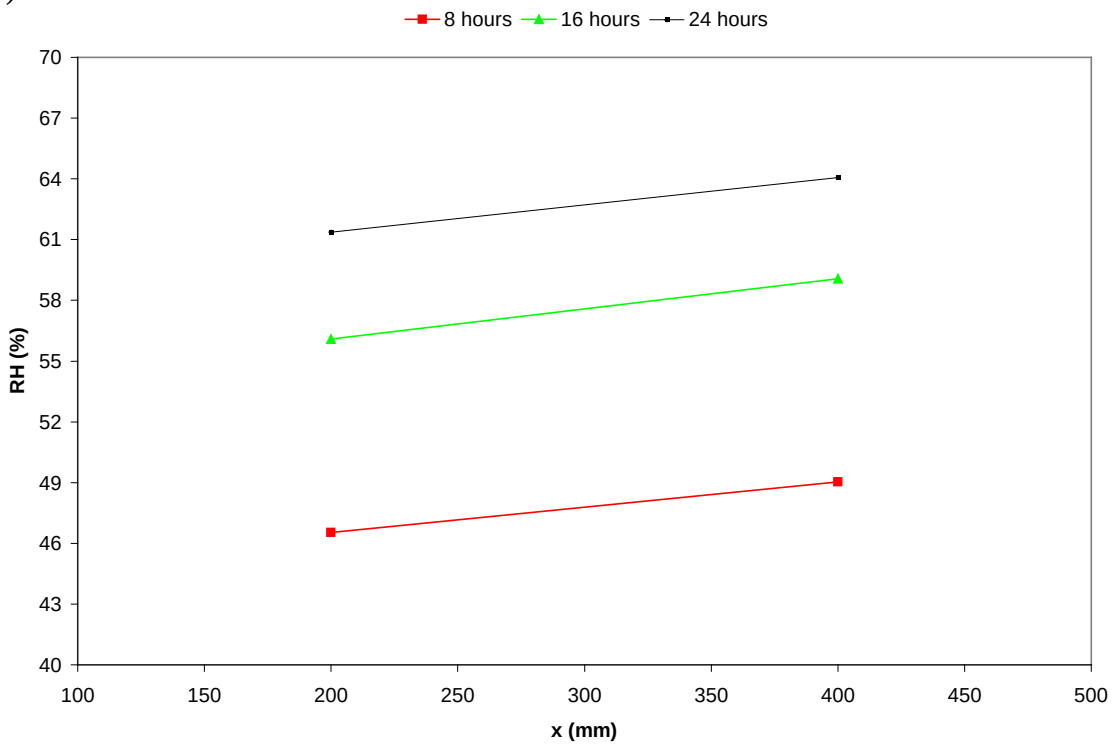

Figure 2.8: Relative humidity along x-axis from leading edge at different times at depths of y = 12.5 mm (a) and y = 25 mm (b) when the top layer is coated with acrylic paint.

The planar relative humidity, shown in Figure 2.8, should show a decrease in measured humidity as the distance from the leading edge increases. The moisture content of the air passing above the bed is reduced from the adsorption of moisture by the gypsum boards; therefore the moisture transfer driving potential and mass transfer coefficient should be decreasing. The opposite trend is seen, in Figure 2.8, indicating that the paint layer may be offering an increased resistance in some areas of the bed. Figure 2.8 shows that the variation in relative humidity seen in Figure 2.7 is more likely due to the thickness variations in the acrylic coat than to systematic measurement errors or developing boundary layers. The results in the coated gypsum bed indicate 1-Dimensional heat and mass transfer thus supporting the use of average heat and surface transfer coefficients with simulations.

2.4 Actual Relative Humidity vs. Average Test Relative Humidity Values

To simplify the simulations, the modelers were supplied with an average value of the inlet temperature and humidity as opposed to time dependent air temperature and relative humidity which varied slightly during the testing. The average value was taken as the average of the inlet and outlet conditions. To ensure that the use of an average value instead of the actual measured values did not sacrifice accuracy, the results were compared ahead of time using a simulation from the University of Saskatchewan [Olutimayin, 2004]. Results from Case 2 (Table 2.1) are shown for comparison. The results from the comparison of average versus actual results for relative humidity are presented in Figure 2.9 (a); the humidity difference detected between sensors at the same depth were at most 1.5% RH which is less than the ±2% RH measurement uncertainty of the in-bed sensors. The result from using the average inlet temperature versus the use of

actual measured temperature is contained in Figure 2.9 (b); the largest difference between the results was less than 0.25°C.

(a)

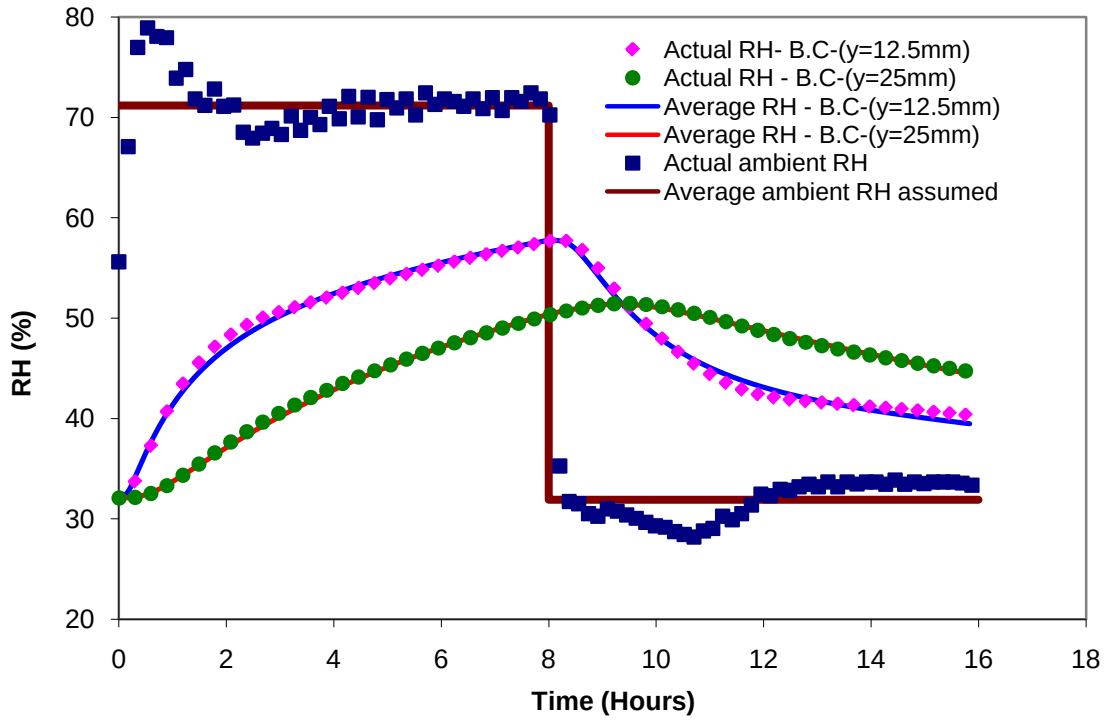

(b)

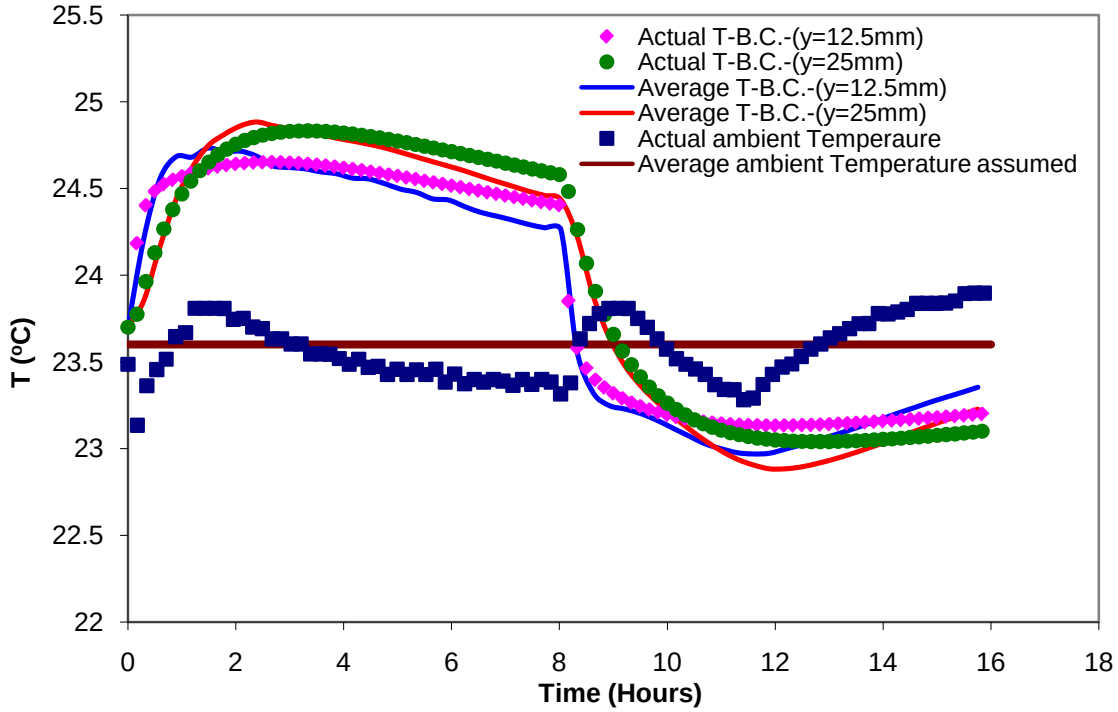

Figure 2.9: Results of (a) relative humidity and (b) temperature at depths of 12.5 and 25 mm in the gypsum bed obtained from a numerical simulation comparing the use of an average value versus actual measured data.

The coated gypsum beds also showed little difference in results when using the time averaged relative humidity and temperature for simulation and are not presented.

2.5 Repeatability

In order to check the repeatability of the experiment, an uncoated gypsum bed was tested 3 times and the results are presented in Figure 2.10. The controlled relative humidity was higher during test 3 and so the relative humidity measured in the gypsum bed is higher than the other two tests. The measured humidity of the air passing above the gypsum beds has been left out for clarity, but is presented in Table 2.4.

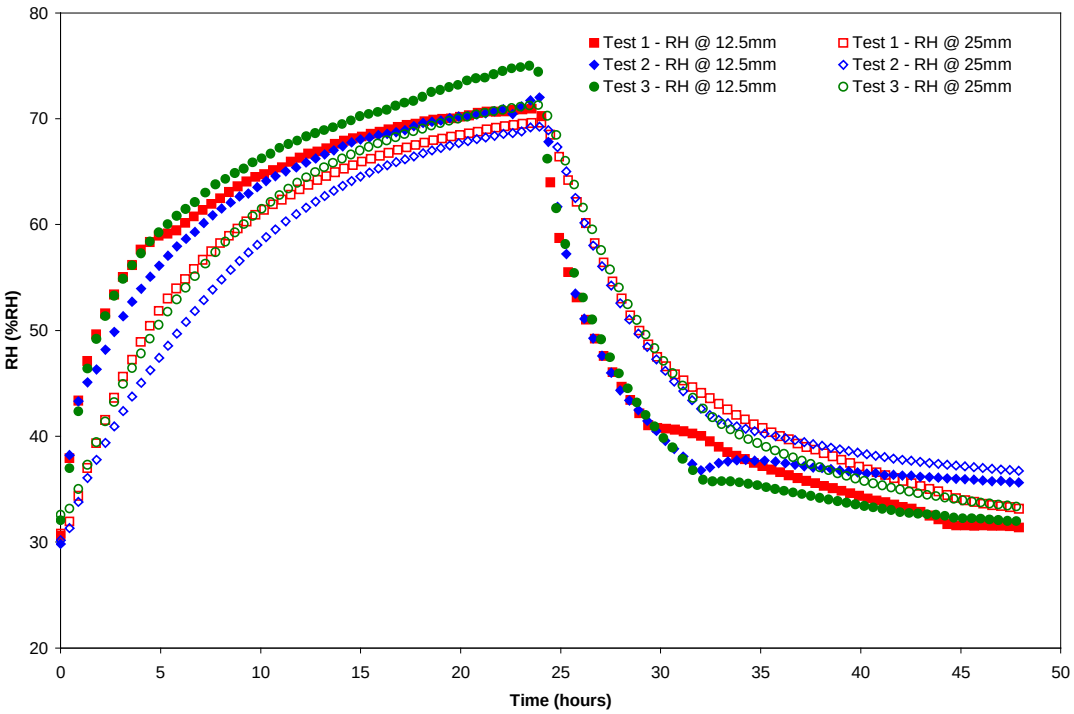

Figure 2.10: Repeatability tests using an uncoated gypsum bed.

The sharp changes during the desorption phase, as seen in Figure 2.10, of the test were caused by unsteady conditions in the environmental chamber. There were difficulties in controlling the humidity of the air to 30% at times during the testing program.

Table 2.4: Experimental conditions for repeatability testing of the uncoated gypsum bed; shown for both adsorption and desorption air conditions.

Test	T_i (ºC)	RH_i(%)	T_∞ (ºC)	RH_∞ (%)
1	23.3	30.7	23.8	71.4
			22.6	29.7
2	23.4	30.0	22.7	71.7
			22.5	32.9
3	23.4	32.3	22.6	74.7
			22.6	29.6

The results from Figure 2.10 show that there is a repeatable nature to the testing and the relative humidity in the gypsum boards is mostly affected by the moisture content of the air passing above the bed.

2.6 Simulations Requested from Modellers

The numerical models submitted for validation in this thesis, were submitted as part of a benchmarking exercise with IEA/ECBCS Annex 41. The numerical model validations are presented in two separate phases. In the first phase, the modelers were provided with all the information required to perform the "blind" simulation of the five experiments. The simulations were considered "blind" because no experimental results were provided, so the actual response of the gypsum bed to cyclic moisture loading was unknown to the modelers. An average temperature and humidity was given for each step in the cycles (Table 2.1) and gypsum material properties such as density, specific heat, sorption and permeability data (Appendix A) were given along with convective and heat and moisture transfer coefficients (Tables 2.2 and 2.3). Participants, of this validation exercise, used their existing models to predict the temperature and relative humidity at y = 12.5 and 25 mm in the gypsum bed, as well as the moisture

accumulation of the entire bed for the five tests listed in Table 2.1. When examining the effects of the paint layer on the gypsum bed, two different methods were utilized. The first method treated the bed as homogeneous material with a surface resistance due to the paint. The second method simulated the paint as a separate porous layer and material properties were supplied for this step (Appendix A).

2.7 Institutions Models

The following institutions provided numerical results for validation. A reference to each institution's simulation is provided for further information on the models.

- Katholieke Universiteit Leuven, Belgium [Janssen *et al.*., 2007]
- Slovak Academy of Science, Slovakia [Kunzel, 1994]
- Concordia University, Canada [Tariku, 2008]
- Concordia University, Canada [Neale, 2006]
- IRC-NRC, Canada [Tariku *et al.*., Aug. 2006]
- Technical University of Dresden, Germany [Perschk *et al.* 2007]
- Chalmers University of Technology, Sweden [Kalagasidis, 2004]
- Thermal Science Centre of Lyon, France [Kwiatkowski, 2007]
- Ghent University, Ghent, Belgium [Steeman, 2009]
- University of Saskatchewan, Canada [Olutimayin, 2005]

The models used in this common exercise are 1-D or 2-D models solving diffusion of heat and moisture transfer within a porous bed. In most of the models, the convective heat and moisture transfer between the air and the porous bed are calculated using convective boundary conditions with specified transfer coefficients (Tables 2.2 and 2.3) while 2 CFD models calculated the heat and moisture transfer coefficients.

Chapter 3

Results of Simulations and Experimental Measurements for all Tests

The tests performed were outlined in Table 2.1. As previously stated, the tests examined 5 different cases: a base test of an uncoated gypsum bed, a shorter time for step changes, a higher air flow rate, and two coatings namely acrylic and latex paint applied to the top sheet.

3.1 Case 1: Uncoated gypsum (Δt = 24 hours, Re = 2000)

This test is the "baseline" test using an uncoated gypsum bed. The time between humidity changes is 24 hours (Δt = 24 h) and the airflow Reynolds number (Re) is 2000 above the gypsum bed. This test will be the basis to see how other tests involving a shorter test time, a higher Re and surface coatings affect the heat and moisture transfer in the gypsum bed.

The experimental conditions for the testing are given in Table 2.1 and shown in Figure 3.1.

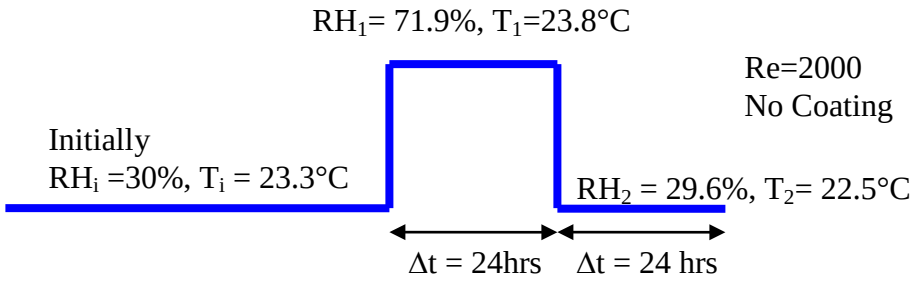

Figure 3.1: Schematic representation of test conditions used for Case 1.

The experimentally measured results of relative humidity at depths of y = 12.5 and 25 mm in the gypsum bed are presented in Figure 3.2 There is significant moisture diffusion into the bed during the 24 hour period resulting in very small differences between relative humidity at depths of y = 12.5 and 25 mm in the bed.

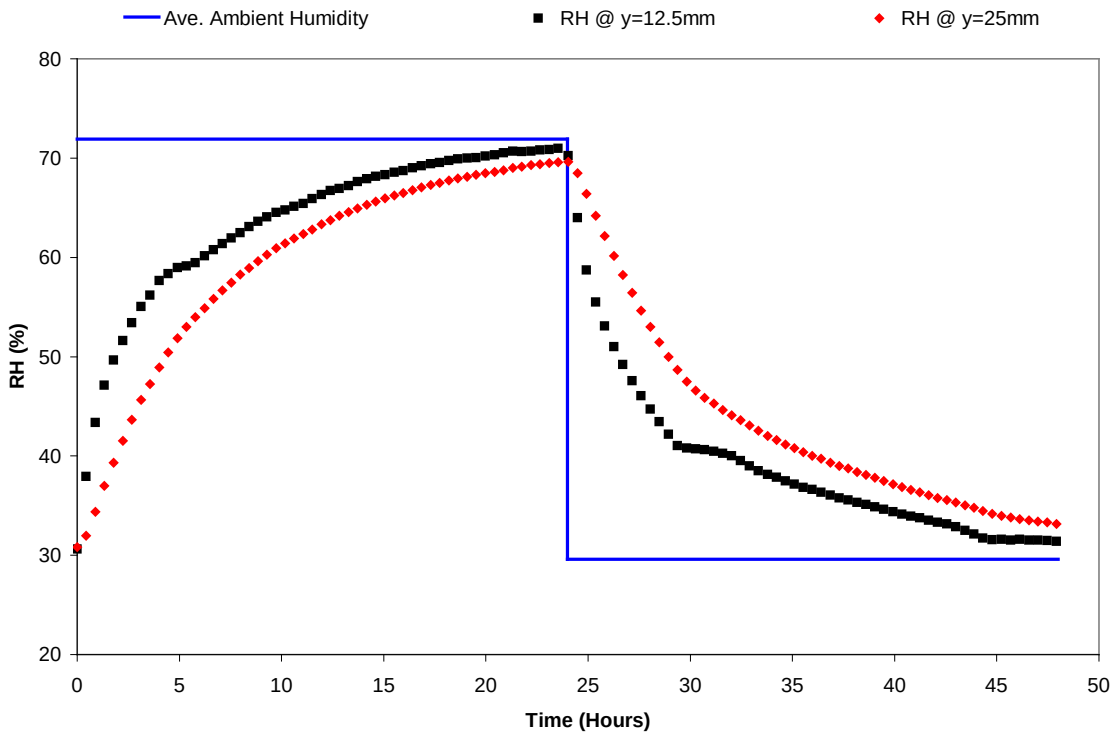

Figure 3.2: Experimentally measured relative humidity at depths of y = 12.5 and 25 mm in the gypsum bed for Case 1.

The comparison of relative humidity, measured and simulated, at depths of 12.5 mm and 25 mm in the gypsum bed are provided Figure 3.3. Each simulation is given a corresponding number, 1 to 10, for anonymity reasons. The thicker dashed lines show the two CFD models used in the common exercise. The data from the different numerical simulations are in good agreement and follow the same trend as the experimental data with the exception of one of the CFD model results. The simulation results are closer to the experimentally measured results at a depth of 12.5 mm than at a

depth of 25 mm in the bed. The simulations also agree better during the adsorption phase than during the desorption loading of the test, indicating that hysteresis may warrant examination for the test on uncoated gypsum boards.

(a)

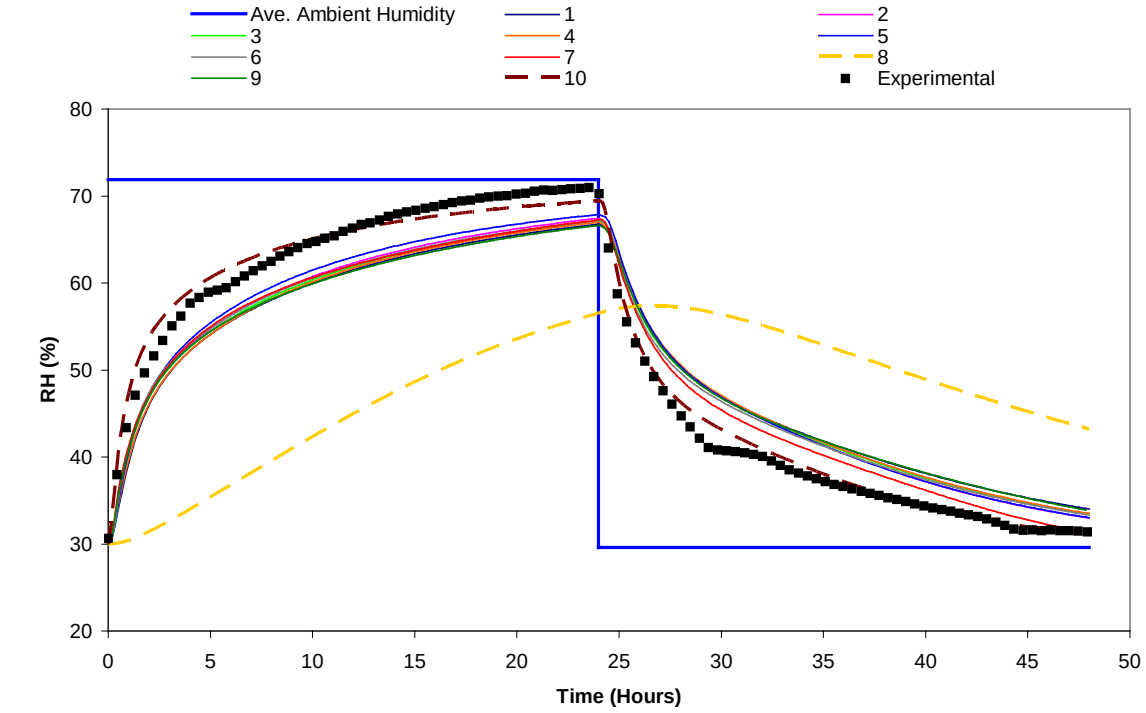

(b)

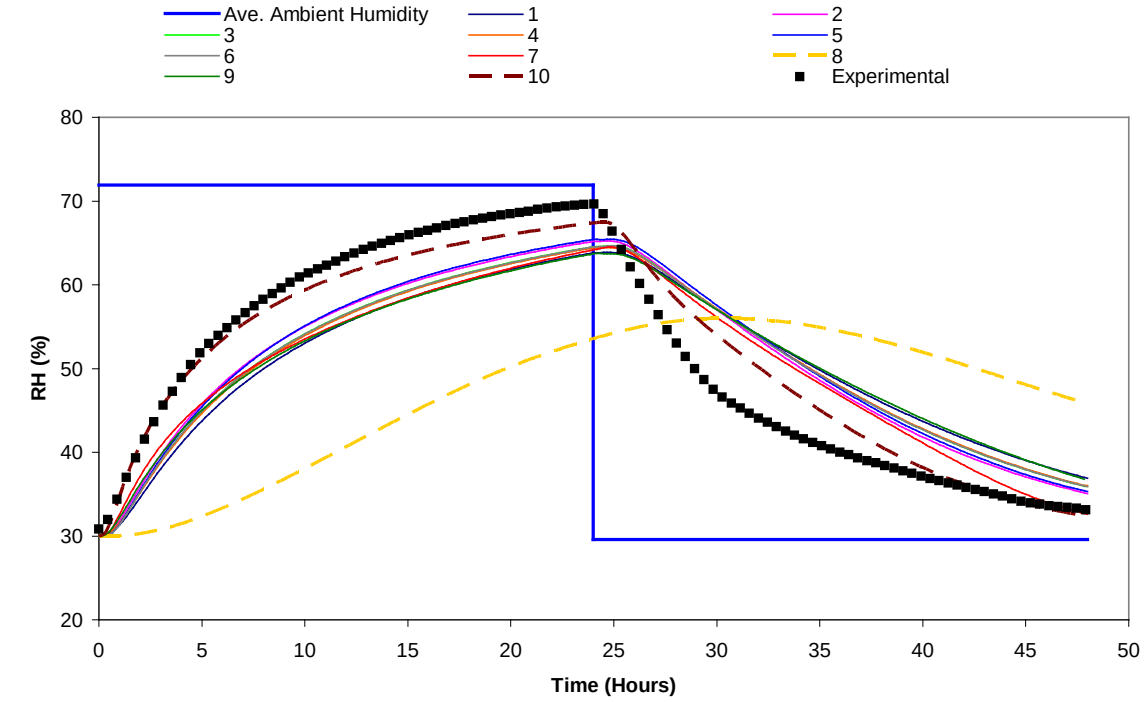

Figure 3.3: Measured and simulated relative humidity at a depth of (a) 12.5 mm and (b) 25 mm in uncoated gypsum bed of Case 1.

The measured and simulated temperatures in the gypsum boards at depths of y = 12.5 and 25 mm are presented in Figure 3.4. In the adsorption phase, there is an initial heating due to the high rate of adsorption of water vapor in the gypsum boards. Near the end of the adsorption phase, the rate of adsorption decreases and the temperature of the boards approach the temperature of the air flow. In the beginning of the desorption phase of the test, the higher desorption rate results in a cooling of the gypsum and later in the desorption phase the boards approach the temperature of the air flow. There is little difference between the temperature at depths of 12.5 and 25 mm in the gypsum bed because the test is nearly isothermal for its duration. In fact, some numerical simulations did not solve for temperature, but rather used a constant temperature for the duration of the test, with little apparent influence on the relative humidity results. The measured and simulated temperature data are only presented for the first test as the focus of this thesis is more on moisture transfer in an isothermal test. There was little difference in the simulation and measured temperature results for Cases 1 to 5 unlike the relative humidity and moisture accumulation.

(a)

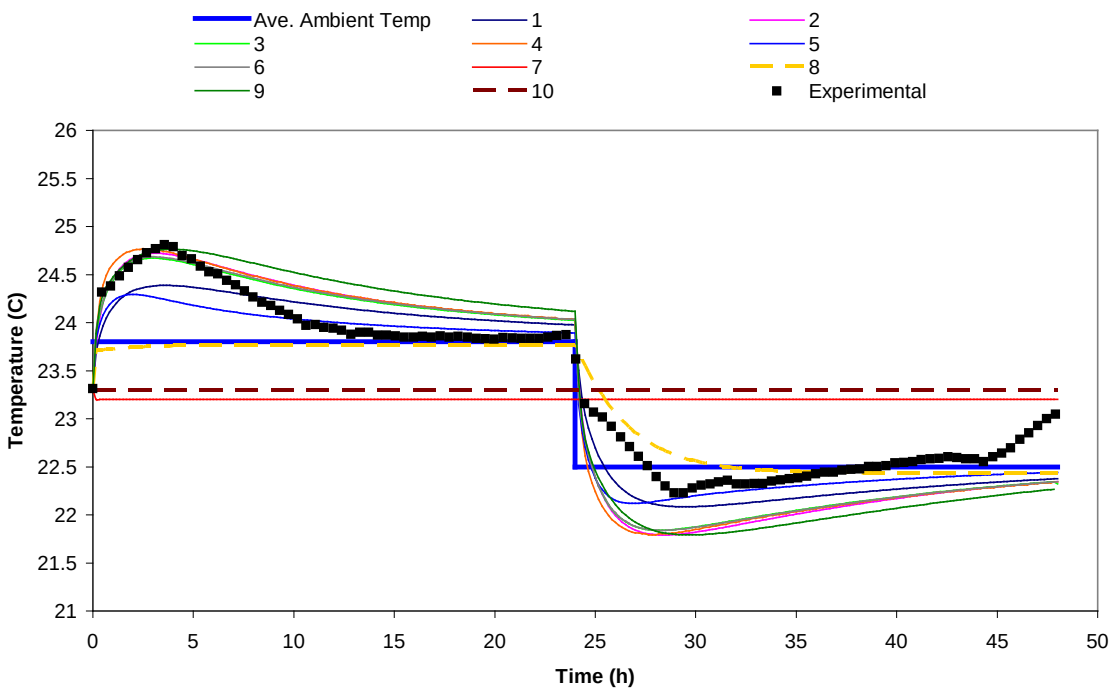

(b)

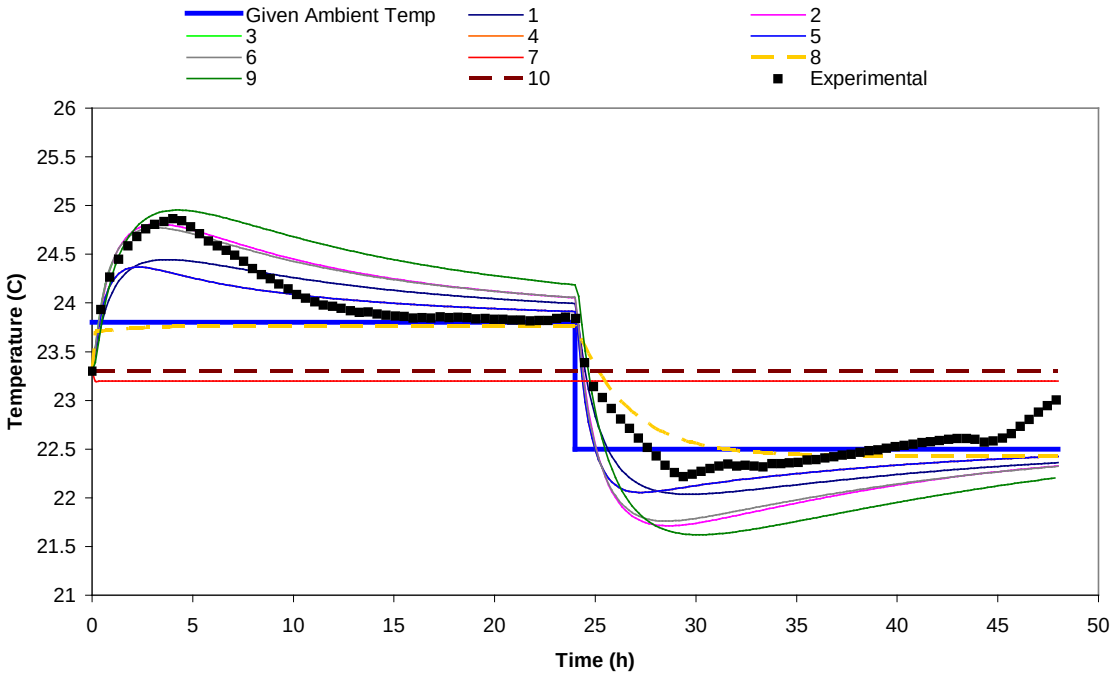

Figure 3.4: Measured and simulated temperature at a depth of (a) 12.5 mm and (b) 25 mm in the uncoated gypsum bed (Case 1).

The calculated vapor pressure from the measured and simulated temperature and relative humidity is presented in Figure 3.5. The vapor pressure was calculated using the Hyland and Wexler equations found in ASHRAE Fundamentals [2001]. The vapor pressure includes the measured or simulated temperature as well as the relative humidity, so it should remove any temperature effects from the relative humidity results since relative humidity is temperature dependent. The results show very good agreement between the experimental and the majority of the simulated results for Case 1. For the other tests performed, the agreement is very similar to the agreement of the relative humidity results and is not presented in this thesis.

(a)

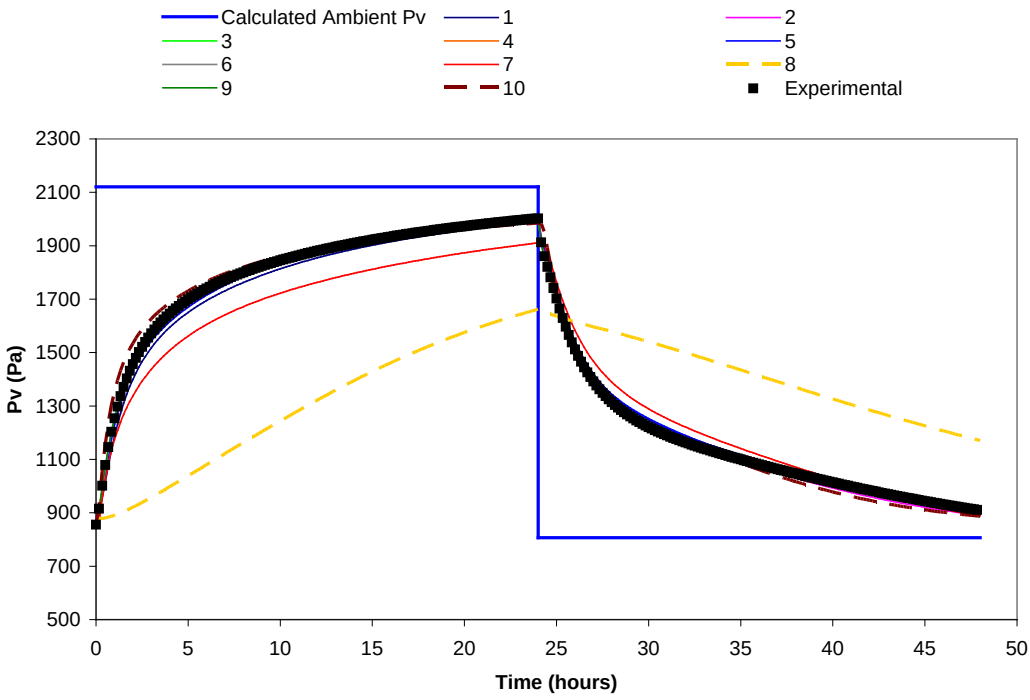

(b)

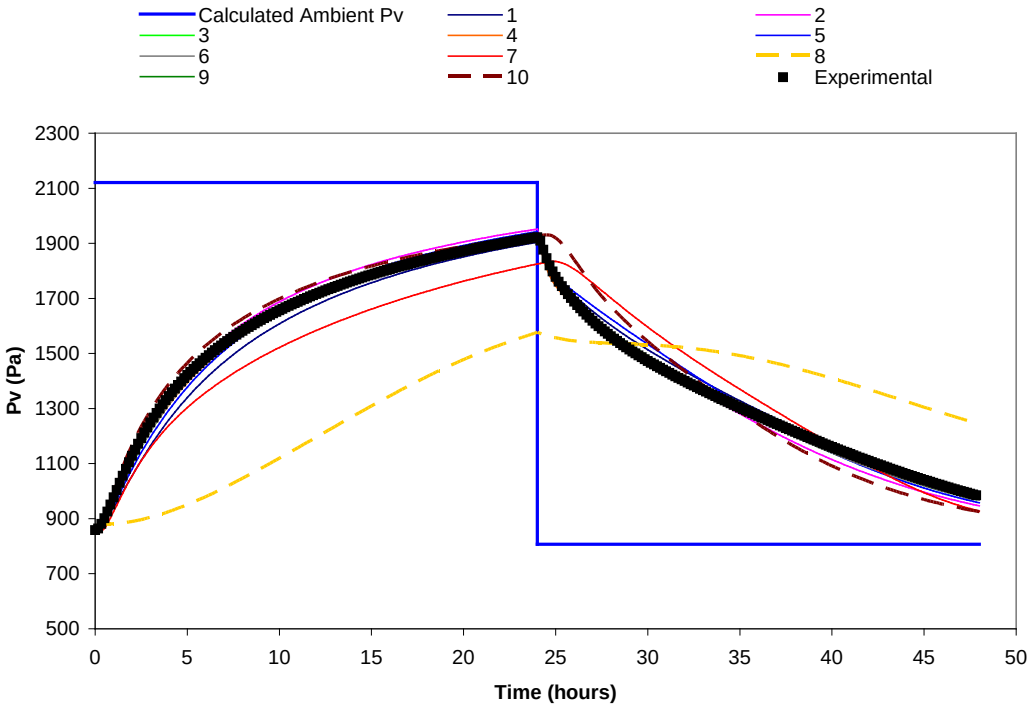

Figure 3.5: Measured and simulated vapor pressure at a depth of (a) 12.5 mm and (b) 25 mm in the uncoated gypsum bed (Case 1).

The mass accumulation in the gypsum bed was measured and simulated by the participants (Figure 3.6). Considering the uncertainty in the measured data, the agreement between the participants and the experimental results is quite good. All of the simulation results are in close agreement, except for simulation 8 which is the CFD model which has had disagreement with the other data for this case.

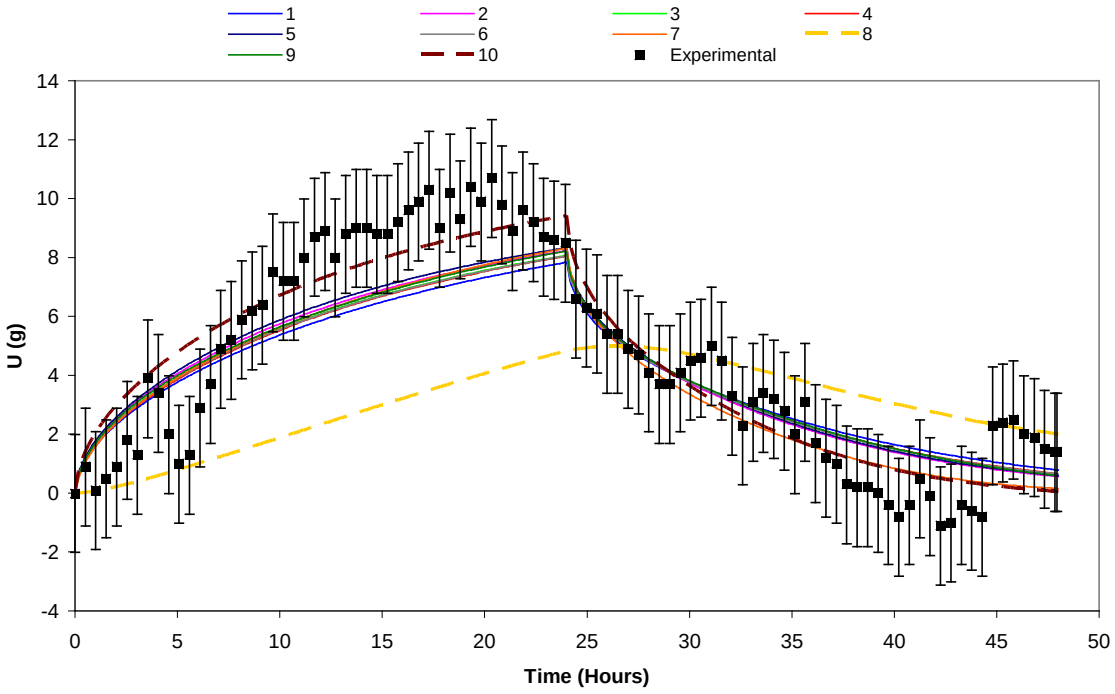

Figure 3.6: Measured and simulated change in mass during Case 1 in the uncoated gypsum bed.

The simulated and measured results of the change in mass in the gypsum bed will not be shown for the remaining cases. The focus of this chapter will be on the simulated and measured relative humidity in the gypsum bed. A summary of the mass accumulation results for all cases will be presented in Chapter 4.

3.2 Case 2: Uncoated gypsum (Δt = 8 hours, Re = 2000)

In this case the effect of a shorter step change time was examined. The adsorption phase was 8 hours long, followed by an 8 hour desorption test. The test conditions are presented in Figure 3.7.

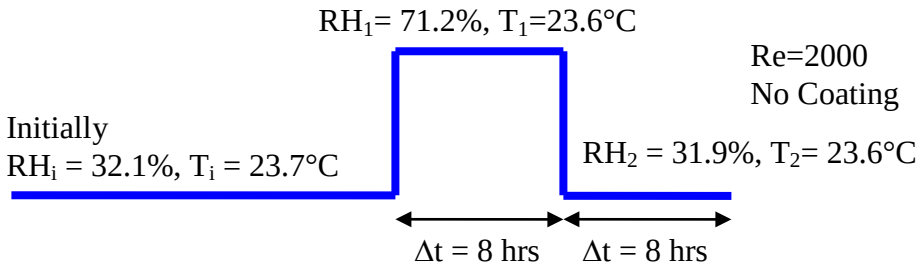

Figure 3.7: Schematic representation of test conditions used for Case 2.

The experimentally measured results for Case 2 are presented in Figure 3.8. The measured relative humidity at a depth of y = 12.5 mm in the gypsum bed attained a maximum level of 62% RH during the 8 hour adsorption phase.

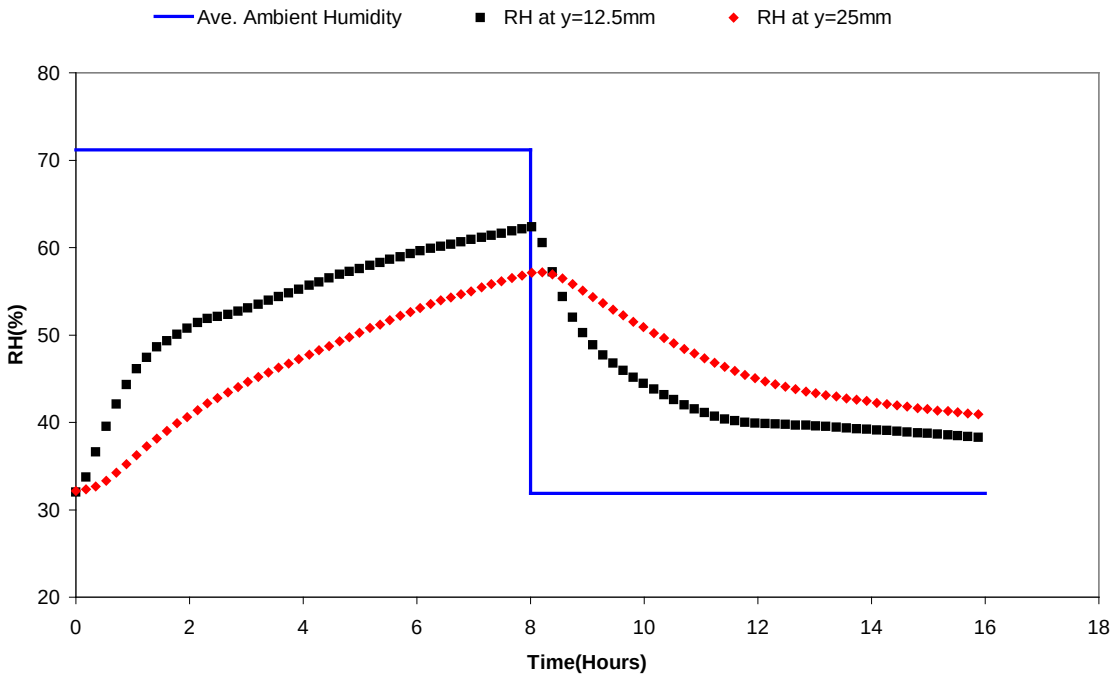

Figure 3.8: Experimentally measured relative humidity at depths of y = 12.5 and 25 mm in the gypsum bed for Case 2.

The measured and simulated results of relative humidity for the shorter test (Case 2) are presented in Figure 3.9. Similar to Case 1, there is good agreement between the numerical and the experimental data except for one CFD simulation, labeled number 8.

(a)

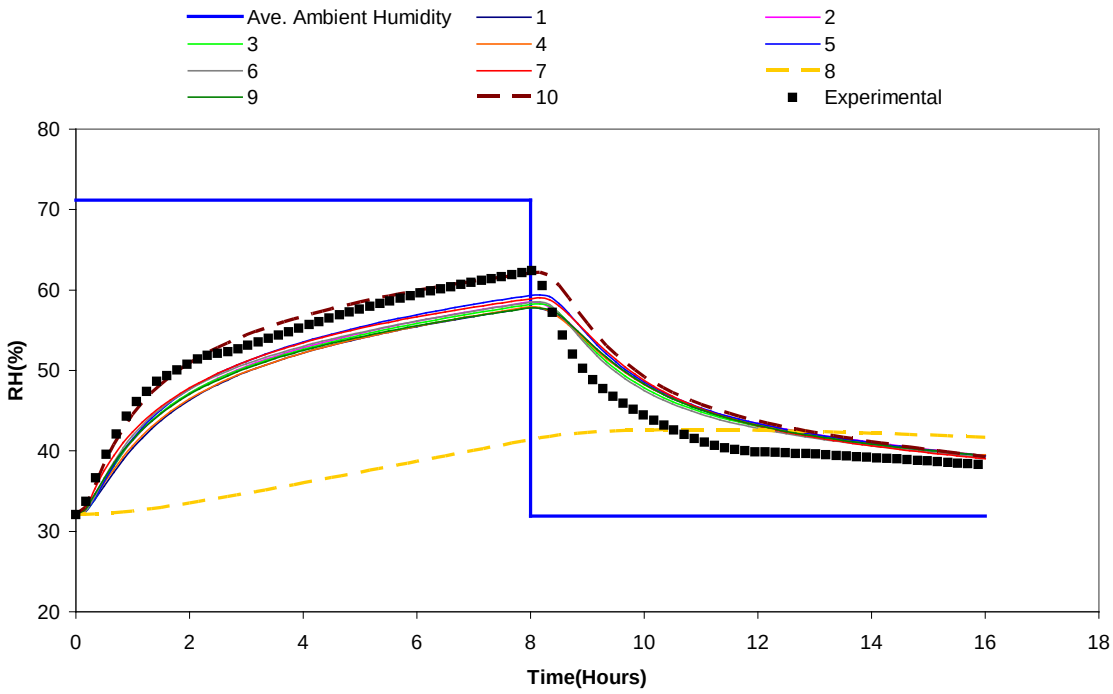

(b)

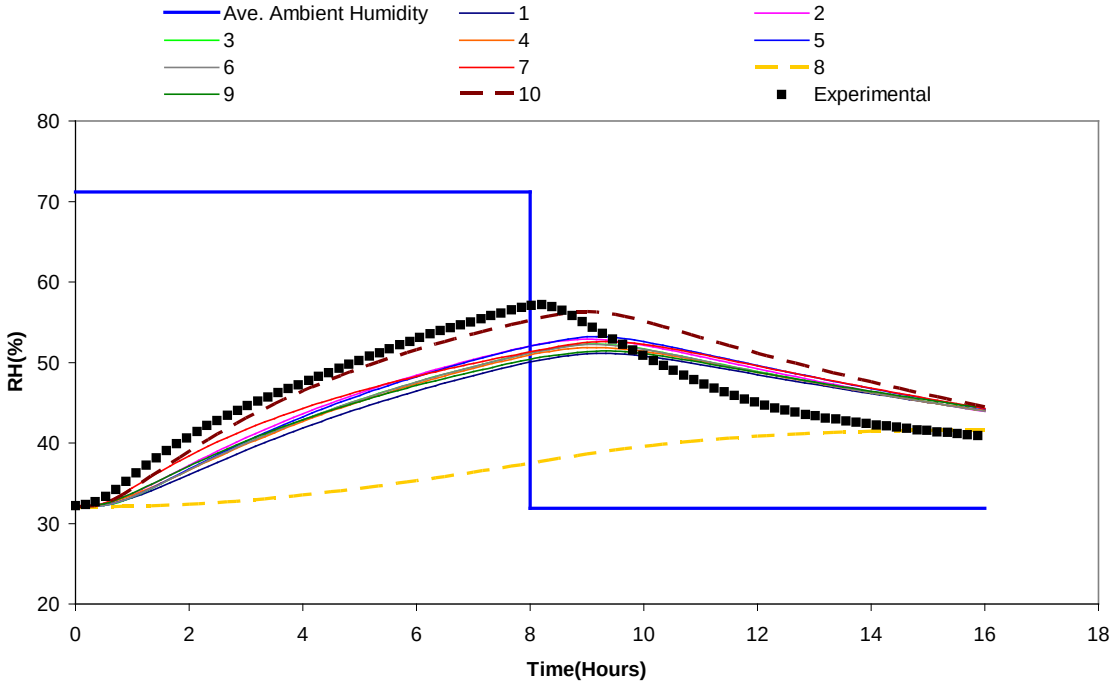

Figure 3.9: Measured and simulated relative humidity in the uncoated gypsum bed at a depth of (a) 12.5 mm and (b) 25 mm for Case 2.

The effect of the length of the adsorption and desorption phases is shown in Figure 3.10. Comparing the measured relative humidity in the gypsum bed for the first 8 hours, of Cases 1 and 2, shows that there is little difference; further demonstrating the repeatability of the experiment. .

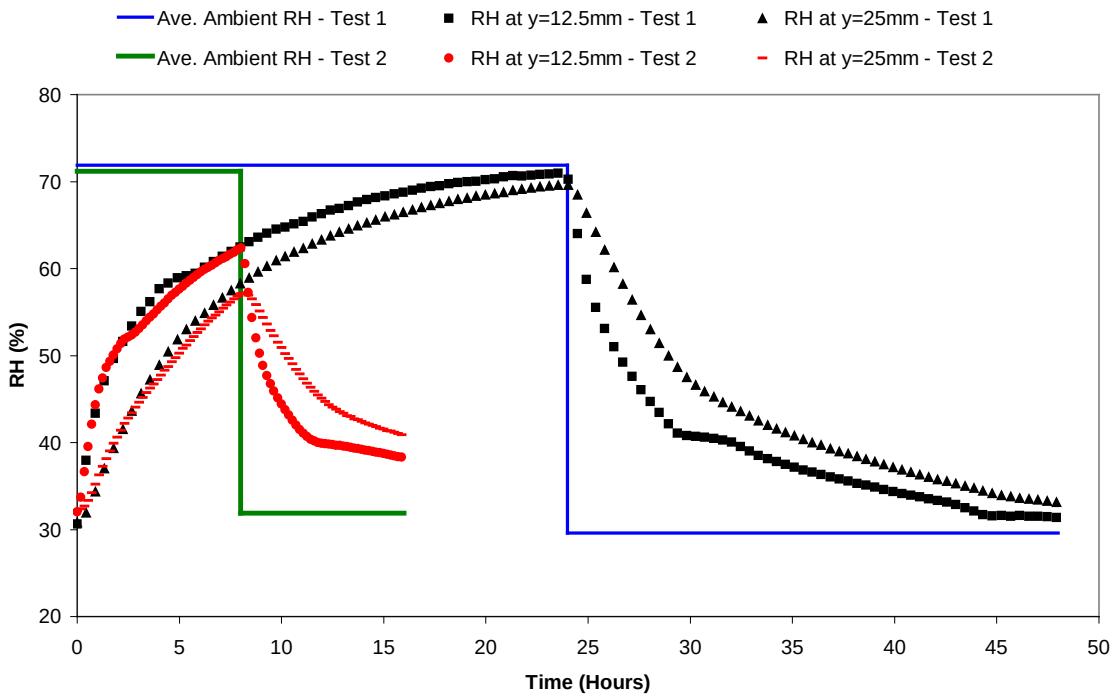

Figure 3.10: Experimentally measured relative humidity in an uncoated gypsum bed for Δt = 24 h (Case 1) and Δt = 8 h (Case 2).

3.3 Case 3: Uncoated gypsum (Δt = 24 hours, Re = 5000)

In this test, the effect of Reynolds (Re) number was examined. The increased air flow rate should increase the heat and mass transfer in the gypsum bed due to the increased heat and mass transfer coefficients between the air and the top gypsum board of the bed. The test conditions are presented in Figure 3.11.

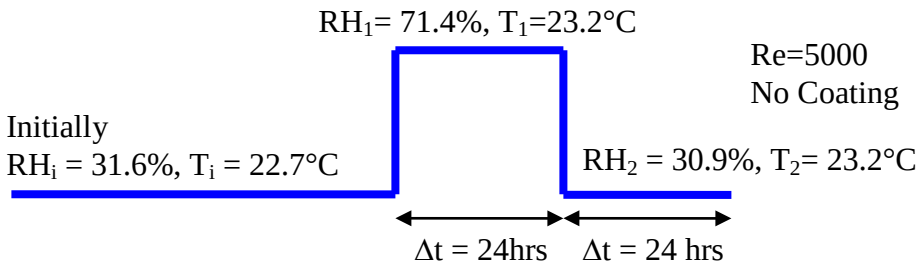

Figure 3.11: Schematic representation of test conditions used for Case 3.

The experimentally measured relative humidity in the gypsum bed is presented in Figure 3.12. The results are very similar to the results from Case 1 which had a laminar flow rate.

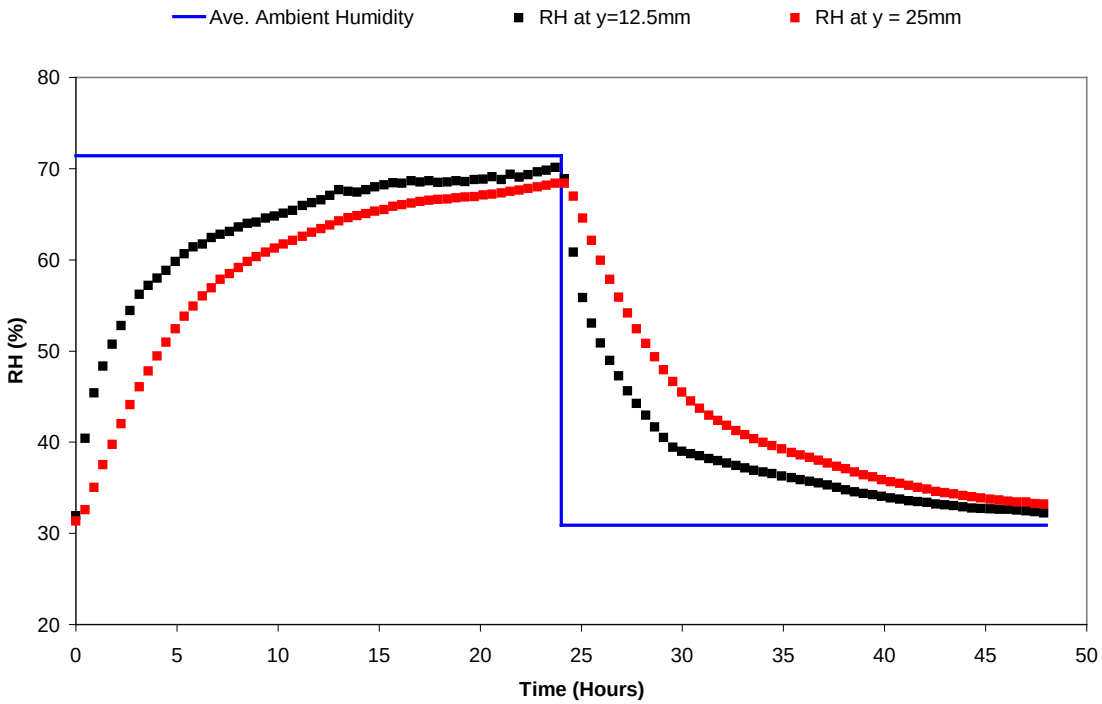

Figure 3.12: Experimentally measured relative humidity at depths of y = 12.5 and 25 mm in the gypsum bed for Case 3.

The results from the simulations and experimentally measured relative humidity at depths of 12.5 and 25 mm in the gypsum bed are presented in Figure 3.13. Again, there was very good agreement between the simulations and the experiment except for one CFD simulation which predicts a different response in the gypsum bed.

(a)

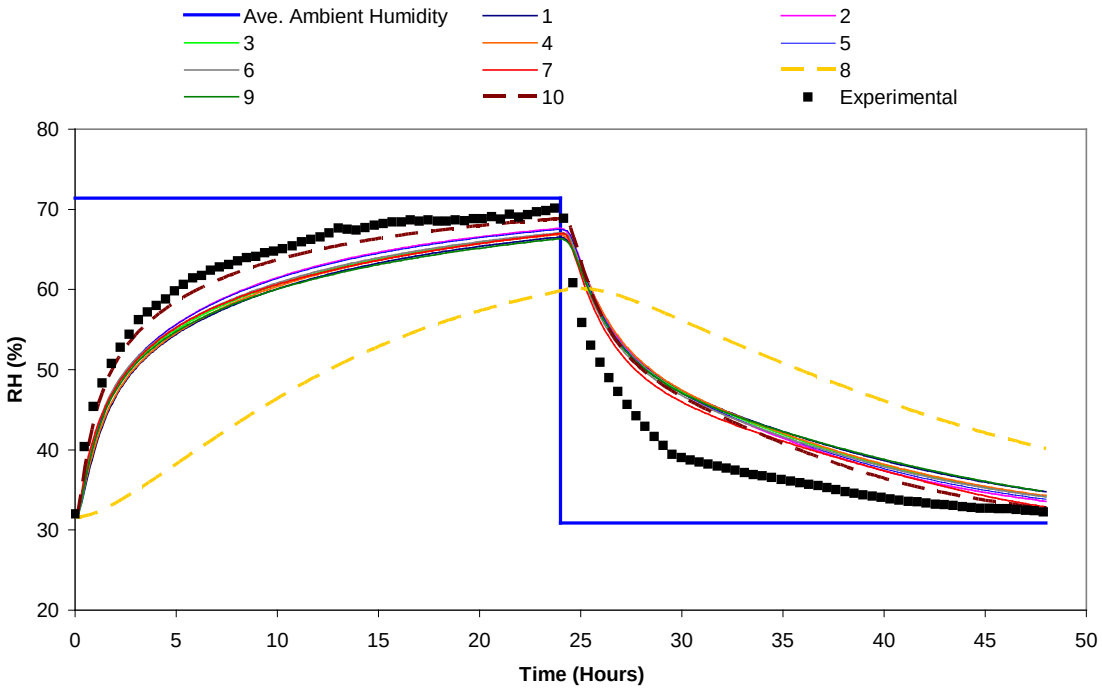

(b)

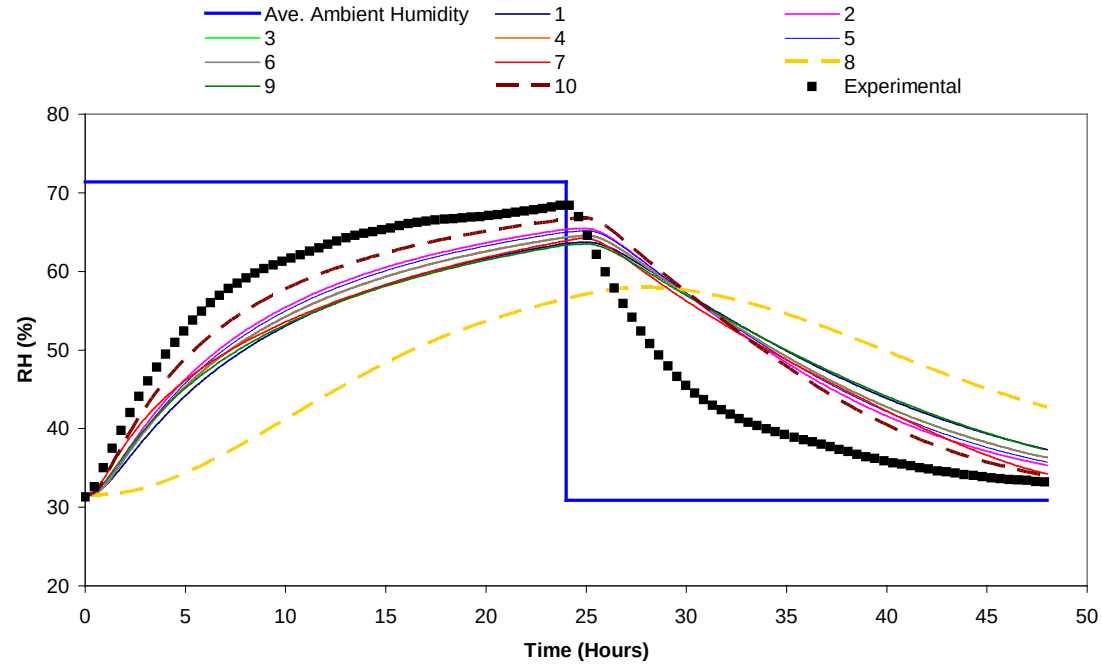

Figure 3.13: Measured and simulated relative humidity at depths of (a) 12.5 mm and (b) 25 mm in the gypsum bed for Case 3.

The effect of air flow rate on relative humidity at depths of 12.5 and 25 mm can be seen in Figure 3.14. The difference between the base experiment (Case 1), which had Re = 2000 (laminar), and Case 3, which had Re = 5000 (turbulent), is very small indicating that the range of flow rates studied had a negligible effect on the measured relative humidity in the gypsum bed.

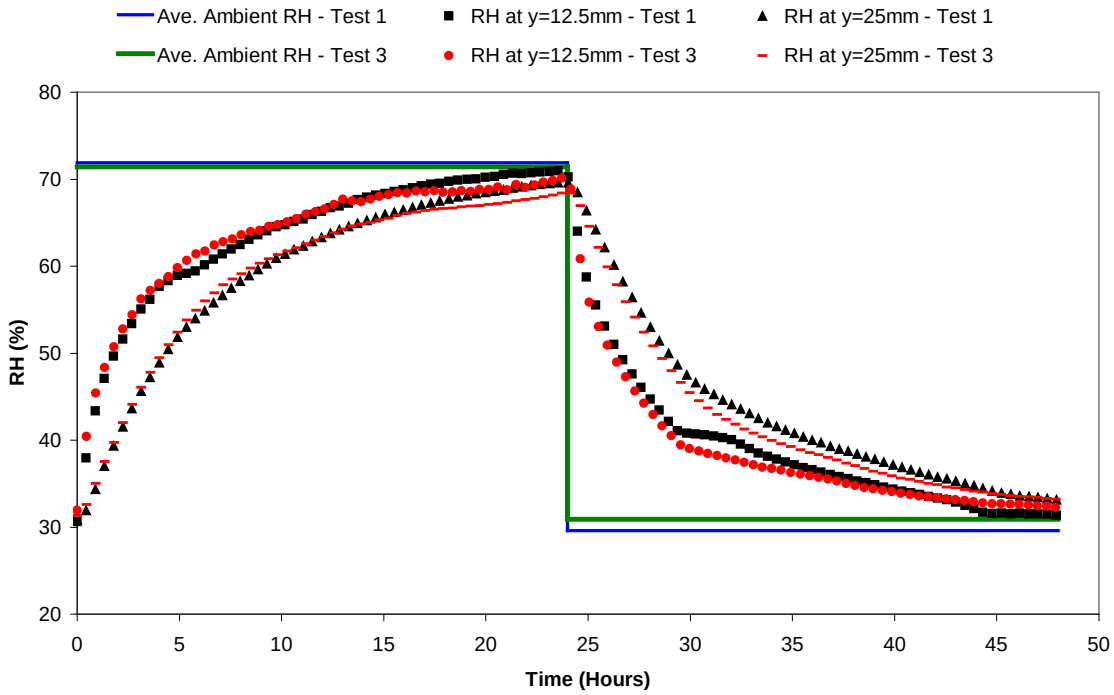

Figure 3.14: Measured relative humidity at a depth of y=12.5 mm and 25 mm in the gypsum bed for Case 1 (laminar) and Case 3 (turbulent).

3.4 Case 4: Acrylic coated gypsum (Δt = 24 hours, Re = 2000)

In this test, the effect of applying a coat of acrylic paint to the top of the bed was examined. Acrylic paint, like gypsum, will allow moisture storage in and transport through its porous matrix. The test conditions are presented in Figure 3.15.

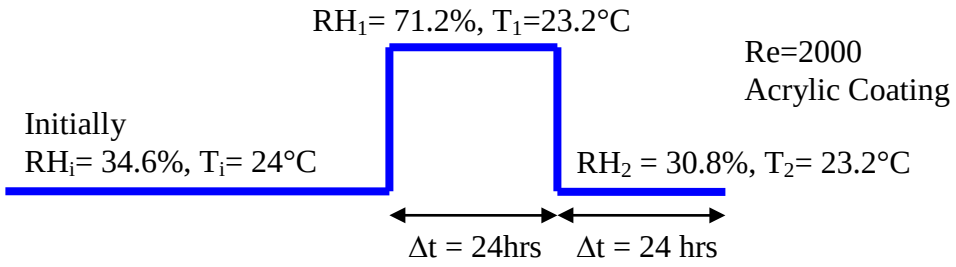

Figure 3.15: Schematic representation of test conditions used for Case 4.

The experimentally measured relative humidity at depths of 12.5 and 25 mm in the gypsum bed are presented in Figure 3.16.

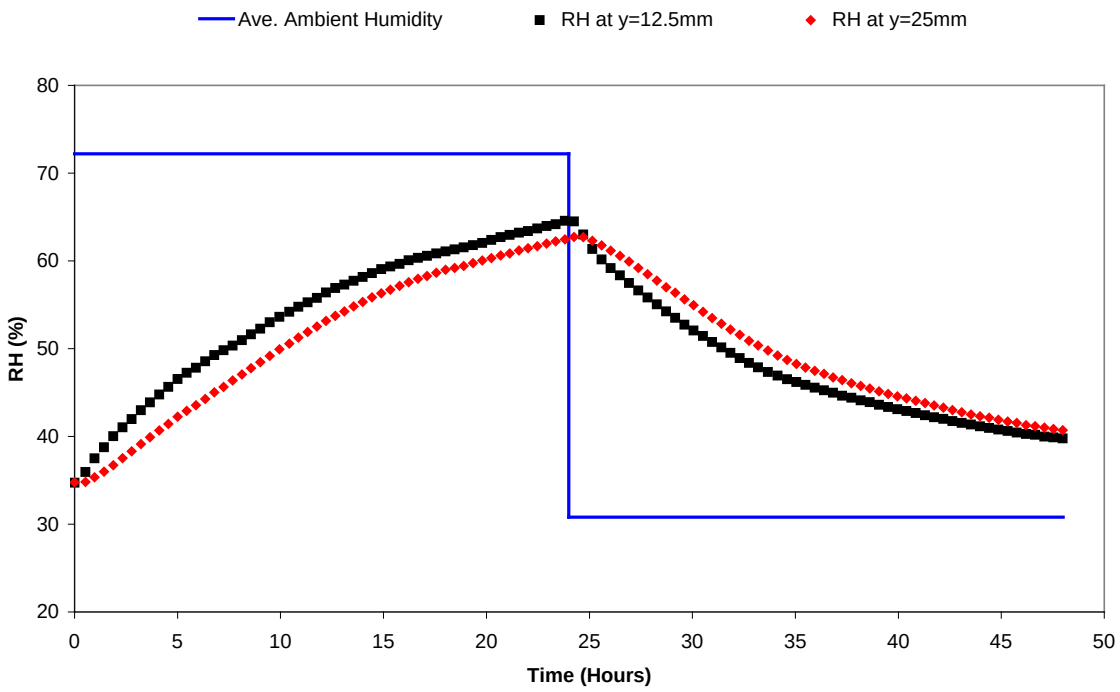

Figure 3.16: Experimentally measured relative humidity at depths of y = 12.5 and 25 mm in the gypsum bed where the top board was painted with acrylic paint for Case 4.

The relative humidity at depths of y =12.5 and 25 mm in the gypsum bed for all simulations and experimental measurements are presented in Figures 3.17 and 3.18. Two different methods were used to simulate the paint layer on the gypsum bed. The first method involved treating the paint as a vapor resistance included in the mass transfer coefficient (Table 2.2) supplied to the modelers (Figure 3.17). This simplified approach was then checked against the second method of treating the paint layer as a separate porous layer on top of the gypsum bed (Figure 3.18). Material properties for the two paints were supplied to the modelers (Appendix A). The two methods produced different simulated results for the response of the gypsum bed and are compared to the measured results for the acrylic coated case. There was a larger spread in the results of the simulation when the paint layer was treated as a separate porous layer compared to combining it in the surface transfer coefficient. Numerical simulations 8 (CFD) and 9 (1-D vapor diffusion) only examined treating the paint layer as an added resistance in the surface transfer coefficient, while simulation 10 (CFD) examined only treating the paint as a separate porous layer. The other models considered both ways of modeling the paint layer.

(a)

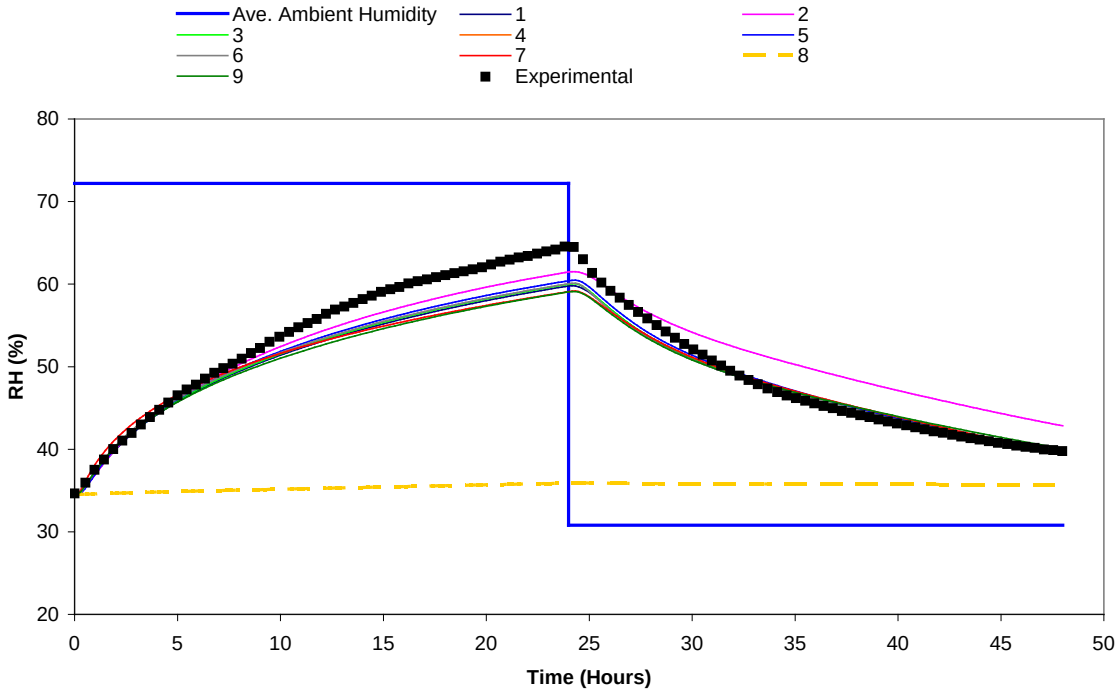

(b)

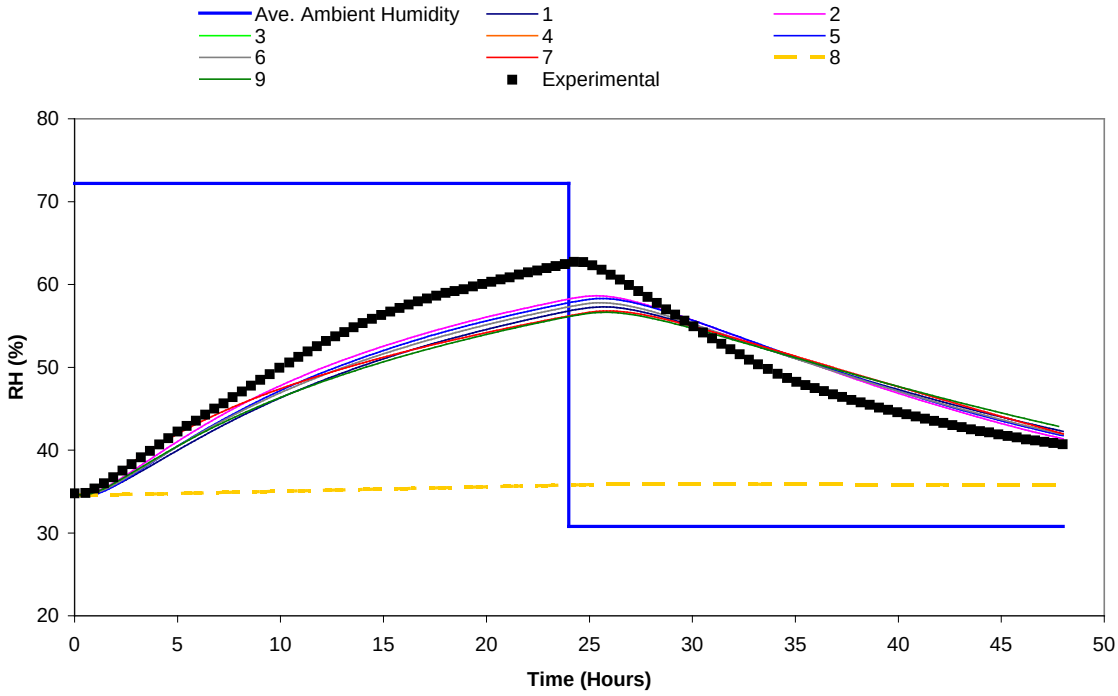

Figure 3.17: Measured and simulated relative humidity at a depth of (a) y = 12.5 mm and (b) y = 25 mm in the acrylic coated gypsum bed treating the paint layer as a vapor resistance in the surface transfer coefficient (Case 4).

(a)

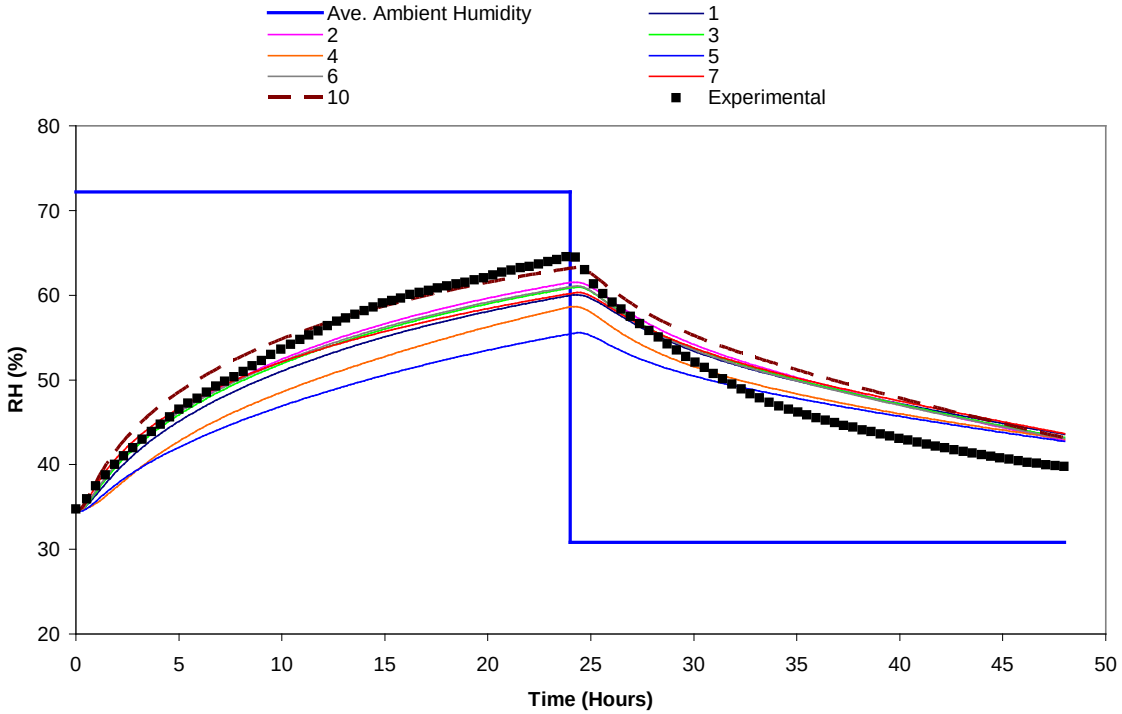

(b)

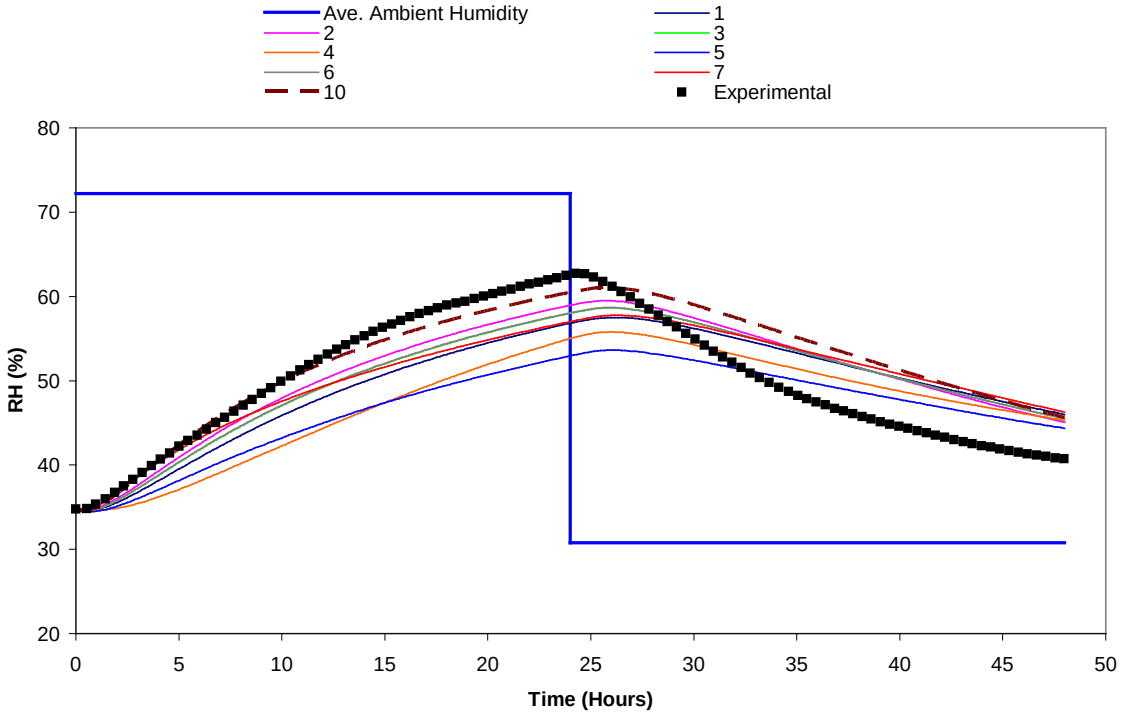

Figure 3.18: Measured and simulated relative humidity at a depth of (a) y = 12.5 mm and (b) y = 25 mm in the acrylic coated gypsum bed treating the paint layer as a separate porous layer on top of the gypsum bed, Case 4.

The acrylic paint had a large effect on the moisture transfer in the gypsum bed due to its increased vapor transfer resistance. The comparison of the acrylic paint coated bed to the base test is presented in Figure 3.19.

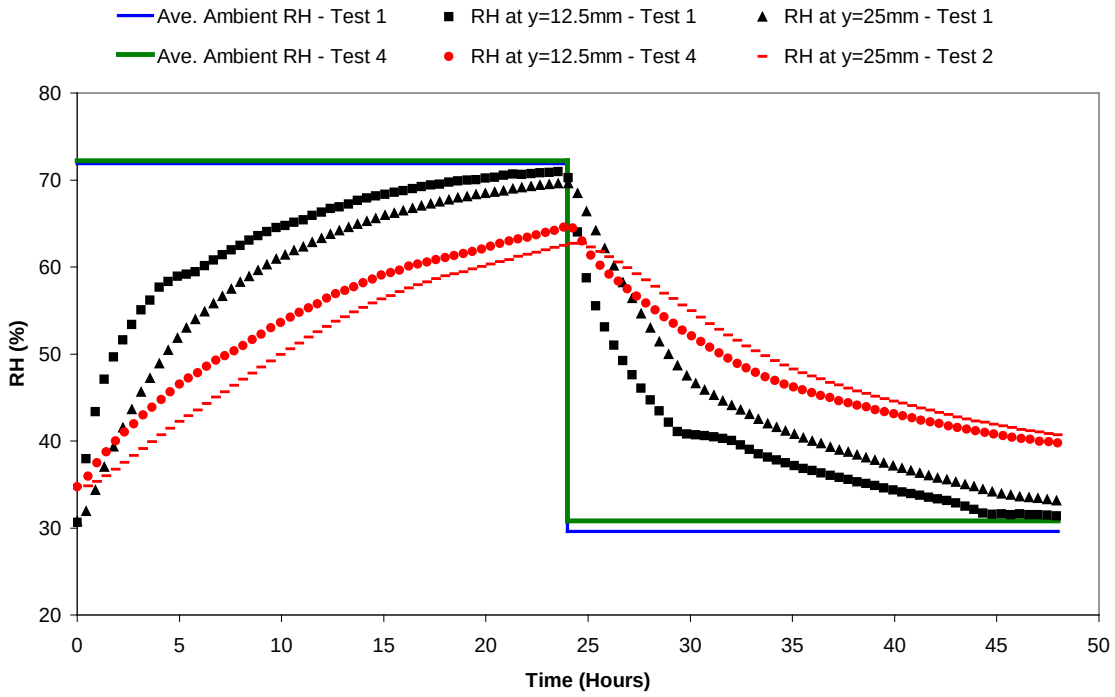

Figure 3.19: Comparison of the measured relative humidity for the uncoated case (Case 1) and the acrylic coated case (Case 4).

3.5 Case 5: Latex coated gypsum (Δt = 24 hours, Re = 2000)

In this test, the effect of the second surface coating, latex paint, was examined. The latex paint has a very large resistance to moisture transfer. The test conditions are presented in Figure 3.20 and the experimental results are presented in Figure 3.21.

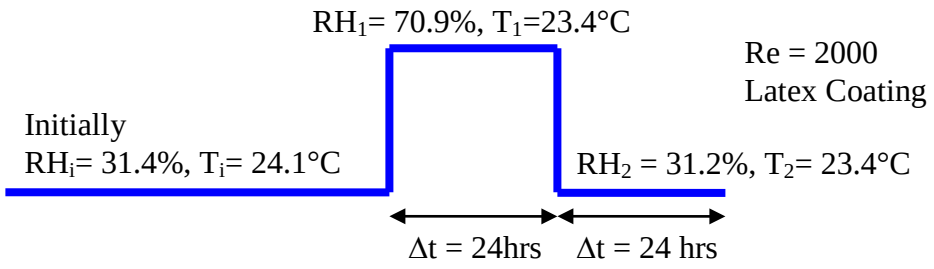

Figure 3.20: Schematic representation of test conditions used for Case 5.

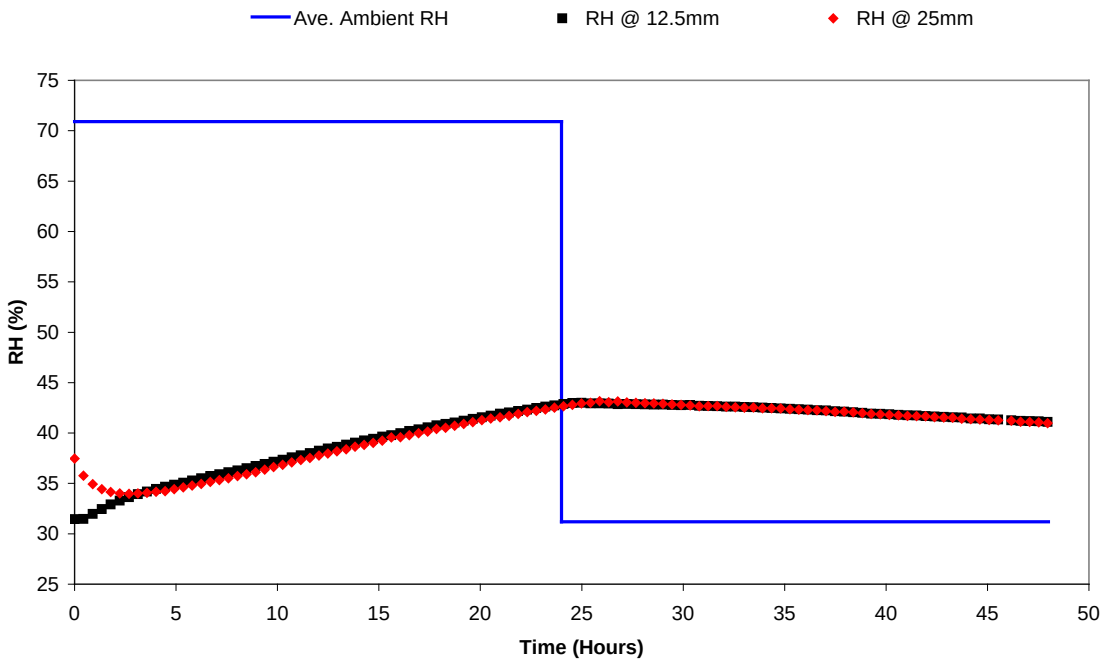

Figure 3.21: Experimentally measured relative humidity at depths of y = 12.5 and 25 mm in the gypsum bed where the top board was painted with latex paint for Case 5.

As shown in Figure 3.21, there was a difference between the initial conditions of the interfaces between the three boards in the bed. This difference was caused by

utilizing two methods of conditioning prior to the test starting because preconditioning in the bed was too slow. Two boards were conditioned in a chamber using a magnesium chloride saturated salt solution [ASTM E104-02] to produce a relative humidity of approximately 33% at 23°C. The other sheet was placed in the environmental chamber held at 30% RH. Due to the different conditions, there were differences in the initial moisture content in the bed. The initial conditions of the bed were provided to the participants as the initial relative humidity at a depth of 12.5 mm in the bed. Since the latex paint does not allow much moisture transfer, the relative humidity in the bed increased only slightly during the adsorption phase of the test. After the conditions were changed, the measured relative humidity did not decrease significantly (~3%) in the bed.

Similar to the test with acrylic paint (Case 4), two different methods were used to simulate the paint layer on the gypsum bed. The first method involved treating the paint as a vapor resistance included in the mass transfer coefficient and the second treated the latex paint as a separate porous layer in the simulation. The measured and simulated relative humidity results for the latex coated gypsum bed when the paint is treated as an added resistance in the transfer coefficient is presented in Figure 3.22. The results from treating the latex paint as a separate porous layer on top of the gypsum bed is presented in Figure 3.23. Again numerical simulations 8 (CFD) and 9 (1-D diffusion) only treated the paint layer as an added resistance in the surface transfer coefficient, while simulation 10 (CFD) only treated the paint as a separate porous layer. The other models provided both simulations for the latex coated case.

(a)

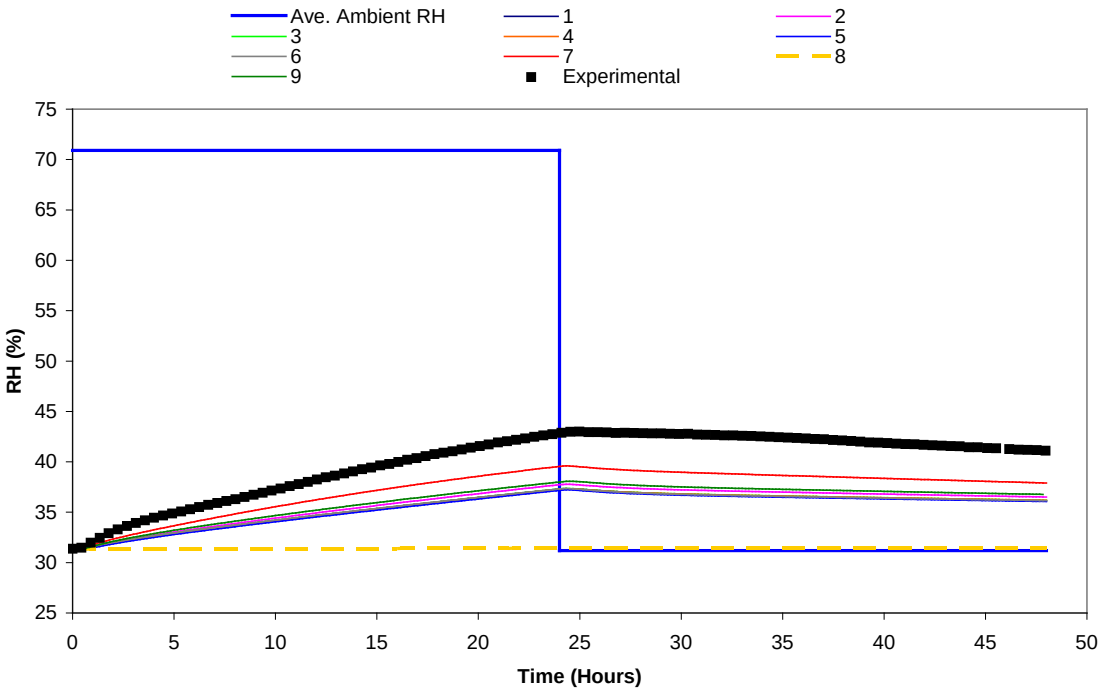

(b)

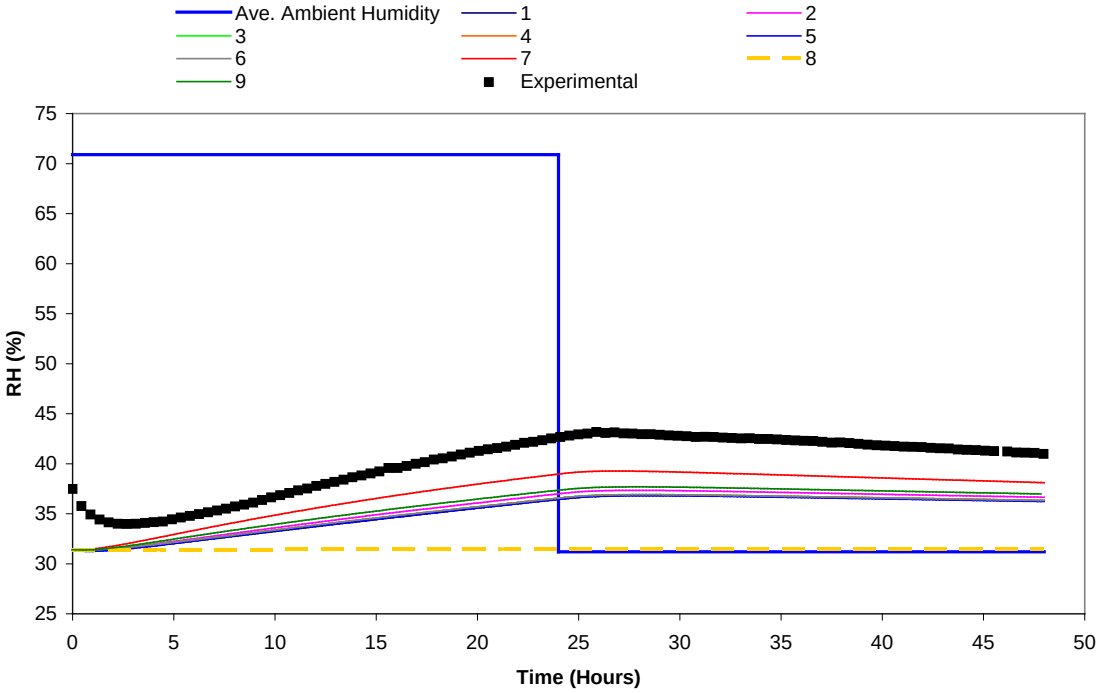

Figure 3.22: Measured and simulated relative humidity at depths of y = (a) 12.5 mm and (b) 25 mm in the latex coated gypsum bed treating the paint layer as a vapor resistance included in the surface transfer coefficient.

(a)

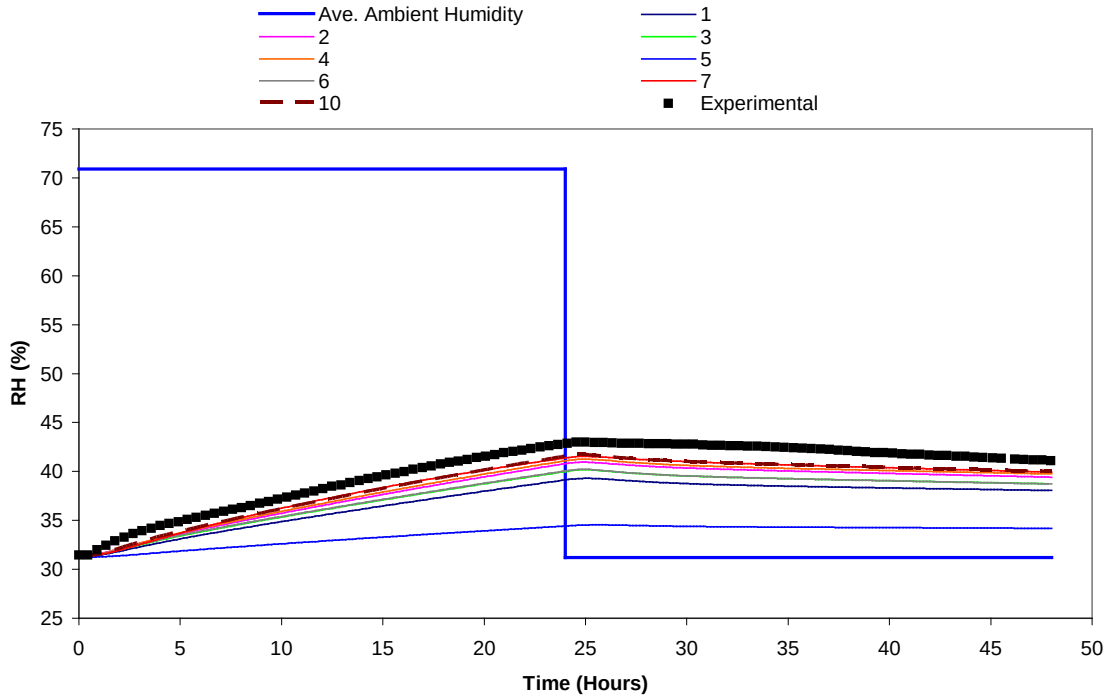

(b)

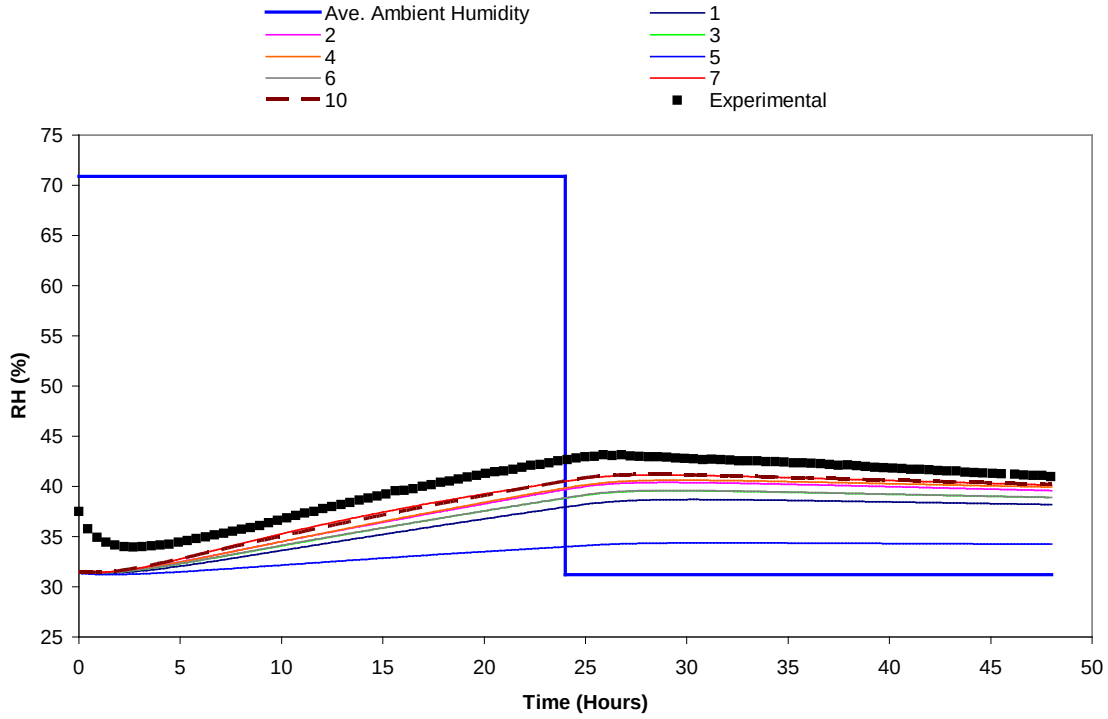

Figure 3.23: Measured and simulated relative humidity at depths of y = (a) 12.5 mm and (b) 25 mm in the latex coated gypsum bed treating the paint layer as a separate porous layer on top of the gypsum bed.

Due to the hydrophobic nature of the latex paint test, there was mostly diffusion within the gypsum bed, below the paint layer, until the relative humidity had come to equilibrium within 3 hours.

The effect of the latex paint on the moisture transfer in the gypsum bed is shown by comparing the latex painted case (Case 5) to the base case (Case 1) with no coating in Figure 3.24. The latex paint offers a very large resistance to moisture transfer and as such there is a large difference between the measured relative humidity in the uncoated and the latex coated gypsum bed.

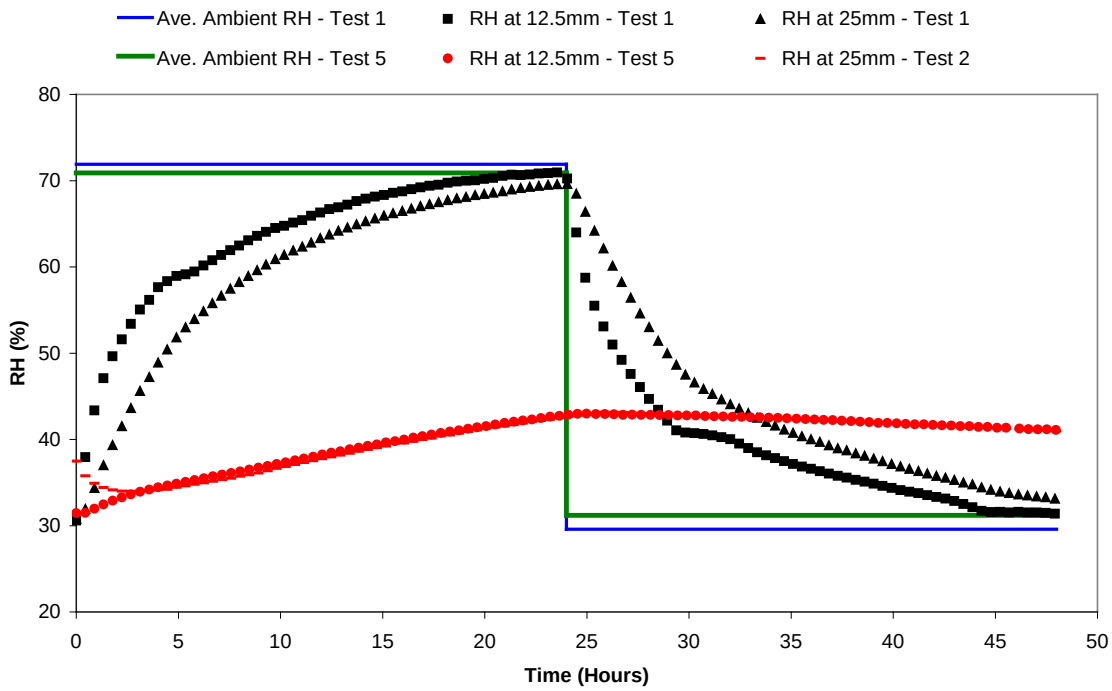

Figure 3.24: Comparison of the measured relative humidity in the uncoated test and the latex coated gypsum bed test.

Chapter 4

Summary Comparisons of Experimental and Numerical Results

Chapter 3 detailed the results of the experimental measurements and simulations for all five cases (Table 2.1) and Appendix B contains the tabulated data. The results showed quite good agreement, but it is difficult to compare or quantify the agreement between the different cases. Therefore this chapter will focus on the maximum change during the adsorption/desorption cycles as shown in Figure 4.1.

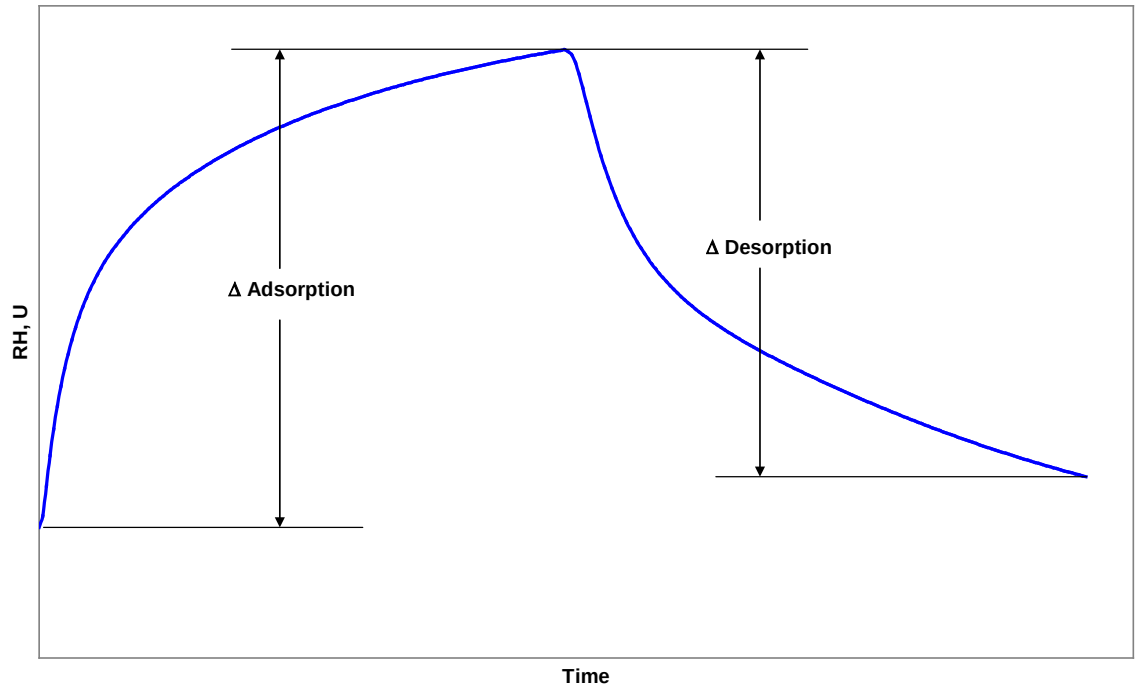

Figure 4.1: Typical response of the measured relative humidity or moisture accumulation in the gypsum bed exposed to a step change in relative humidity.

Comparing the change during each phase will provide a more convenient method of comparing different tests and quantifying the agreement between the numerical and experimental results. The transient response of the experiments and the numerical results showed good agreement and that is why the comparison is made solely on the final values of the adsorption/desorption cycles.

4.1 Methodology for Comparison

Using the nominal value of the change from the adsorption or desorption loading, the simulations can be effectively compared to each other and the experimental results. The change in the value is calculated as the difference of a condition at the end of a cycle and the beginning.

$$\Delta X = X_{end\ of\ cycle} - X_{beginning\ of\ cycle} \quad (1)$$

Where ΔX is the calculated change in relative humidity or mass accumulation between the end ($X_{end\ of\ cycle}$) of the adsorption/desorption cycle and the beginning ($X_{beginning\ of\ cycle}$) of the respective cycle.

Figure 4.2 shows the experimental and simulation results from Case 1 (Uncoated gypsum bed, with Δt = 24 h and Re = 2000) for the simulations and the experimentally measured value for relative humidity. The shaded region in the background is the experimental value with uncertainty bars (95% confidence interval) and each simulation is shown as a bar. Results are the same as in Figure 3.3 but it is easier to see the agreement and quantify the difference between the different simulations and the experimental data. Note that simulations 8 and 10 are the CFD simulations.

(a)

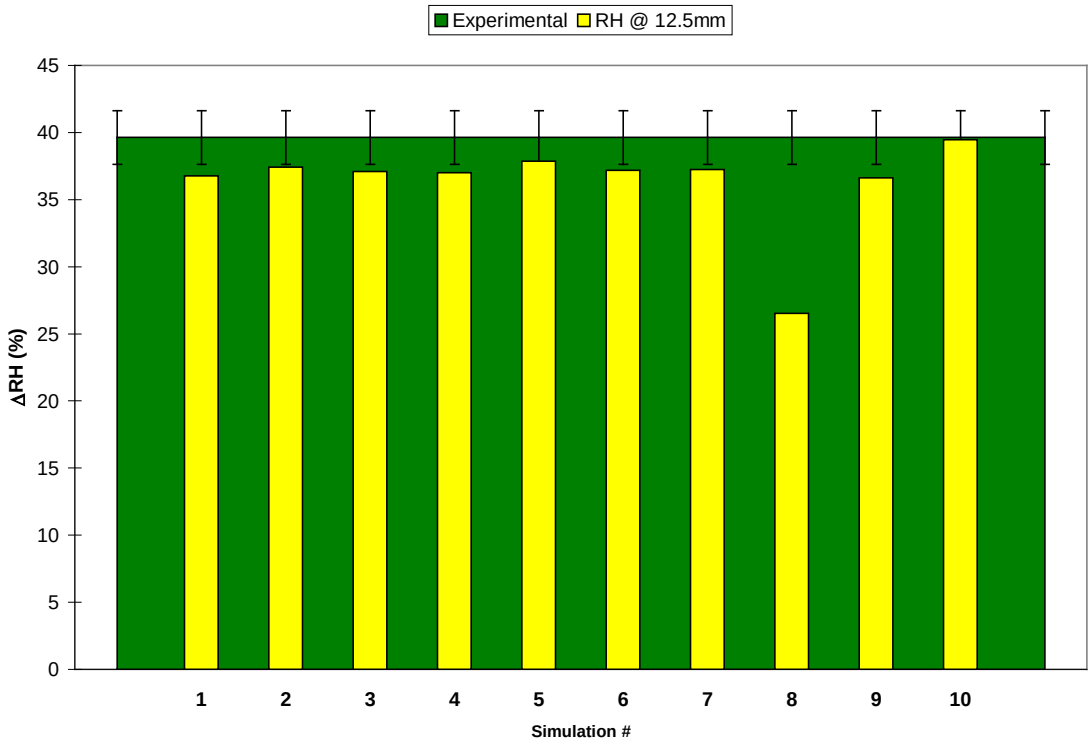

(b)

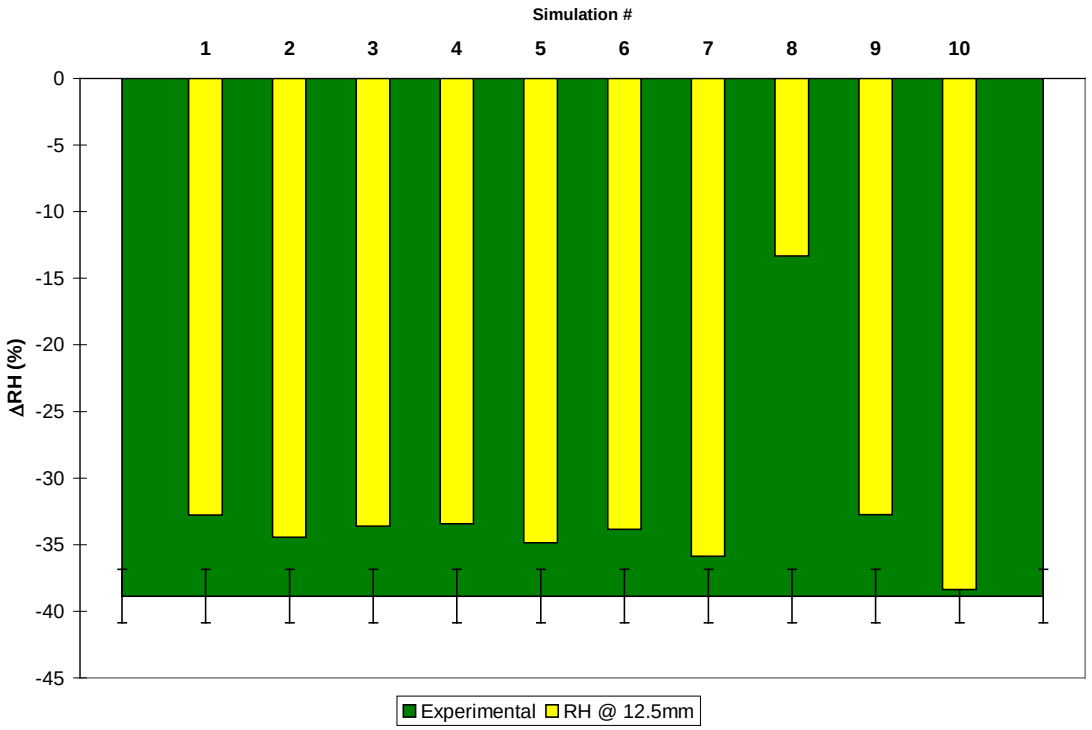

Figure 4.2: Comparison of simulated (bars) and measured (shaded background) relative humidity change during the (a) adsorption and (b) desorption phase of the uncoated gypsum bed case at a depth of 12.5 mm. The error bars represent the 95% uncertainty bound of the experimental values.

4.2 Summary Comparison of Relative Humidity and Moisture Change

If charts like Figure 4.2 were developed for each adsorption/desorption phase of each test, one could examine the agreement of each simulation to the experimental results for each individual test. A better method of comparing the simulations and tests together is a scatter plot as shown in Figures 4.3 and 4.4. The results for the adsorption and desorption phase of each simulation are shown for all tests and methods of simulations for easy comparison. Note that simulations 8 and 10 are the CFD simulations and are denoted with small square symbols.

Figures 4.3 and 4.4 show that the results from the simulations agree better during the adsorption loading than desorption loading. The numerical results from the painted bed (Cases 4 and 5) simulations show better agreement among each other when the paint is treated as an extra resistance in the surface transfer coefficient than when it is treated as a separate porous media. The effect of an increased transfer coefficient above the gypsum bed (Case 3) shows a negligible effect on the relative humidity in the board when compared to the base case (Case 1). The numerical results at a depth of y = 25 mm in the gypsum bed have a larger spread than the results at y = 12.5 mm.

(a)

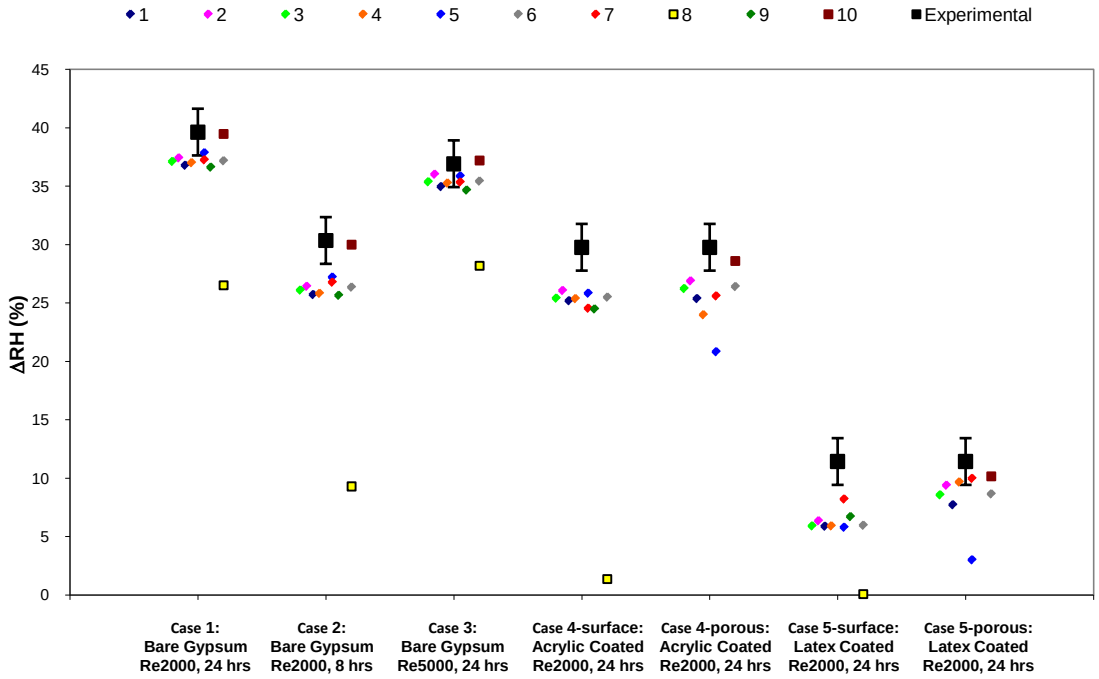

(b)

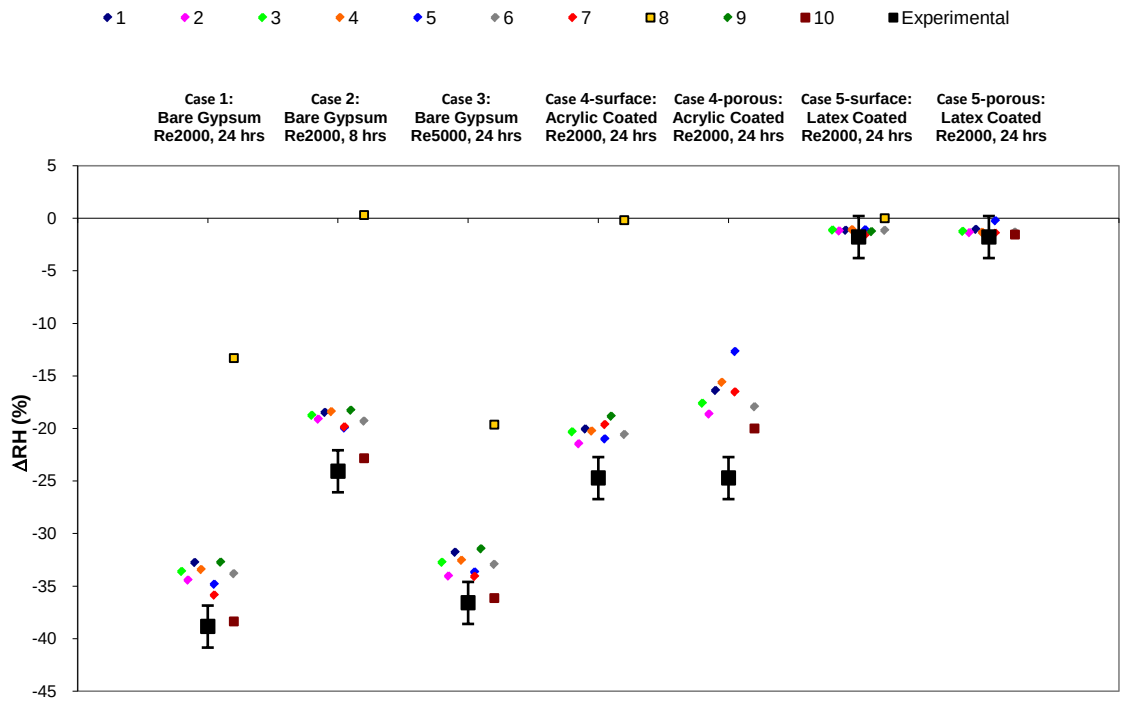

Figure 4.3: Change in relative humidity results for the (a) adsorption and (b) desorption cycle at a depth of 12.5 mm in the gypsum bed.

(a)

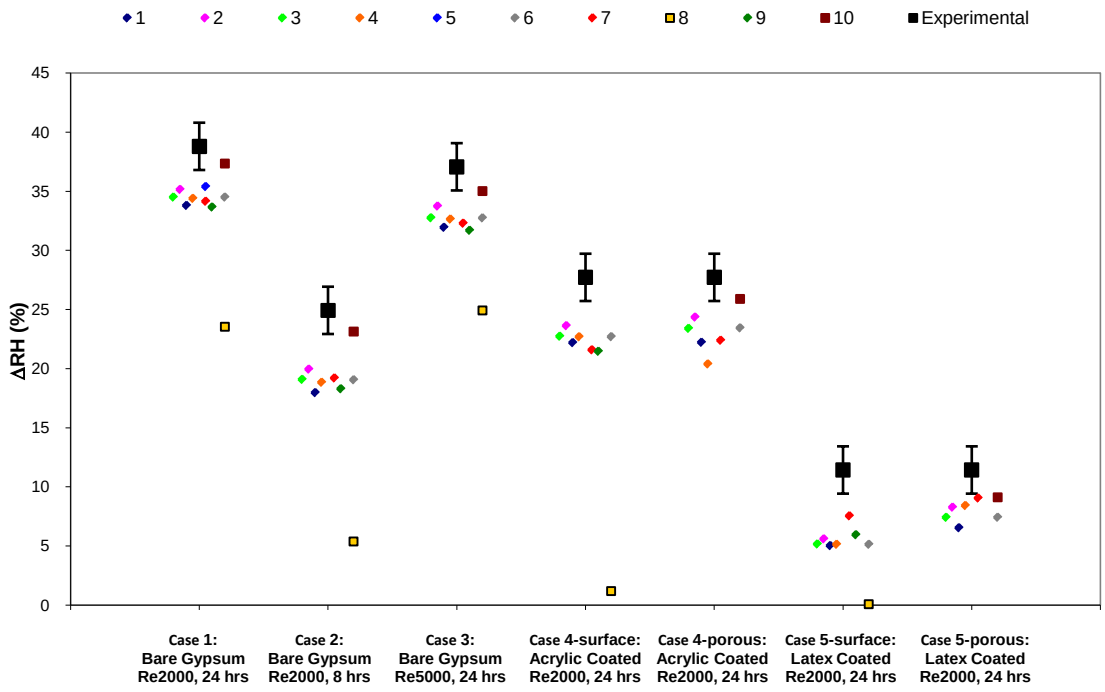

(b)

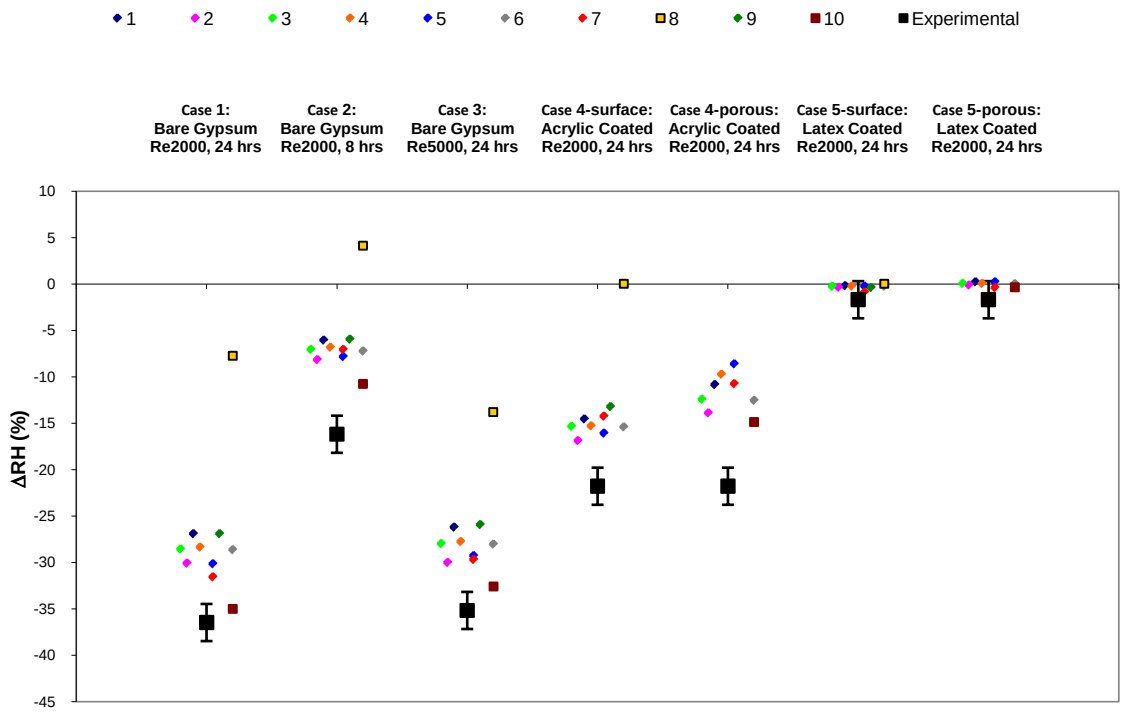

Figure 4.4: Change in relative humidity for the (a) adsorption and (b) desorption cycle at a depth of 25 mm in the gypsum bed.

The mass of the gypsum bed followed the same trend as the relative humidity. The mass increased during the period of high humidity exposure and decreased during the period of low humidity exposure. In the case of the latex coated bed, the change in mass during the adsorption and desorption was below the uncertainty in the sensors which made it difficult to assess the change in mass during each phase of the test. Therefore, the experimentally measured change in mass during the test with latex paint is assumed to be zero. This can be seen in Figure 4.5 along with the other experimental and numerical data. Overall, the moisture gain and loss was simulated quite accurately. There were also very similar results from the different simulations for each test.

(a)

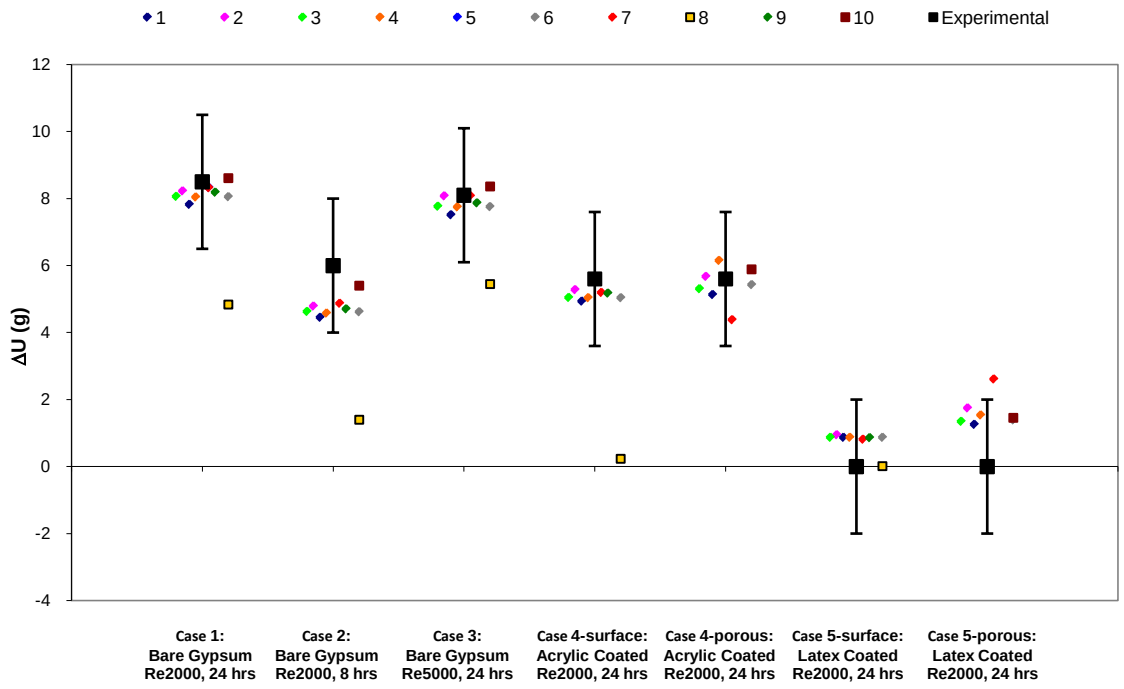

(b)

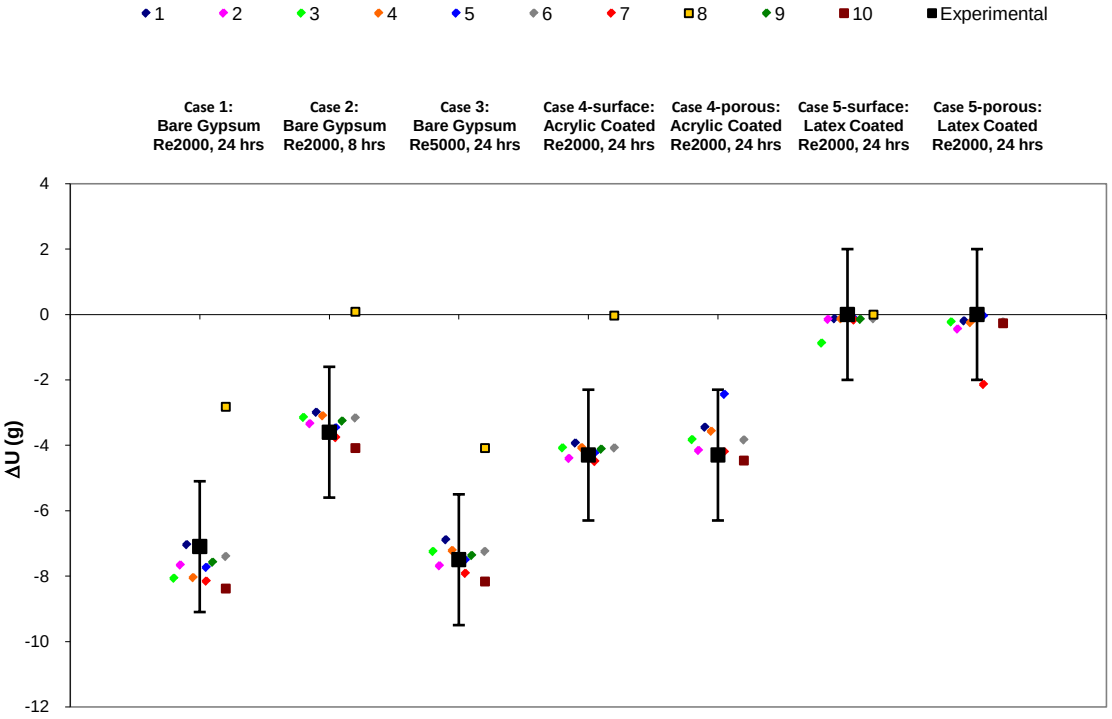

Figure 4.5: Change in mass of the gypsum bed during the (a) adsorption and (b) desorption phases of all tests.

The previous graphs (Figures 4.3 and 4.4) show that the numerical and experimental values are in good agreement, but there is a general trend for the numerical models to underestimate the relative humidity change in the gypsum bed. On the other hand there is no general trend for the numerical models to over predict or under predict the moisture accumulation in the gypsum bed (Figure 4.5). The average of the simulations results, with 95% confidence level, $t\sigma$, (t is 1.890 and is the student-t distribution for the 95% confidence level with 8 degrees of freedom) for relative humidity at a depth of 12.5 mm in the gypsum bed for each test is shown in Figure 4.6 along with the experimental results for each test. The CFD simulations were previously shown for comparison but are not included in any of the statistical analysis. The results are plotted with the adsorption and desorption phases of the tests. The results at a depth of 25 mm in the bed are shown in Figure 4.7.

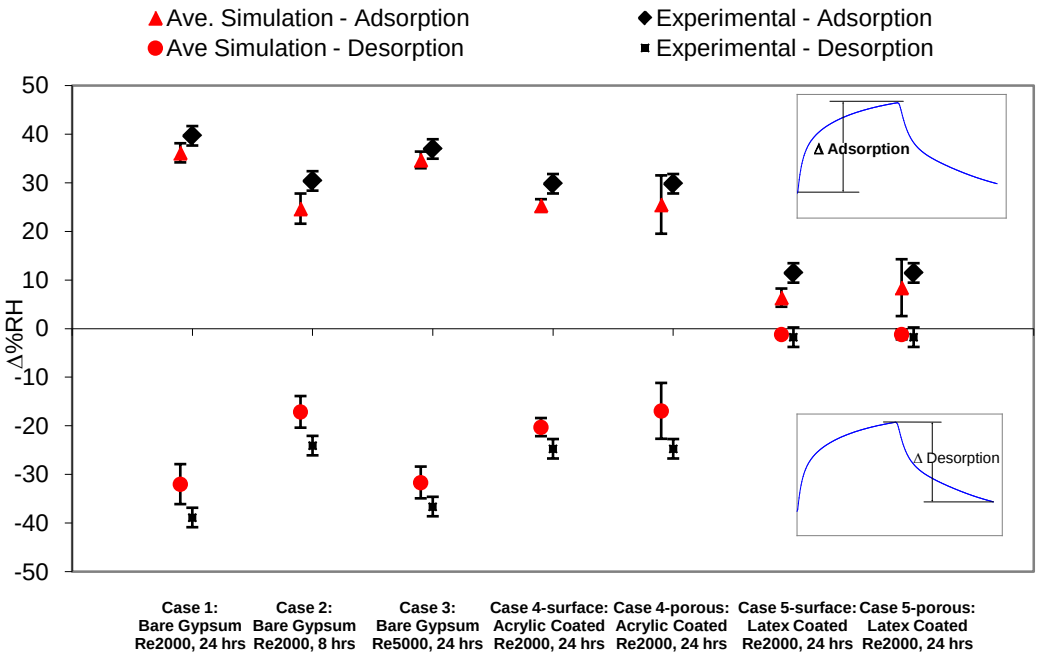

Figure 4.6: Average measured and simulated (excluding CFD models) change in relative humidity (for all tests at a depth of 12.5 mm in the gypsum bed). The error bars are the 95% confidence intervals for the measured and simulated data.

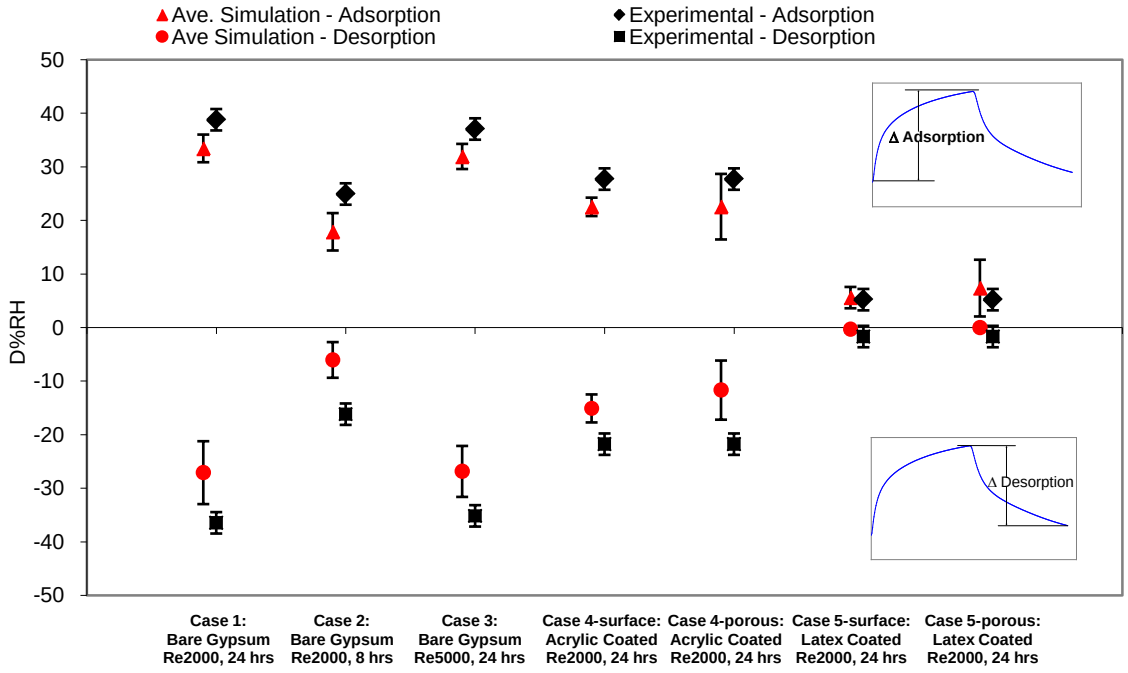

Figure 4.7: Average measured and simulated (excluding CFD models) change in relative humidity (for all tests at a depth of 25 mm in the gypsum bed). The error bars are the 95% confidence intervals for the measured and simulated data.

The results from the adsorption loading of the test showed closer agreement than the results from desorption loading. Hysteresis was not included in the first phase of this common exercise and could contribute to the larger difference between the simulations and the experimental results during desorption loading. When the paint layer was simulated, incorporating the paint into the transfer coefficient gave results closer to the experimental results compared to treating the paint as a separate porous layer. The simulated results also had a much smaller spread when treating the paint as an extra vapor resistance in the surface transfer coefficient.

Similar to the relative humidity results, the simulated mass accumulation is plotted for both the adsorption and desorption phases of each test in Figure 4.8.

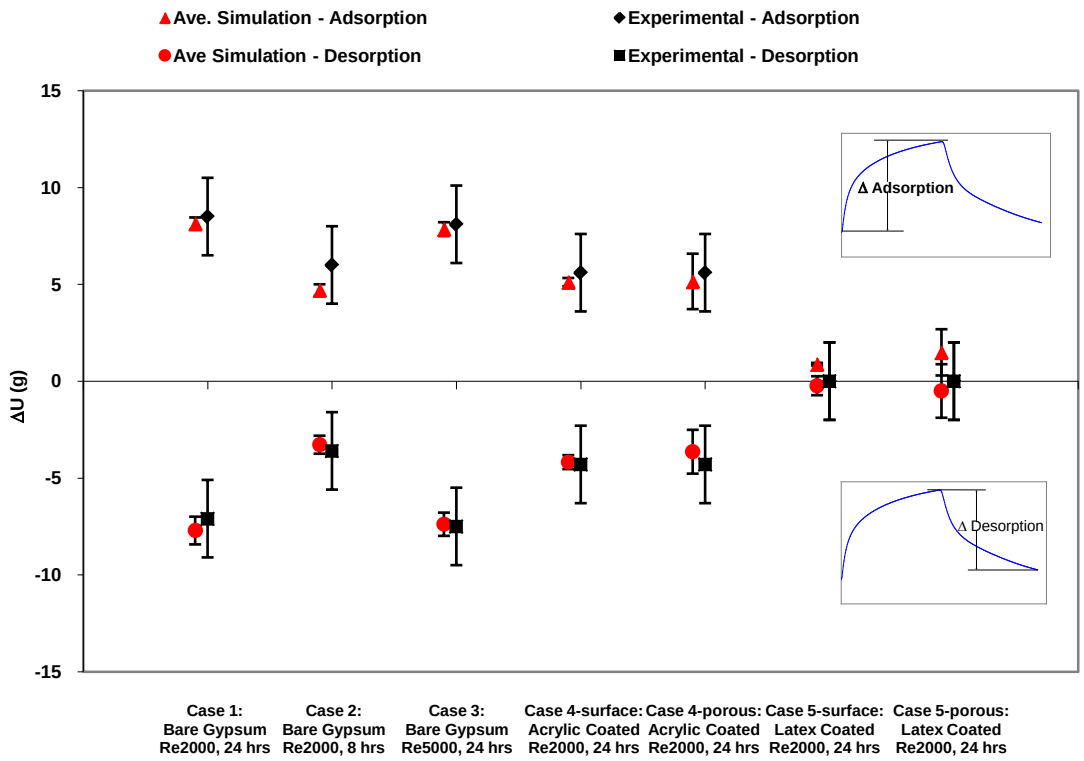

Figure 4.8: Average measured and simulated (excluding CFD models) change in mass for all tests. The error bars are the 95% confidence intervals for the measured and simulated data.

A table of the measured change and average of the numerical models simulated change is contained in Appendix B. Near hourly data for each case is also listed in Appendix B.

The standard deviations (σ) of the simulations results, excluding CFD simulations, are presented in Figure 4.9. The important fact to note is that the standard deviations of the numerical model results are less than 3% RH for each case.

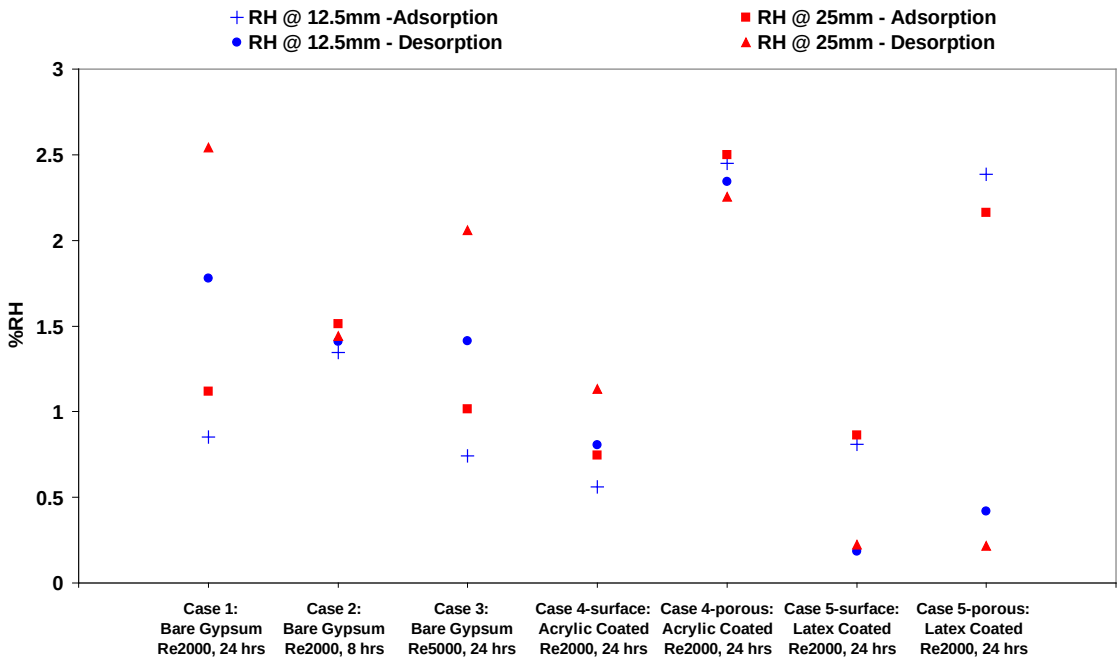

Figure 4.9: Standard deviation (σ) of the relative humidity results from the simulations.

Figure 4.9 shows that the variation in the simulated data is larger at y = 25 mm than at y = 12.5 mm. Incorporating the paint into the transfer coefficient also showed a lower standard deviation than treating the paint as a separate porous layer with its own properties.

The standard deviation (σ) in the mass accumulation simulations is presented in Figure 4.10. The simulations agreed well with each other, with the largest standard deviation (σ) being less than 0.9 g. The results show that treating the paint as separate porous layer created a much larger spread in the results and if these two simulations were discarded, the standard deviation of the samples would be less than 0.5 g for all of the tests.

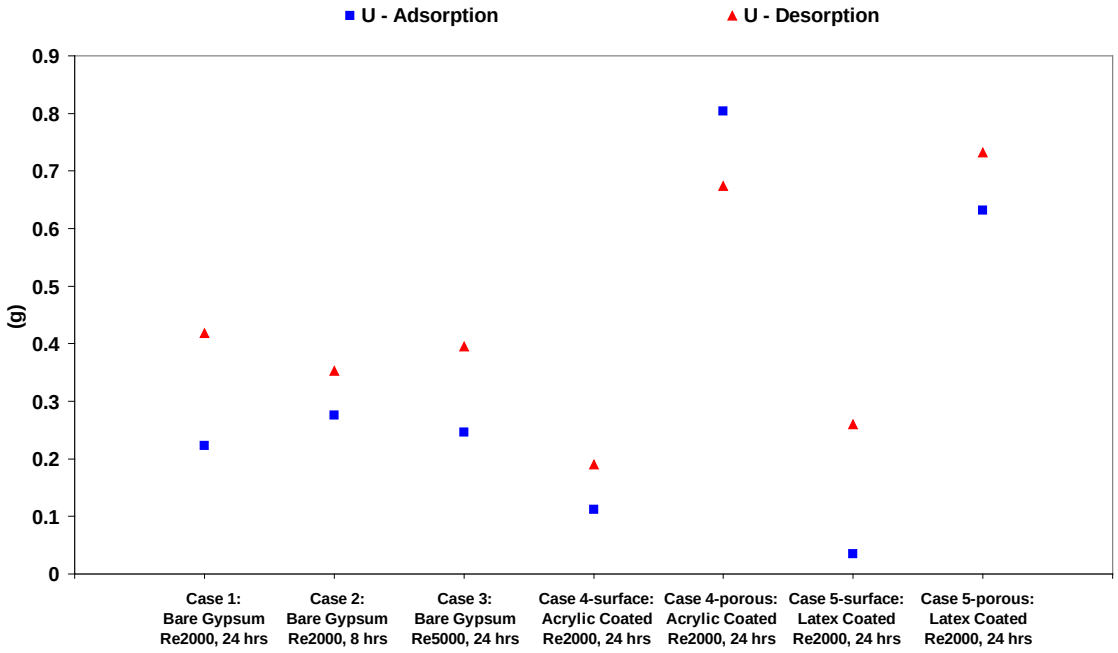

Figure 4.10: Standard deviation (σ) of the simulated moisture accumulation.

Chapter 5

Sensitivity Studies

Chapter 4 showed the comparison of the simulations when only the basic or required information was provided for the simulation of the 5 cases. The transient results were similar between simulations and with the experimental data. This chapter presents a series of sensitivity studies to further enhance the benchmark data.

The results of the "blind" simulations show that there are small discrepancies between the measured results and the simulated data. A sensitivity study was performed to determine which properties (sorption, vapor diffusion, or transfer coefficients) have an important impact on the results of the simulation.

During the round-robin testing on the gypsum boards and the paints [Roels 2008a], the laboratories measured the sorption and water vapor permeability. From the submissions, the mean of each property was supplied for the simulations in the blind simulations. For the sensitivity study, minimum and maximum values were provided (Appendix A). For the sorption isotherm these values correspond to the minimum and maximum measured isotherms from the round robin testing. For the vapor permeability the minimum and maximum represent the spread of the most reliable measurements from cups that used a high quality sealing method [Roels 2008a]. The sensitivity of the transfer coefficients was tested using a ±10% value of the transfer coefficient, based on

the work done by Iskra [2007] which shows an uncertainty of ±10% for the transfer coefficients in the TMT facility.

The effect of hysteresis was also investigated. Hysteresis is a common effect observed in sorption measurements. The effect of loading (i.e. adsorption or desorption) can produce two distinct measurements of sorption for a given relative humidity. Since half of each test included desorption loading on the gypsum bed, it is important to understand the effect of hysteresis on the simulated results. The hysteresis is only presented for the uncoated gypsum bed as it will have the largest effect for this case.

5.1 Property Sensitivity Study

There were 3 modelers who submitted results for the sensitivity/hysteresis study, Katholieke Universiteit Leuven, Slovak Academy of Science and Technical University of Denmark. One participant completed a full sensitivity of the results for sorption, vapor permeability and the transfer coefficients as per their assigned deviance. Another participant completed a sensitivity study examining an increase in the vapor permeability of the gypsum. The last participant examined the effect of hysteresis on the results with the uncoated gypsum bed. The results from one participant, for the simulated relative humidity at a depth of 12.5 mm in an uncoated bed are presented in Figure 5.1.

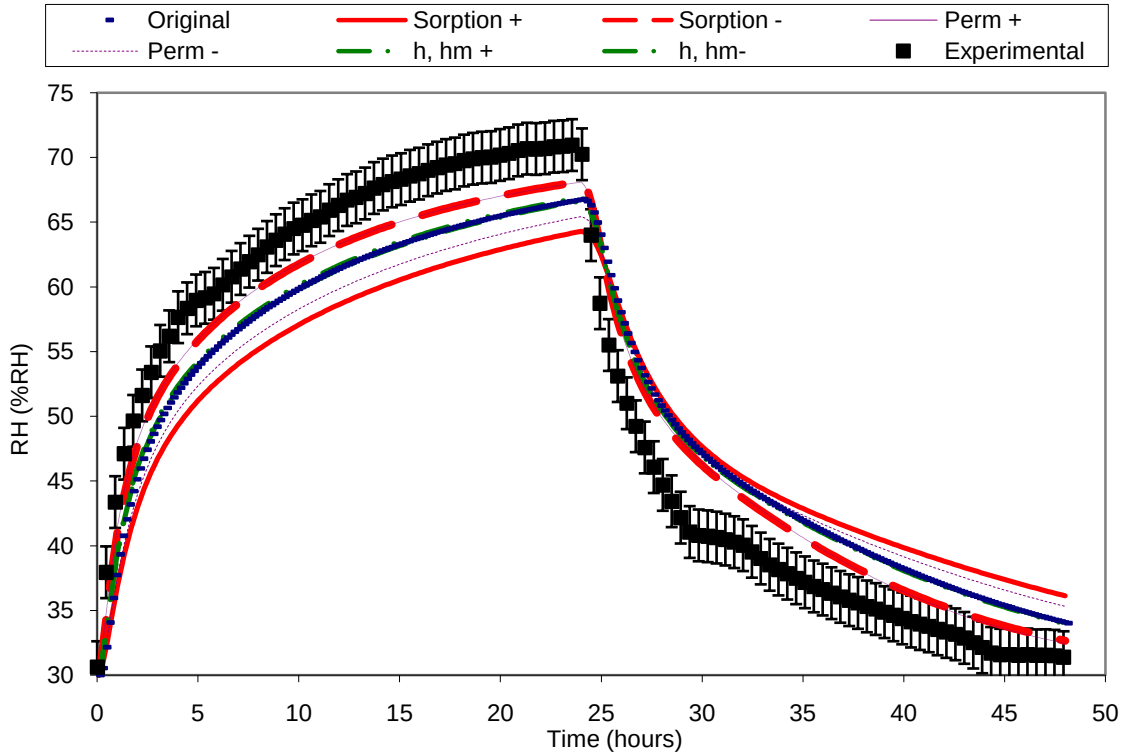

Figure 5.1: Simulated results of relative humidity at a depth of 12.5 mm in the uncoated gypsum bed showing the effects of changing the sorption and vapor permeability of the gypsum and the heat (h) and surface transfer (hm) coefficients.

The results in Figure 5.1 show that a simulated increase in vapor permeability or a decrease in sorption will result in an improved agreement with the experimentally measured relative humidity in the uncoated gypsum bed at a depth of 12.5 mm. A decrease in vapor permeability or increase in sorption will cause the difference between the experimental and numerical data to increase. The simulated results show little sensitivity to the change in transfer coefficients.

The sensitivity results of relative humidity are shown for the acrylic coated gypsum bed in Figure 5.2. Similar results to Figure 5.1 are seen when the sorption isotherm, vapor permeability and transfer coefficients are modified.

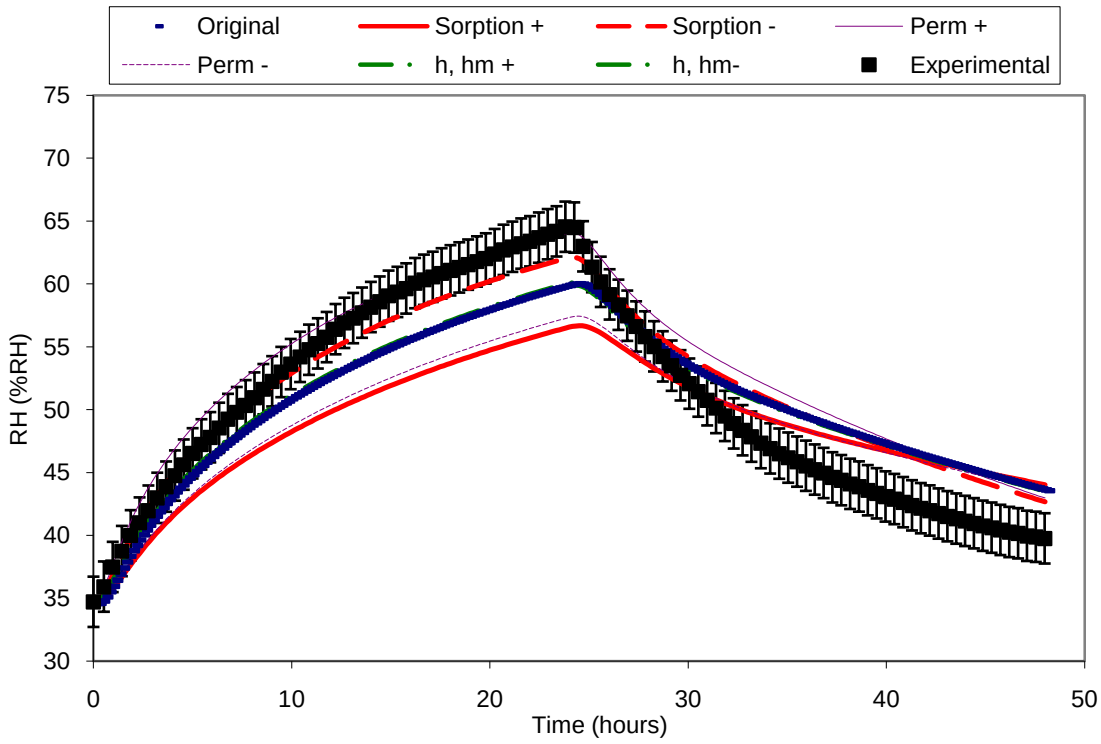

Figure 5.2: Simulated results of relative humidity at a depth of 12.5 mm in the acrylic coated gypsum bed showing the effects of changing the sorption and vapor permeability of the gypsum and the heat and surface transfer coefficients.

The sensitivity results of relative humidity at a depth of 12.5 mm in the latex coated gypsum bed are shown in Figure 5.3. The results parallel the trends seen in both the uncoated and acrylic coated cases.

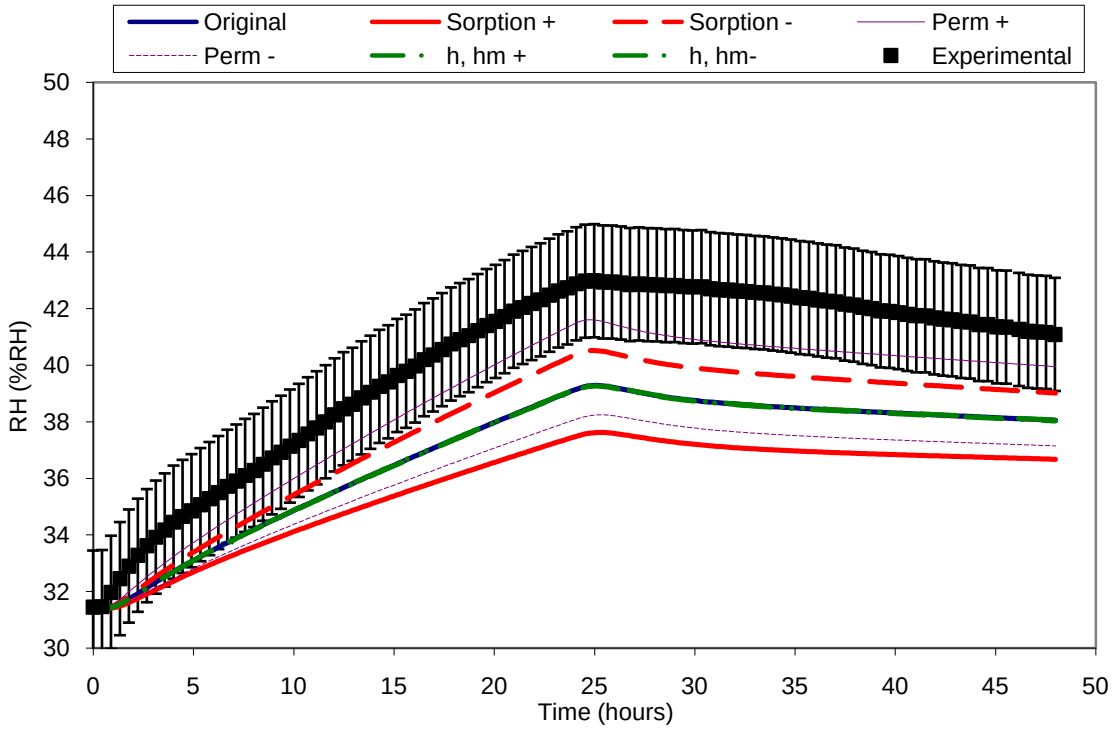

Figure 5.3: Simulated results of relative humidity at a depth of 12.5 mm in the latex coated gypsum bed showing the effects of changing the sorption and vapor permeability of the gypsum and the heat and surface transfer coefficients.

5.2 Hysteresis Study

One participant examined the effects of hysteresis on the uncoated gypsum bed. The results are shown in Figure 5.4. Details of the model can be found in Janssen [2002].

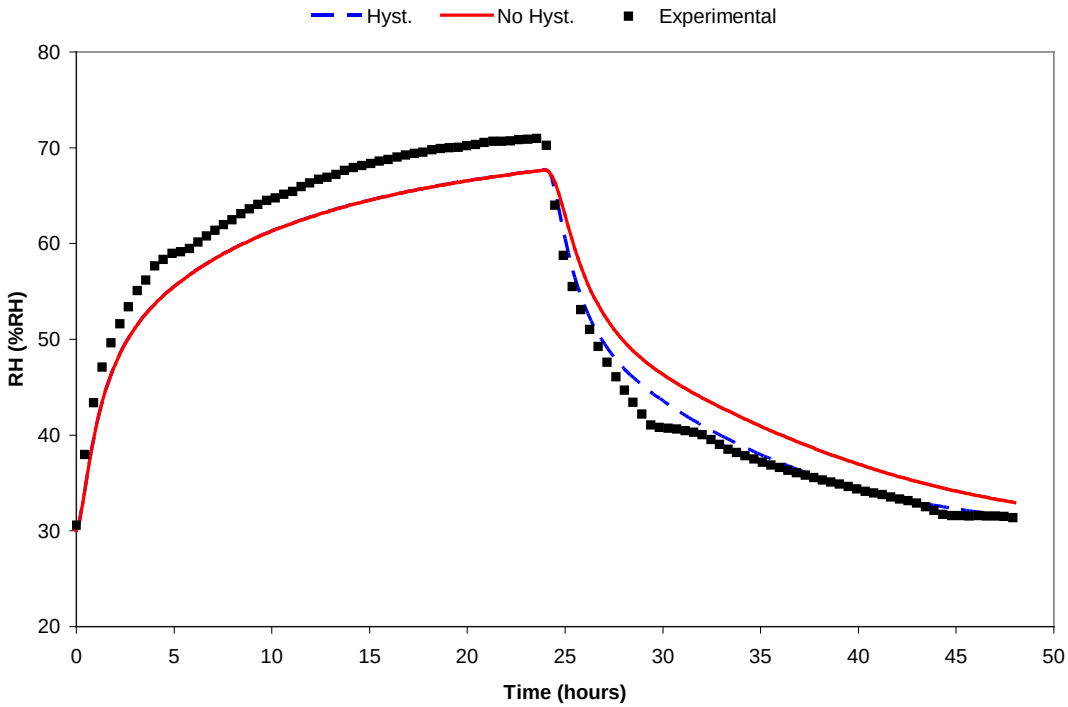

Figure 5.4: Experimental and simulated results showing the results when a hysteresis model is included in the simulation (uncoated gypsum bed).

The simulated results in Figure 5.4 show that the effects of the sorption isotherm hysteresis will improve the simulated relative humidity during a desorption loading compared to the case when no hysteresis is considered. The results are the same for the first 24 hours (adsorption phase) when hysteresis was and was not considered.

5.3 Summary of the Property and Hysteresis Study

If the same method of comparison presented in Chapter 4 is used to compare the sensitivity for all the cases, a better understanding of the results can be achieved. Figures 5.5 – 5.7 show the results of the sensitivity analysis for the uncoated, acrylic and the latex coated tests. The sensitivity results are not presented for the shorter test (Case 2) or the high flow rate test (Case 3), see Table 2.1, as the sensitivity results remain practically unchanged for all of the uncoated gypsum bed tests. In Figures 5.5 – 5.7, the

points indicate the original simulated change in relative humidity and the error bars show the minimum and maximum values corresponding to an increase or decrease in the material property, transfer coefficient or hysteresis model.

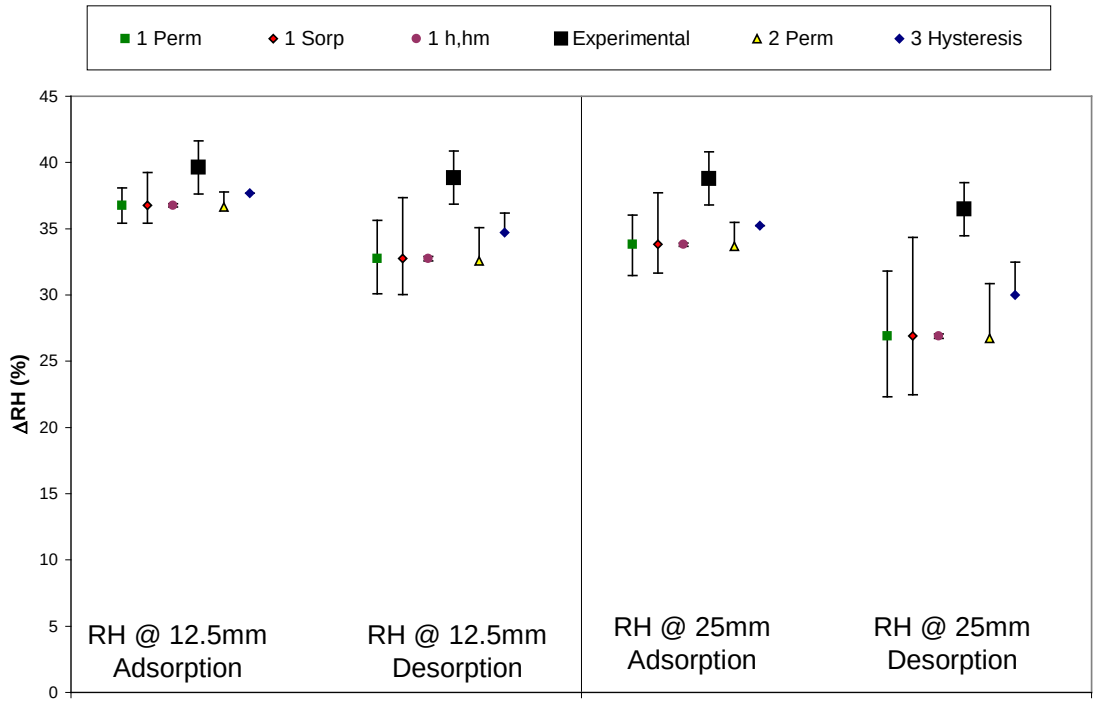

Figure 5.5: Simulated and the absolute sensitivity change of relative humidity in an uncoated gypsum bed, including the effects of hysteresis.

The sensitivity results in the uncoated bed, Figure 5.5, show that a change in the sorption isotherm of the gypsum boards will cause the largest change in the relative humidity. The ±10% change to the transfer coefficients had a very small effect on the simulated results at the two depths in the gypsum bed over the course of the test. When comparing the results of an increased vapor permeability of the gypsum bed, the results of participant 1 and 2 show a very similar change in simulated relative humidity, indicating the two codes have a similar sensitivity to vapor permeability changes. The

effect of hysteresis only had an effect during desorption loading and had a smaller effect when compared to the sensitivity of sorption or vapor permeability. The property changes had a greater effect during desorption loading than during the adsorption loading and a greater effect at a deeper depth in the gypsum bed.

Figure 5.6 shows the sensitivity study results for the acrylic coated gypsum bed.

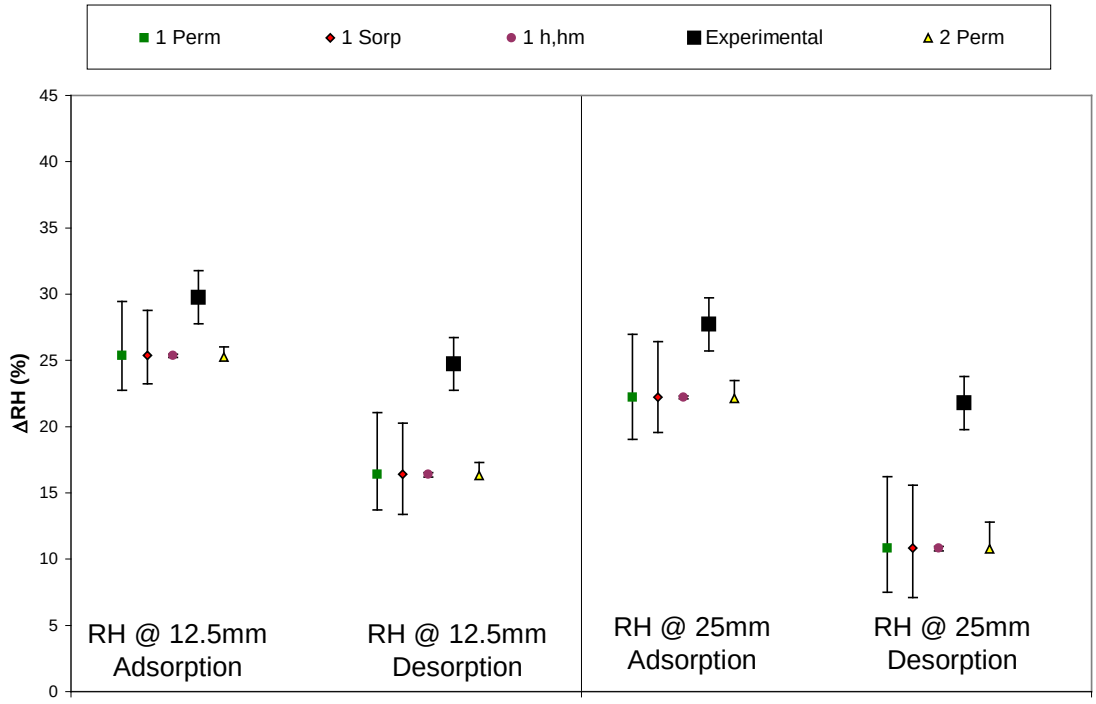

Figure 5.6: Simulated and sensitivity change of relative humidity in the acrylic coated gypsum bed.

When comparing the results in Figure 5.6, there is a noticeable difference between the results of the increased vapor permeability of the two participants' submittals. The results from Participant 1 include an increased vapor permeability of the paint, while the results of Participant 2 only include the increased vapor permeability of the gypsum boards. In the acrylic coated case, it appears that permeability has a larger effect than

sorption, unlike the uncoated case. Again the relative humidity sensitivity is more sensitive at deeper depths during desorption loading.

Figure 5.7 shows the sensitivity study results on the latex coated gypsum bed.

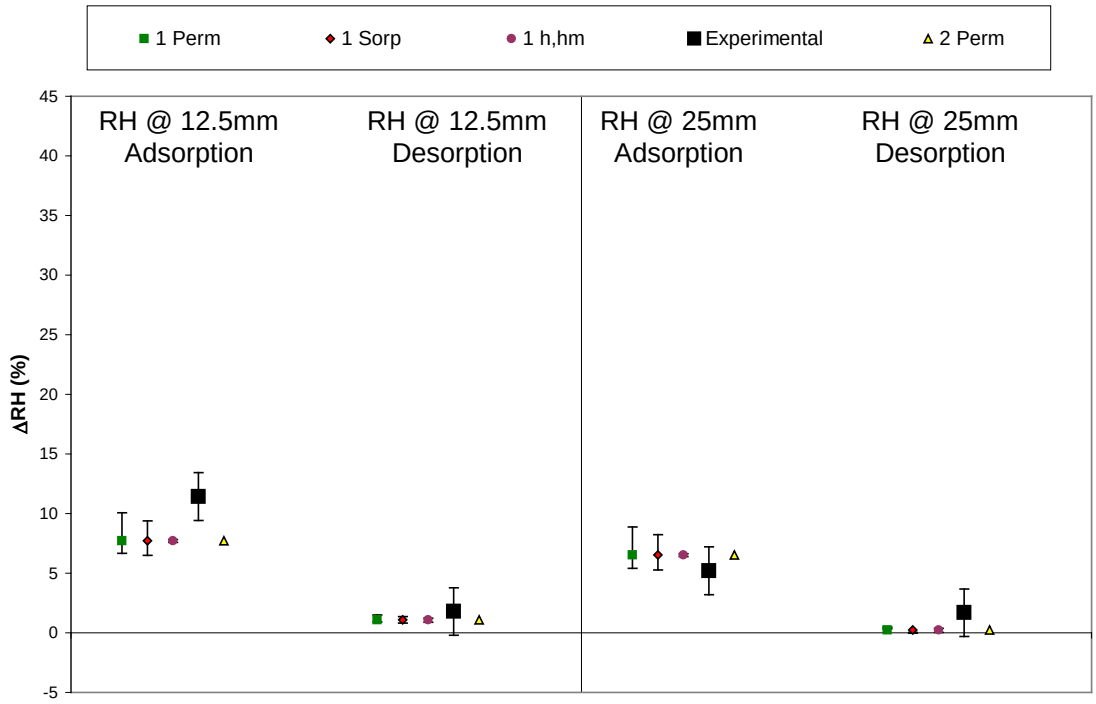

Figure 5.7: Absolute simulated and the sensitivity change of relative humidity in the latex coated gypsum bed.

The sensitivity results of relative humidity in the latex coated bed (Figure 5.7) show a slightly different trend than the results for the uncoated and acrylic coated bed (Figures 5.5 and 5.6). The vapor permeability results from Participant 1 show a much larger effect than the results of Participant 2 most likely due to the paint layer properties being adjusted as well as the gypsum bed's properties.

The effects of changing the properties on moisture accumulation were also examined. The results for the uncoated, acrylic and latex coated gypsum bed are provided in Figure 5.8.

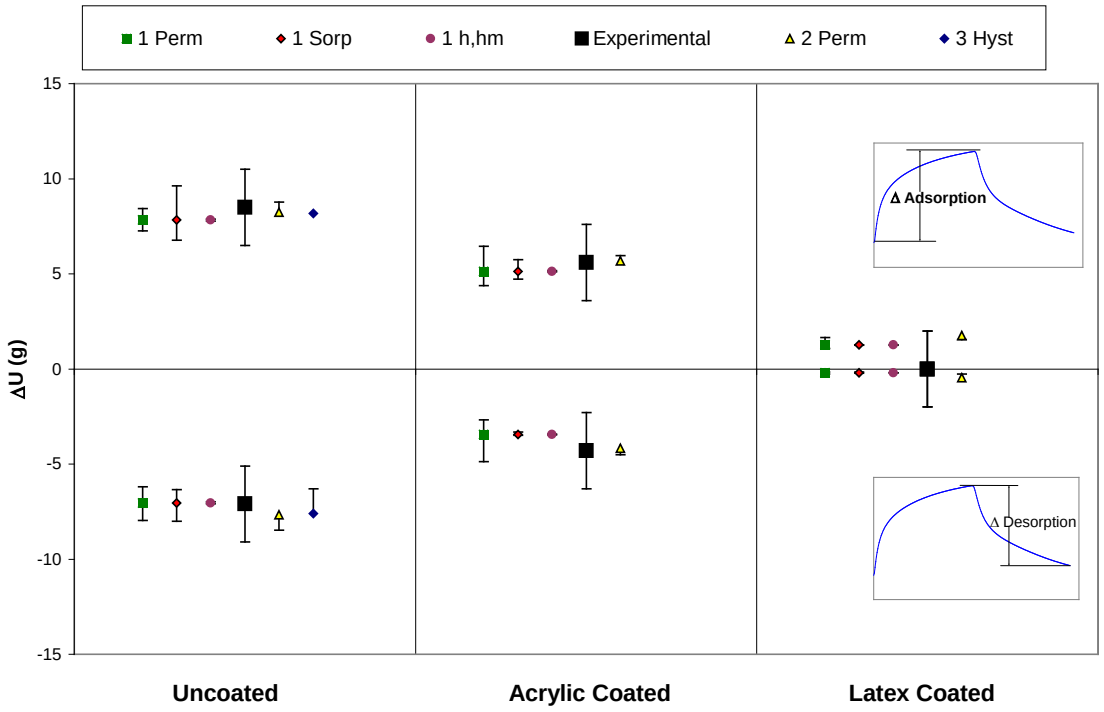

Figure 5.8: Results of the sensitivity analysis of moisture accumulation in the uncoated, acrylic and latex coated gypsum beds.

Similar to the sensitivity study results of the relative humidity simulations, the moisture accumulation is most affected by the sorption if uncoated and the vapour permeability when coated.

The results of the blind simulation agree with the experimental results well within the associated measurement uncertainty. The sensitivity analysis helped to determine which properties affected the moisture accumulation in the gypsum bed. The results in Figure 5.8 show that a change of ±10% to the transfer coefficients has little effect on the simulated results similar to the relative humidity sensitivity results. The sorption

isotherm has the largest effect on the simulated moisture accumulation in the uncoated gypsum bed while the vapor permeability has the largest effect on the simulated moisture accumulation in the coated beds.

5.4 Steady State Results

Three participants, Thermal Science Centre of Lyon, Slovak Academy of Science and Technical University of Denmark, submitted results for some or all three arrangements (Table 2.1) for the case of the bed being exposed to 100 repeated cycles, or at steady state conditions. The buffering resistance of the paint can be examined numerically from simulations of this nature. In this section, the steady state results are presented for the uncoated, acrylic coated and latex coated gypsum beds after 100 cycles. Figure 5.9 shows the relative humidity results at a depth of 12.5 mm in the uncoated gypsum bed.

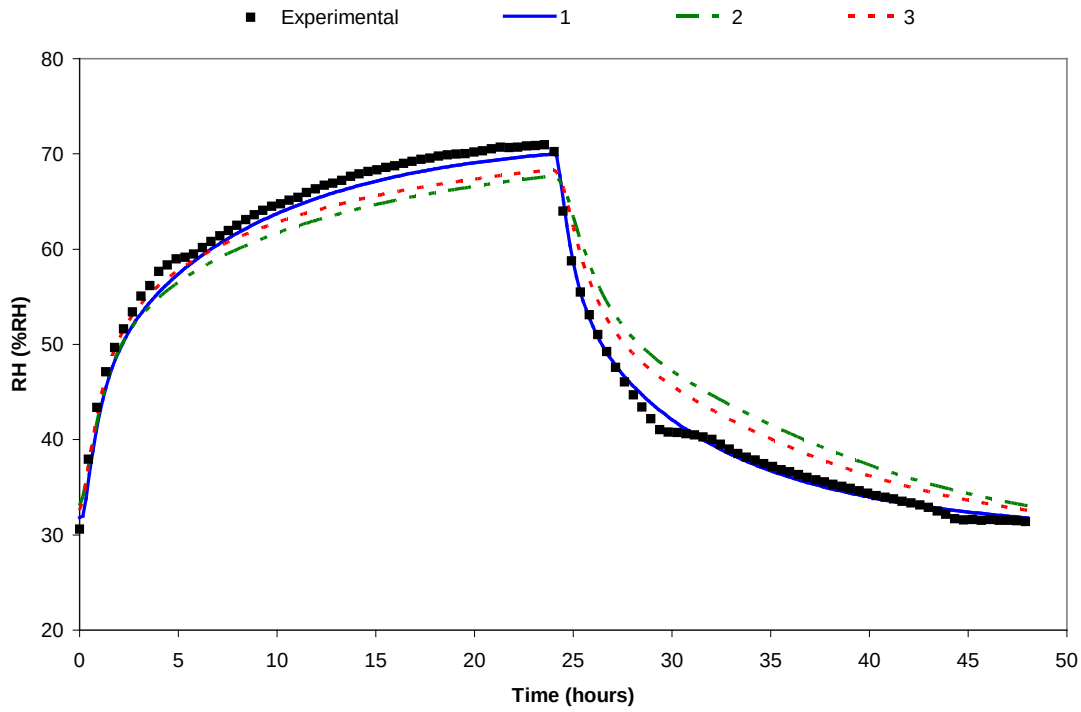

Figure 5.9: Simulated steady state results and single cycle experimental measurements of relative humidity at a depth of 12.5 mm in an uncoated gypsum bed.

Two of the simulations in Figure 5.9 (labeled 1 and 3) included hysteresis in the heat and moisture transfer models of the uncoated gypsum bed. The results of simulation 1 are almost identical to the results of the single cycle experimental measurements. The method of conditioning the gypsum bed for the experiments induced the type of cyclical loading simulated which could be the major cause of the similar results. The gypsum boards were conditioned from 70% to 30% RH before a new test was carried out. Due to hysteresis in the sorption isotherm (Appendix A), the moisture content of the gypsum may have been higher than expected at the beginning of the test. If the gypsum bed was allowed to condition to a relative humidity lower than 30% RH before it was initially conditioned to 30% RH, the boards would have been in a

state of adsorption instead of desorption and the simulated steady state results might differ from the experimental measurements.

Only one participant, Thermal Science Centre of Lyon, submitted simulation results after 100 cycles in the acrylic coated gypsum bed. The results of the relative humidity at depths of 12.5 and 25 mm in the acrylic coated bed are shown in Figure 5.10.

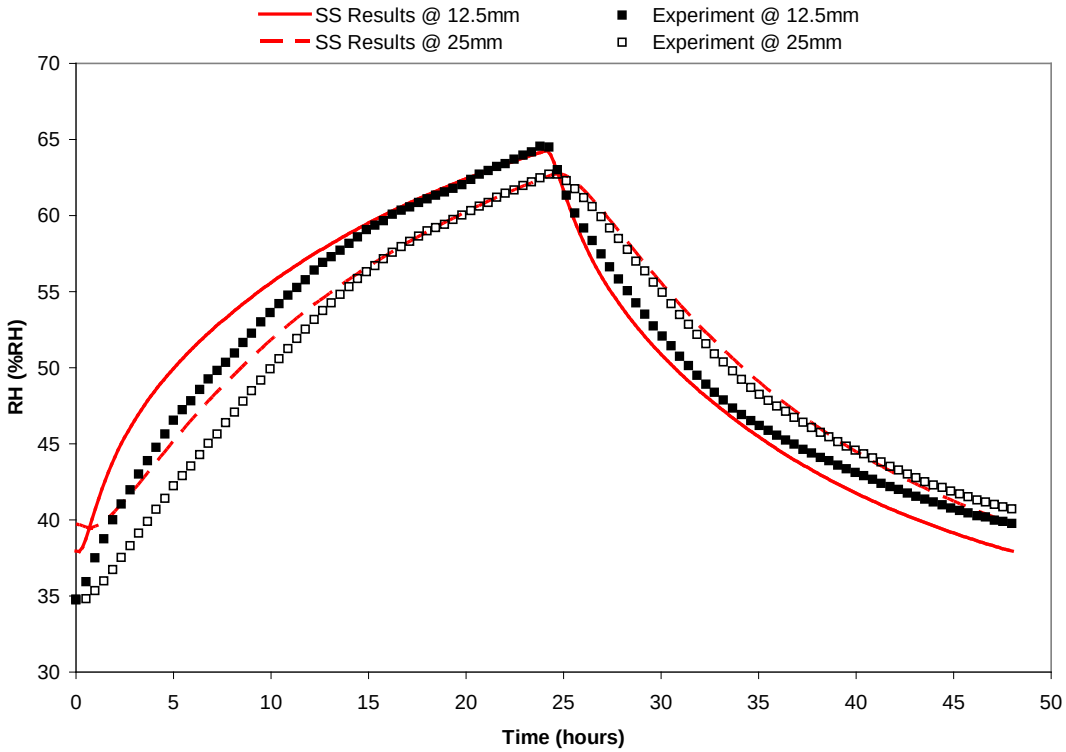

Figure 5.10: Simulated steady state results after 100 cycles and experimental measurements of one cycle for relative humidity in the acrylic coated gypsum bed.

The acrylic paint allows significant moisture transfer as shown in Figure 5.10.

Two participants (Thermal Science Centre of Lyon and Slovak Academy of Science) submitted results for the latex coated gypsum bed. The steady state relative humidity results are shown for the latex coated gypsum bed in Figure 5.11.

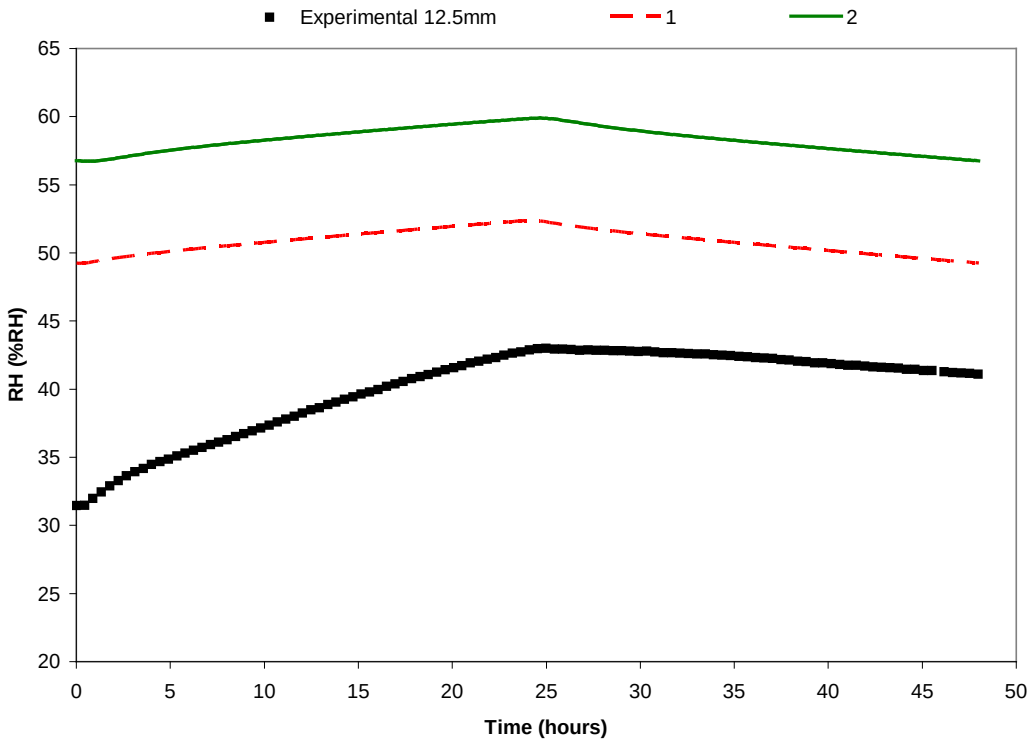

Figure 5.11: Relative humidity simulated after 100 cycles and measured for one cycle at a depth of 12.5 mm in the latex coated gypsum bed.

The latex paint provides a great barrier to moisture transfer as shown in the simulated results of Figure 5.11. The relative humidity in the gypsum bed is only shown at a depth of 12.5 mm in the gypsum bed. The simulated and measured relative humidity is the same at 25 mm due to the paint allowing very little moisture transfer and the bed reaching equilibrium. The relative humidity in the gypsum bed increases from the first cycle significantly as the gypsum desorbs much less moisture than it adsorbs, with the major resistance to moisture transfer being the latex paint coating. Somewhere between the first and hundredth cycle, the relative humidity change in the adsorption equals the change in the desorption loading.

The mass accumulation and removal in the gypsum bed could be considered a 24 hour moisture buffering simulation after 100 cycles. The results can help interpret how

much moisture the gypsum boards could buffer if uncoated or coated with acrylic or latex paint. The results of the steady state moisture accumulation and removal for the uncoated and coated gypsum beds are shown in Figure 5.12.

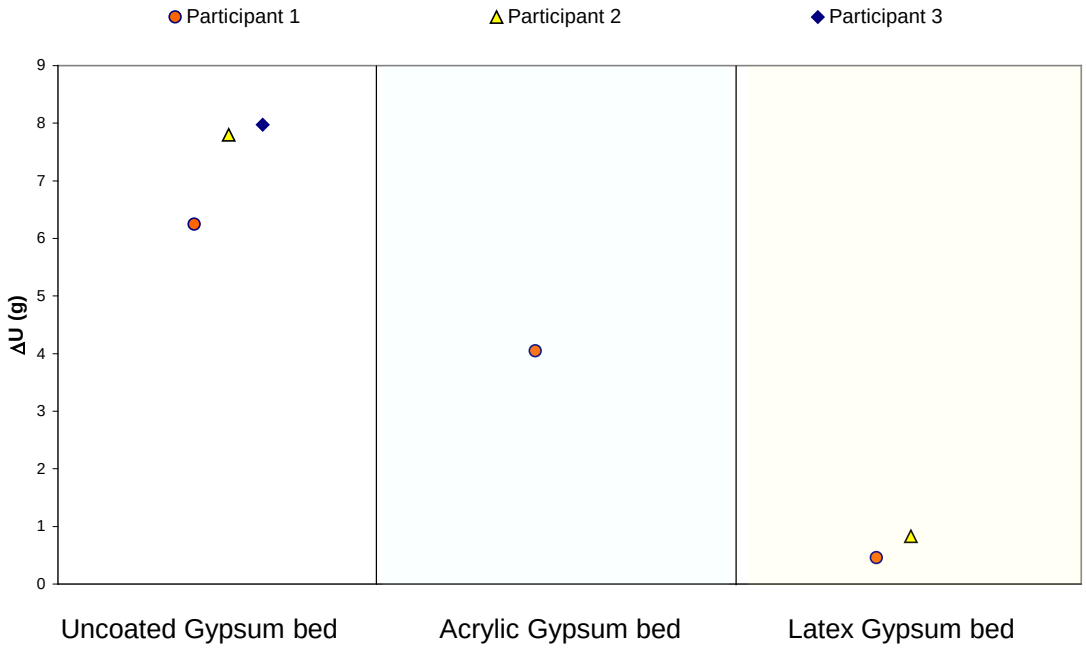

Figure 5.12: Moisture accumulation/desorption simulated after 100 cycles for an uncoated, acrylic coated and latex coated gypsum bed.

The results in Figure 5.12 show that the latex coated gypsum bed allows significantly less moisture accumulation/removal than the acrylic and uncoated gypsum beds.

5.5 Interaction of Different Sensitivity Parameters

In Sections 5.1 to 5.3, the sensitivity analysis examined the effect of individual parameters, while this section will examine the sensitivity if multiple parameters are changed simultaneously. One participant submitted results that improved the agreement

between the simulated and measured results by changing multiple material properties, within their given uncertainty bounds from the round robin testing (Appendix A). The "fine-tuned" simulation results of the uncoated gypsum bed used an increased vapor permeability of the uncertainty bound and a sorption value that was decreased by half of the uncertainty bound. The uncertainty bounds refer to the range of the measured values for the sorption and vapour permeability data for the materials from the round-robin testing [Roels 2008a]. The results of the uncoated case are presented in Figures 5.13 and 5.14.

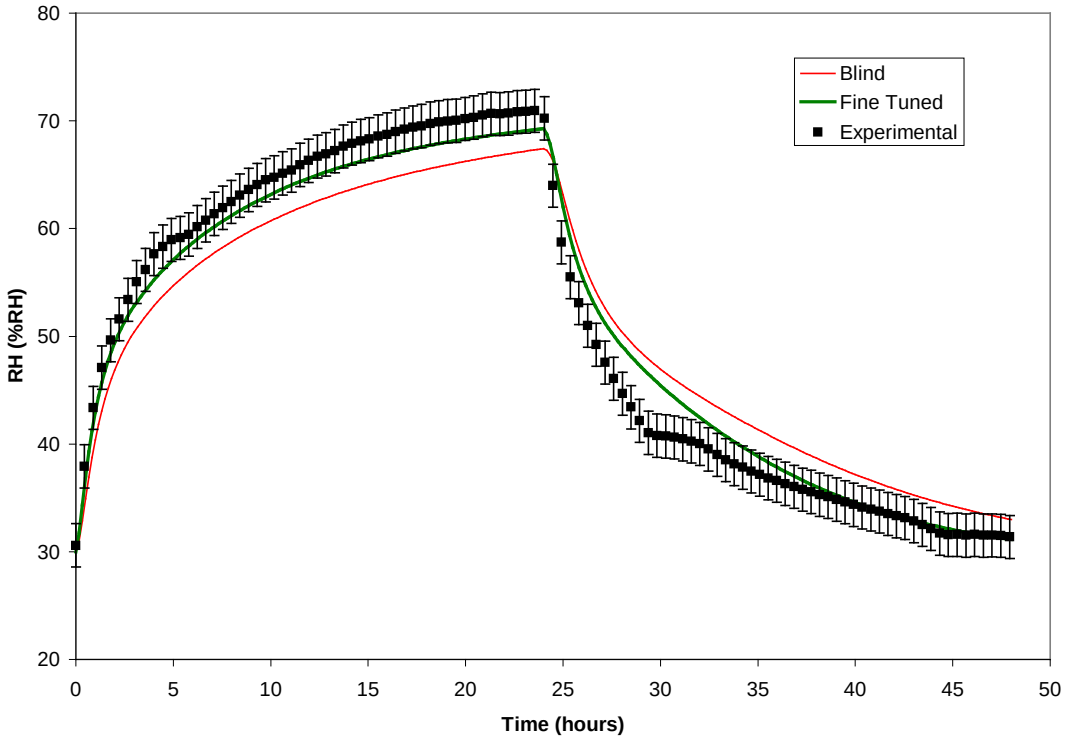

Figure 5.13: Fine tuned and blind simulations compared to the experimental measurements of relative humidity at a depth of 12.5 mm in the uncoated gypsum bed.

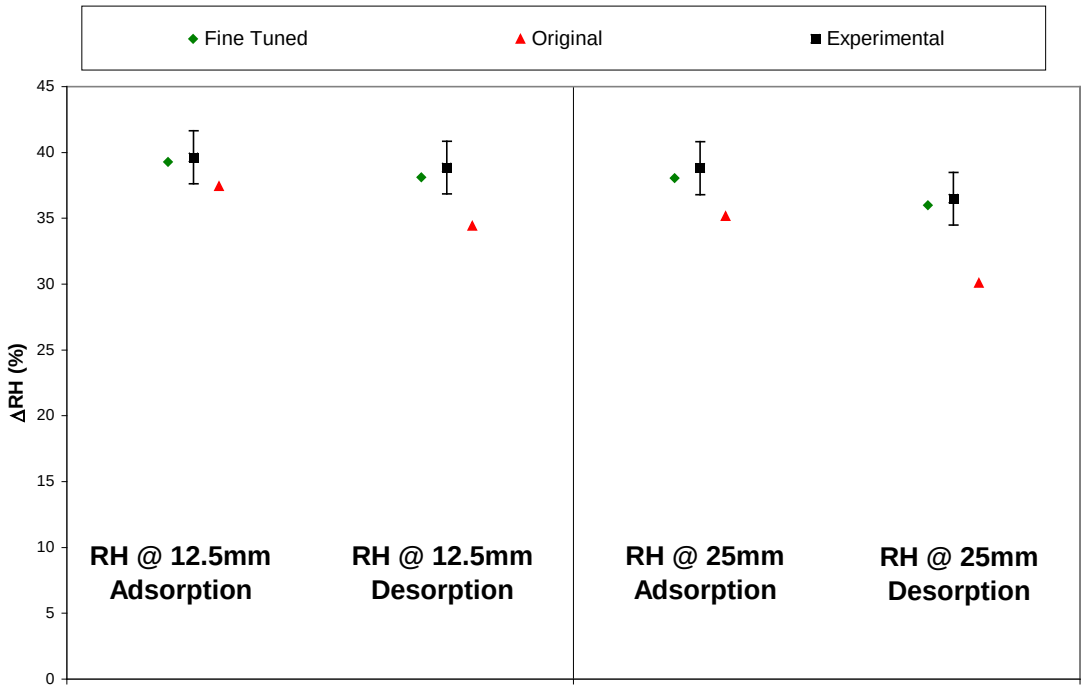

Figure 5.14: Fine tuned relative humidity results of the uncoated gypsum bed.

The "fine-tuned" results of the acrylic coated gypsum bed are shown in Figures 5.15 and 5.16. The "fine-tuned" results are developed using the same gypsum properties as in the uncoated case with no further change to the paint material properties.

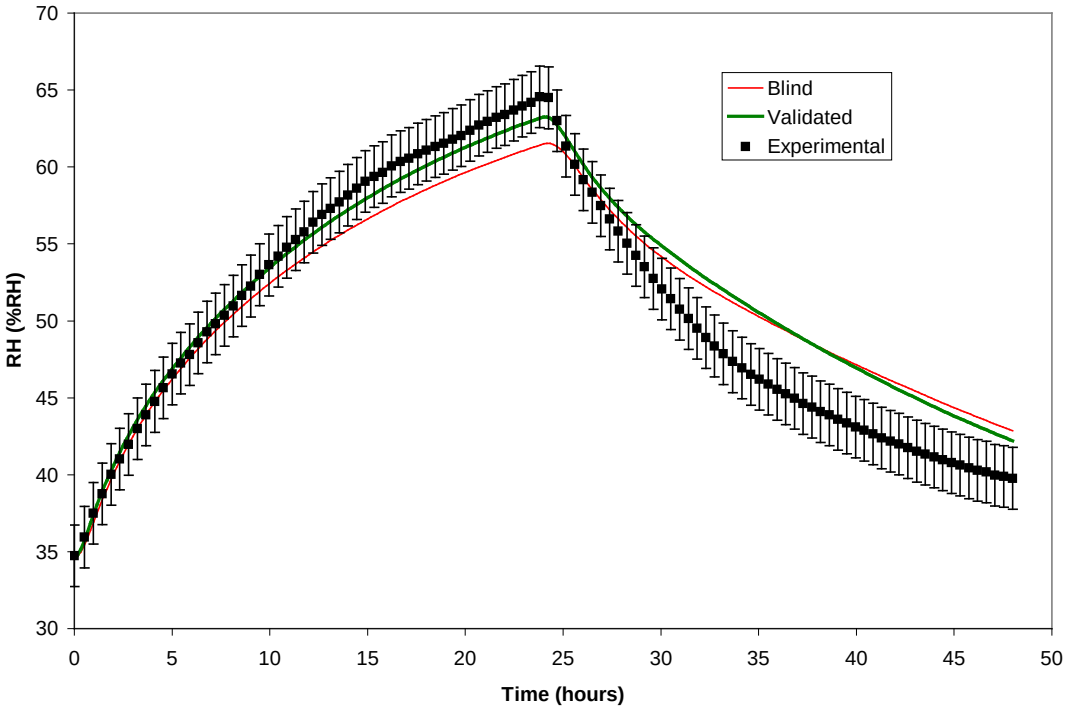

Figure 5.15: Fine tuned and blind simulations compared to the experimental measurements of relative humidity at a depth of 12.5 mm in the acrylic coated gypsum bed.

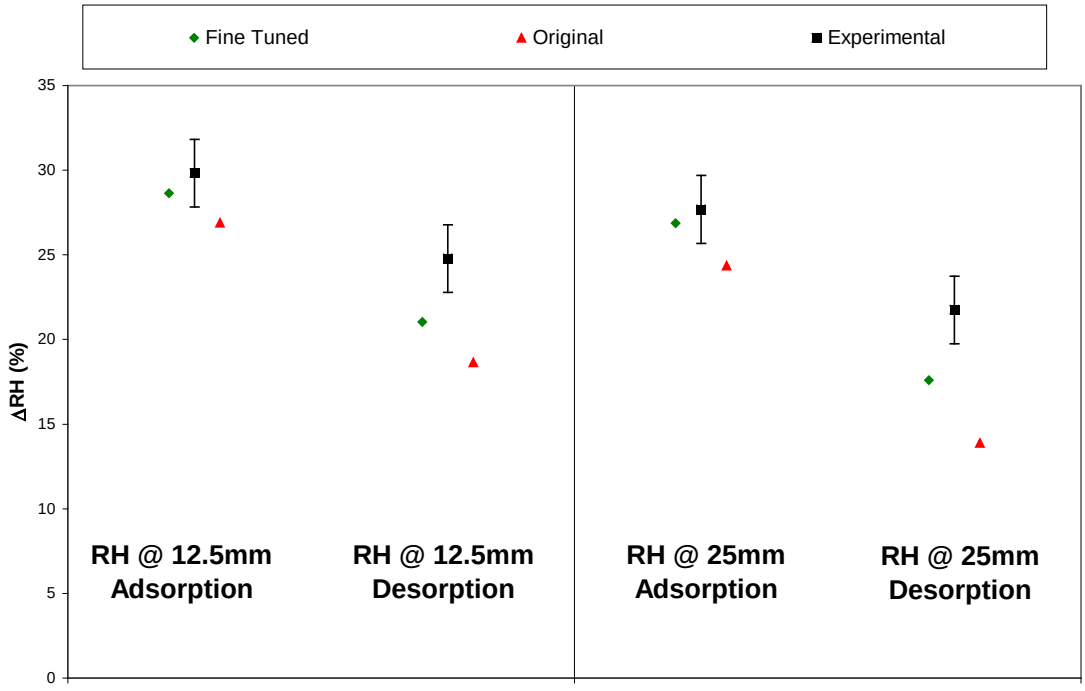

Figure 5.16: Fine tuned relative humidity results of the acrylic coated gypsum bed.

The “fine-tuned” results of the acrylic coated gypsum bed agree quite well with the experimental results at a depth of 12.5 mm as seen in Figure 5.16. There is a larger difference between the “fine-tuned” simulated and experimental relative humidity change in the acrylic coated gypsum bed during desorption loading than during the adsorption loading, indicating an influence of the paint. The simulated results compare very well with the experimental measurements for the uncoated case.

The improved simulation results for the latex coated gypsum bed are shown in Figures 5.17 and 5.18. The further validated results were developed by using the same gypsum properties as in the uncoated “fine-tuned” sensitivity study and increasing the vapor permeability of the latex paint by half the uncertainty bound from the round robin testing.

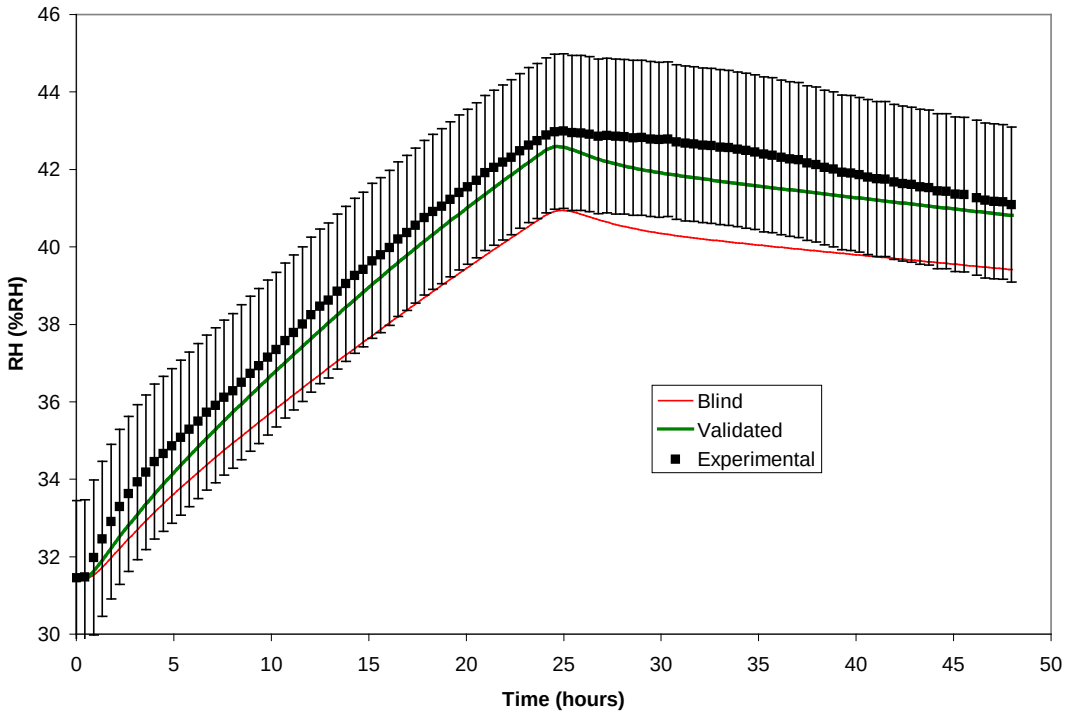

Figure 5.17: Fine tuned and blind simulations compared to the experimental measurements of relative humidity at a depth of 12.5 mm in the latex coated gypsum bed.

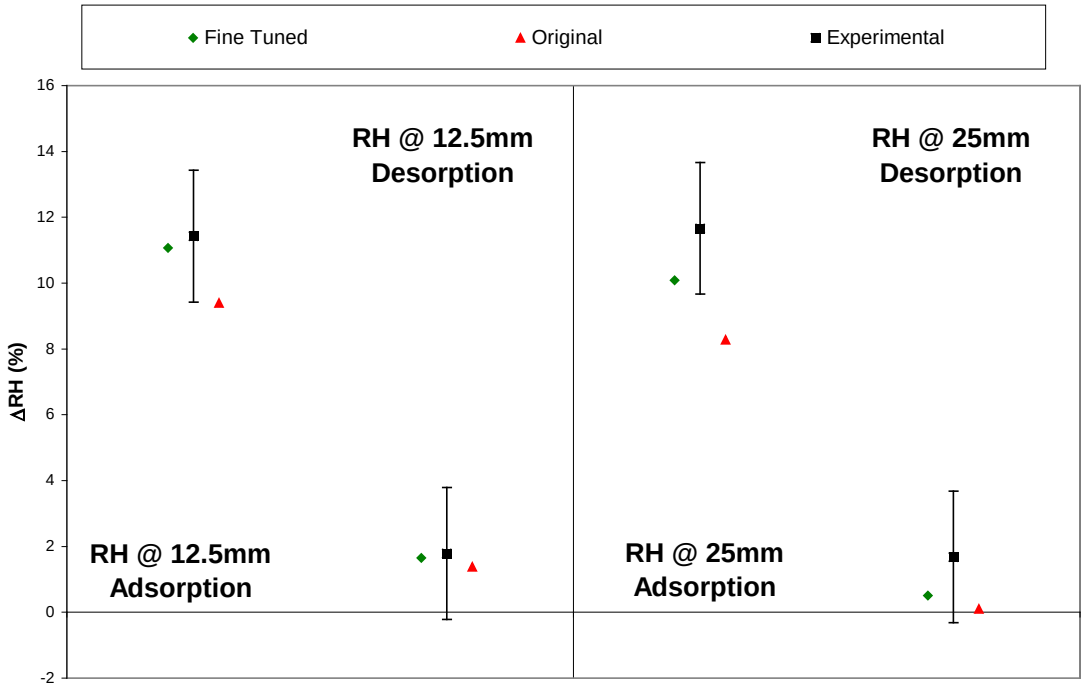

Figure 5.18: Fine tuned relative humidity results for the latex coated gypsum bed.

The results of fine tuned relative humidity in the latex coated gypsum bed are in good agreement with the experimental data and within the measurement uncertainty. The problem seen during the desorption loading of the acrylic simulation is not seen with the latex paint due to its very small desorption relative humidity change.

Chapter 6

Conclusions and Recommendations

The experimental data obtained in this thesis validated numerous numerical models. The modelers were supplied with very tight constraints to simulate in the "blind" section of the validation exercise and the results were an overall success. The participants of the validation exercise simulated 1-D heat and moisture transfer in a gypsum bed subject to constant surface transfer coefficients for a step change in relative humidity, from 30% to 70% and back to 30%, at a constant temperature of 23°C. The relative humidity and temperature at two depths in a gypsum bed were measured for five different cases. The first case was the base test run with 24 hours between step changes, the second examined a shorter test length (8 hour between step changes), the third examined a higher flow rate (turbulent) above the gypsum bed and the fourth and fifth test examined the effect of surface coatings, acrylic and latex paint respectively. The testing produced confident experimental data for future numerical model validation and for benchmarking other 1-D heat and moisture simulations.

The results of the numerical simulations were close to the experimental measurements for the blind simulation. The eight 1-D vapor diffusion models used for the exercise produced very similar results for relative humidity and moisture accumulation when compared to each other, due mostly to the tight constraints provided to the participants, which disallowed too many creative inputs which could have caused

large differences. The simulations also compared well with the experimental measurements, but there was a need for a sensitivity and hysteresis study to better understand the effects of material properties and transfer coefficients on the simulated results. The temperature in the gypsum bed changed only slightly during the test and the simulated temperature results followed a similar trend. The focus of validation was placed on the relative humidity and moisture accumulation.

A sensitivity study was performed to determine the effects of the sorption isotherm, vapor permeability and transfer coefficients on the simulated relative humidity and moisture accumulation. From the round robin material testing of the coated and uncoated gypsum performed by Roels [2008a], the participants were supplied with the uncertainty bounds of the measured properties as the upper and lower bands to use in the sensitivity analysis. The participants also adjusted the transfer coefficients by ±10% to determine their influence on the results. The results presented in Chapter 5, show that gypsum sorption had the largest effect on the simulated relative humidity and moisture accumulation in the uncoated gypsum bed. The vapor permeability had a larger effect than sorption on the simulated relative humidity and moisture accumulation results in the coated gypsum beds. The transfer coefficients studied in the sensitivity analysis showed little influence on the relative humidity or moisture accumulation results. An accurate determination of the sorption isotherm and vapor permeability, of both the gypsum and coatings, will assist with an accurate simulation, as the material properties affected the simulation results substantially.

Hysteresis of the gypsum boards was considered to be one material characteristic that would have a large impact on the simulated relative humidity and moisture accumulation. A hysteresis model was incorporated into an existing 1-D heat and mass

transfer model to study hysteresis in the gypsum bed. The simulation showed that including hysteresis will improve the results during desorption loading but the influence on the results was not as large as the influence of sorption and vapor permeability.

The paint layer was simulated by two different methods. One method included the paint in the surface transfer coefficient while the other treated the paint as a separate porous layer with its own material properties. Incorporating the paint into the surface transfer coefficient proved to be a very accurate method of simulation with results that were comparable to treating the paint as a separate porous layer.

When coating the gypsum bed, acrylic paint allowed substantially more moisture transfer than latex paint.

The most important considerations when simulating 1-D heat and moisture transfer in a gypsum wall would be the type of surface coating applied to the gypsum. Of the parameters studied in this exercise, the surface coating had the largest effect on the moisture transfer in the gypsum. The next most important issue is accurate sorption isotherm and vapor permeability data. These two material properties greatly affect the simulated relative humidity and moisture accumulation. In the testing performed, the top of the gypsum bed was exposed to a convective boundary layer. Changing the values of the heat and mass transfer coefficient by ±10% shows little influence on the measured and simulated results of relative humidity and moisture accumulation in the gypsum bed.

An adjustment of multiple properties simultaneously resulted in better agreement between the measured and simulated values. These “fine-tuned” simulation results show that the material properties can be adjusted inside their measured uncertainty bounds to yield relative humidity results within the relative humidity measurement uncertainty.

6.1 Recommendations

The measurement of the mass of the gypsum bed requires a very accurate instrument, due to the small change in mass during the test. The uncertainty in the measurement of the moisture accumulation was in the same range as the actual change, especially for the latex coated bed testing. A more accurate measurement of the mass of the bed would be recommended for further testing of this type.

The data obtained for this work included extensive measurements of material properties of gypsum and the acrylic and latex paint used. More extensive material property databases are required for future heat and moisture transfer studies. These will be useful to building designers incorporating passive heat and moisture control techniques.

The hygric response of gypsum boards to a step change in relative humidity was determined. Testing using the TMT facility at the University of Saskatchewan has produced accurate data on the hygric response of numerous building materials. The testing of a wall assembly could be the next phase of testing. This would produce data that could be used for further improvements to numerical models.

The results presented in this thesis show that an acrylic painted gypsum wall could be used for passive moisture control in buildings. One problem that could be encountered if buildings are designed to incorporate this type of wall/ceiling passive moisture control is occupants modifying the space, by repainting. If paint with a large resistance to moisture transfer is used, nearly all moisture control could be lost. Occupancy education would help with this issue.

References

Abuku M, Janssen H, Roels S, 2008, "Impact of wind-driven rain on historic brick wall buildings in a moderately cold and humid climate: Numerical analyses of mould growth risk, indoor climate and energy consumption", *Energy and Buildings*, Article in Press

Ampofo F, Karayiannis T, 2003, "Experimental benchmark data for turbulent natural convection in an air filled square cavity", *International Journal of Heat and Mass Transfer*, 46: 3551-3572

ASHRAE, 2001. Fundamentals Handbook, Atlanta, GA

ASTM E 104, 1985. "Maintaining Constant Relative Humidity by Means of Aqueous Solutions", *American Society for Testing and Materials*, West Conshohocken, PA

Belarbi R, Qin M, Aït-Mokhtar A, Nilsson L, 2007, "Experimental and theoretical investigation of non-isothermal transfer in hygroscopic building materials", *Energy and Buildings*, Article in Press

Blocken B, Roels S, Carmeliet J, 2007, "A combined CFD-HAM approach for wind-driven rain on building facades", *Journal of Wind Engineering and Industrial Aerodynamics*, 95: 585-607

Clarke J, Johnstone, C, Kelly N, McLean R, Anderson J, Rowan N, Smith J, 1998, "A technique for the prediction of the conditions leading to mould growth in buildings", *Building and Environment*, 34: 515-521

Cunningham M, 1990. "Modeling of Moisture Transfer in Structure-2. A Comparison of a Numerical Model, an Analytical Model and Some Experiment Results", *Building and Environment*, 25-2: 85-94

Dalgliesh W, Surry D, 2003, "BLWT, CFD and HAM modeling vs. the real world: Bridging the gaps with full-scale measurements", *Journal of Wind Engineering and Industrial Aerodynamics* 91: 1651-1669

Gupta S, Khare M, Goyal R, 2007, "Sick building syndrome-A case study in a multistory centrally air-conditioned building in Delhi City", *Building and Environment*, 42: 2797-2809

Hagentoft C-E, Kalagasidis A, Adl-Zarrabi B, Roels S, Carmeliet J, Hens H, Grunewald J, Funk M, Becker R, Shamir D, Adan O, Brocken H, Kumaran K, Diebbar R, 2004, "Assesment Method of Numerical Prediction Models for Combined Heat, Air and Moisture Transfer in Building Components: Benchmarks for One-Dimensional Cases", *Journal of Thermal Envelope and Building Science* , 27 (4): 327-352

Hirano T, Kato S, Murakami S, Ikaga T, Shiraishi Y, 2005, "A study on a porous residential building model in hot and humid regions: Part 1 – the natural ventilation performance and the cooling load reduction effect of the building model", *Building and Environment*, 41: 21-32

Holm A, 2008, "Volume 4: Applications: Indoor Environment, Energy, Durability", *IEA/ECBCS-Annex 41 Whole Building Heat, Air and Moisture Response*:*MOIST-ENG Final Report*, 177pp.

Hu H, Zhang Y, Wang X, Little J, 2007, "An analytical mass transfer model for predicting VOC emissions from multi-layered building materials with convective surfaces on both sides", *International Journal of Heat and Mass Transfer*, 50: 2069-2077

Iskra C, Simonson C, 2007, "Convective mass transfer coefficient for a hydrodynamically developed airflow in a short rectangular duct", *International Journal of Heat and Mass Transfer*, 50: 2376-2393.

Iskra C, 2007, "Convective mass transfer between a hydrodynamically developed airflow and liquid water with and without a vapor permeable membrane", MSc Thesis, University of Saskatchewan, Canada

Janssen H. 2002. "The influence of soil moisture transfer on building heat loss via the ground", Ph.D. thesis, Department of Civil Engineering, Katholieke Universiteit Leuven, Belgium

Janssen H, Blocken B, Carmeliet J, 2007, "Conservative modelling of the moisture and heat transfer in building components under atmospheric excitation", *International Journal of Heat and Mass Transfer*, 50:1128-1140

Kalagasidis A, 2004, "HAM-Tools. An Integrated Simulation Tool for Heat, Air and Moisture Transfer Analyses in Building Physics", Doctoral thesis, Chalmers University of Technology, Sweden

Kalagasidis A, Weitsmann P, Nielson T, Peuhkuri R, Hagentoft C-E, Rode C, 2006, "The International Building Physics Toolbox in Simulink", *Energy and Buildings*, 39: 665-674

Kumaran K, Sanders C, 2008, "Volume 3: Boundary Conditions and Whole Building HAM Analysis", *Annex 41 MOIST-ENG Final Report*, 235pp.

Kunzel, H. M, Kiessl, K, 1996, "Calculation of heat and moisture transfer in exposed building components", *International Journal of Heat and Mass Transfer*, 40: 159-167

Kwiatkowski J., Feret K., Woloszyn M., Roux J. J, 2007, "Predicting indoor relative humidity using buildings simulation tools", *The 6th International Conference on Indoor*

Air Quality, Ventilation & Energy Conservation in Buildings, 28-31 October 2007, Sendai, Japan.

Kwiatkowski J., Woloszyn M., Roux J. J, 2007, "Modelling of hysteresis influence on mass transfer in building materials", *The XIth Polish Scientific-Technical Conference, Building Physics in Theory and Practice Lodz*, 19-22 June 2007, Slok, Poland

Li Q, Rao J, Fazio P, 2008, "Development of HAM tool for building envelope design", *Building and Environment*, Article in Press

Lucas F, Adelard L, Garde F, Boyer H, 2001, "Study of moisture in buildings for hot humid climates", *Energy and Buildings*, 34: 345-355

Mendes N, Winkelmann F, Lamberts R, Philippi P, 2002, "Moisture effects on conduction loads", *Energy and Buildings*, 35: 631-644

Neale A, Personal communications with A. Neale, October 2006.

Neuner R, Seidel H-J, 2006, "Adaptation of office workers to a new building – Impaired well being as part of the sick-building-syndrome", *International Journal of Hygiene and Environmental Health*, 209:367-375

Nielsen K, Holm G, Uttrup L, Nielsen P, 2004, "Mould growth on building materials under low water activities. Influence of humidity and temperature on fungal growth and secondary metabolism", *International Biodeterioration and Biodegradation*, 54: 325-336

Ochs F, Heidemann W, Müller-Steinhagen H, 2007, "Effective thermal conductivity of moistened insulation materials as a function of temperature", *International Journal of Heat and Mass Transfer*, 51: 539-552

Olutimayin S, 2004, "Vapor Boundary Layer Growth During Transient Heat and Moisture Transfer in Cellulose Insulation", MSc Thesis, University of Saskatchewan, Canada

Osanyintola O, Simonson C, 2006, "Moisture buffering capacity of hygroscopic building materials: Experimental facilities and energy impact", *Energy and Buildings*, 38: 1270-1282

Pasanen A-L, Kasanen J-P, Rautiala S, Ikäheimo M, Rantamäki J, Kääriäinen H, Kallioski P, 2000, "Fungal growth and survival in building materials under fluctuating moisture and temperature conditions", *International Biodeterioration and Biodegradation*, 46: 117-127

Perschk A, Meinhold U, 2007, "Ein Modell zur hygro-thermischen Gebäude simulation mit Hilfe der Kopplung von Zonen und Feldmodell". *Zeitschrift, Bauphysik* 29. (2007)

Ernst & Sohn Verlag für Architektur und technische Wissenschaften GmbH & Co. DELPHIN4 - Numerical Simulation of Coupled Heat, Moisture and SaltTransport Theoretical Fundamentals and demo versions available: Institute of Building Climatology: http://www.bauklimatik-dresden.de

Peuhkuri R and Rode C, 2005. "Using Dynamic Moisture Loading Tests for Determination of Moisture Buffer Value", *Report A41-T2-Dk-05-1, IEA/ECBCS-Annex 41 Whole Building Heat, Air and Moisture Response*

Qin M, Belarbi R, Aït-Mokhtar A, Seigneurin A, 2005, "An analytical method to calculate the coupled heat and moisture transfer in building materials", *International Communications in Heat and Mass Transfer*, 33: 39-48

Rode C, 1990, "Transient Calculation of Moisture Migration Using a Simplified Description of Hysteresis in the Sorption Isotherms", *Proc. Building Physics In the Nordic Countries*, Trodheim, Norway.

Rode C, Grau K, 2008, "Moisture Buffering and its Consequences in Whole Building Hygrothermal Modelling", *Journal of Building Physics*, 31 (4): 333-360

Roels S, Vandersteen K, Carmeliet J, 2002, "Measuring and simulating moisture uptake in a fractured porous medium", *Advances in Water Resources*, 26: 237-246

Roels S, Moonen P, Proft K, Carmeliet J, 2005, "A coupled discrete-continuum approach to simulate moisture effects on damage processes in porous materials", *Computer methods in applied mechanics and engineering*, 195:7139-7153

Roels S, Janssen H, 2006, "A comparison of the Nordtest and Japanese Test Methods for the Moisture Buffering Performance of Building Materials", *Journal of Building Physics*, 30(2): 137-161

Roels S, 2008a, "Round Robin Testing", *IEA/ECBCS-Annex 41 Whole Building Heat, Air and Moisture Response: Whole Building Heat, Air and Moisture Response:MOIST-ENG Final Report*, pp17-70

Roels S, 2008b, "Volume 2: Experimental Analysis of Moisture Buffering", *Annex 41 IEA/ECBCS-Annex 41: Whole Building Heat, Air and Moisture Response:MOIST-ENG Final Report*, 173pp.

Simonson C, Salonvaara M, Ojanen T, 2002, "The effect of structures on indoor air humidity – possibility to improve comfort and perceived air quality", *Indoor Air*, 12: 1-9

Steeman H, 2009, "Modelling Local Hygrothermal Interaction between Airflow and Porous Materials for Building Application", Ph.D. Thesis, Ghent University, Belgium

Steeman H, Janssens A, Carmeliet J, De Paepe M, 2008, "Modelling indoor air and hygrothermal wall interaction in building simulation: Comparison between CFD and a well-mixed zonal model", *Building and Environment*, Article in Press

Syed A, Izquierdo M, Rodriguex P, maidment G, Missenden J, Lecuona A, Tozer R, 2005, "A novel experimental investigation of a solar cooling system in Madrid", *International Journal of Refrigeration*, 28: 859-871

Talukdar P, Olutmayin S, Osanyintola O, Simonson C, 2007, "Transient moisture transfer between porous building material and humid air-Part-1: experimental facility and property data", *International Journal of Heat and Mass Transfer*, 50: 4527-4539.

Talukdar P, Olutmayin S, Osanyintola O, Simonson C, 2007, "An experimental data set for benchmarking 1-D, transient heat and moisture transfer models of hygroscopic building material. Part II: Experimental, numerical and analytical data", *International Journal of Heat and Mass Transfer*, 50: 4915-4926

Tariku F, Kumaran K, 2006, "Hygrothermal modeling of aerated concrete wall and comparison with field experiment", *3rd International Building Physics Conference*, August 27-31, pp. 321-328, Montreal, Canada.

Tariku F, 2008, "Whole building heat and moisture analysis", Ph.D. Thesis, Concordia University, Montreal, Canada

Vera S, Rao J, Fazio P, 2007, "Moisture Transport Through a Horizontal Opening: Test Setup and Initial Results", *Paper A41-T4-C-07-3, IEA/ECBCS-Annex 41 Whole Building Heat, Air and Moisture Response*

Wang B-L, Takigawa T, Yamasaki Y, Sakano N, Wang D-H, Ogino K, 2007, "Symptom definitions for SBS (sick building syndrome) in residential dwellings", *International Journal of Hygiene and Environmental Health*, 211: 114-120

Woloszyn M, Rode C, 2008, "Volume 1: Modeling Principles and Common Exercises", *IEA/ECBCS-Annex 41 Whole Building Heat, Air and Moisture Response*: *MOIST-ENG Final Report*, 234pp.

Appendix A – Material Properties

The following tables list the material properties determined from the round robin testing [Roels, 2008 (1)]

Table A.1: Basic Properties, sorption isotherm and water vapour diffusion for gypsum board, and paints.

	gypsum board	**acryl coat**	**latex coat**
Basic properties			
ρ (kg/m³)	690	2285	1950
d (m)	0.0125	0.0001	0.0001
Thermal conductivity (W/m.K)	0.198	0.5	0.5
Sorption isotherm u(kg/kg)			
RH(%)			
5	0.001316	0.010872	0.013879
10	0.001552	0.011627	0.015441
15	0.001753	0.012160	0.016594
20	0.001944	0.012607	0.017559
25	0.002135	0.013019	0.018414
30	0.002333	0.013422	0.019197
35	0.002542	0.013837	0.019933
40	0.002769	0.014281	0.020636
45	0.003019	0.014776	0.021321
50	0.003299	0.015345	0.022001
55	0.003620	0.016023	0.022689
60	0.003996	0.016860	0.023401
65	0.004447	0.017932	0.024159
70	0.005007	0.019368	0.024994
75	0.005729	0.021394	0.025958
80	0.006719	0.024444	0.027141
85	0.008195	0.029431	0.028724
90	0.010746	0.038372	0.031157
95	0.016800	0.054171	0.036063
Water vapour diffusion equivalent air layer thickness s_d(m)			
RH(%)			
5	0.136	0.304	3.639
10	0.135	0.299	3.609
15	0.133	0.293	3.564
20	0.132	0.285	3.498
25	0.130	0.276	3.403
30	0.128	0.265	3.269
35	0.125	0.251	3.085
40	0.122	0.235	2.844
45	0.119	0.217	2.544
50	0.115	0.198	2.194
55	0.111	0.176	1.816
60	0.106	0.155	1.441
65	0.101	0.133	1.099
70	0.095	0.113	0.809
75	0.089	0.094	0.578
80	0.083	0.077	0.404
85	0.076	0.062	0.278
90	0.069	0.049	0.189
95	0.063	0.039	0.127

A.1 Extra data to include hysteresis

Based on the results of the round robin test the main desorption curve (from 94% RH down to 33% RH) and one of the intermediate desorption curves (from 79.5% RH down to 33% RH) have been determined.

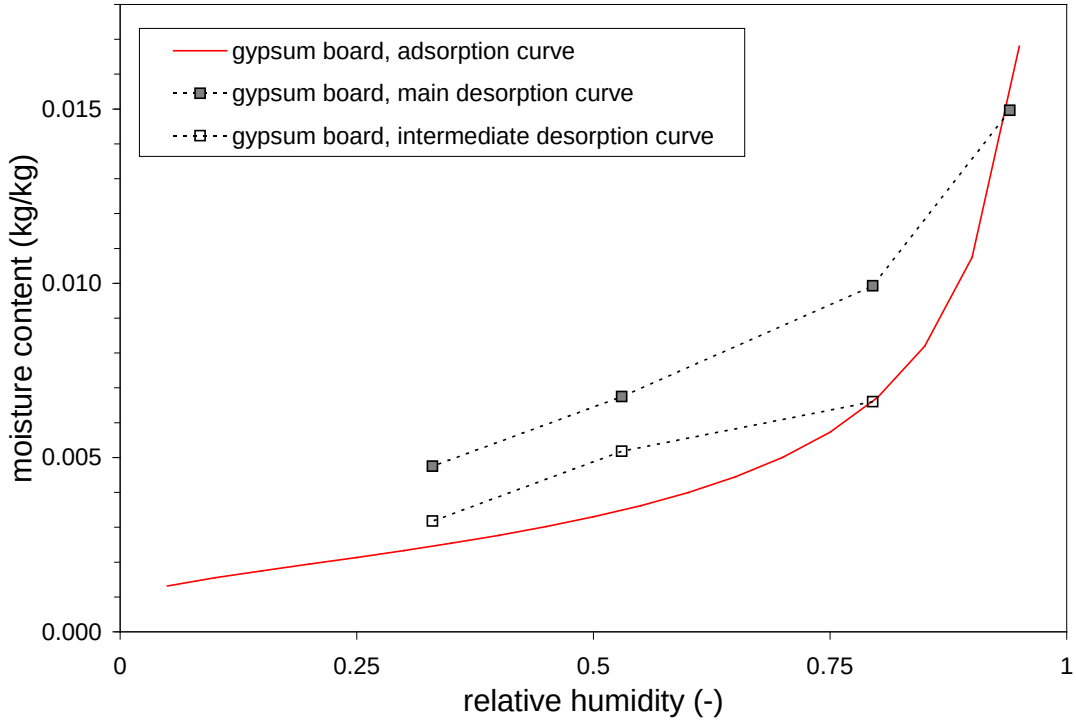

Figure A.1: Desorption isotherms of the gypsum board determined from round-robin testing.

The corresponding values are :

Table A.2: Desorption isotherms from the round-robin testing.

RH (%)	adsorption	desorption 94% - 33%	desorption 79.5% - 33%
94	0.0150	0.0150	
79.5	0.0066	0.0099	0.0066
53	0.0035	0.0068	0.0052
33	0.0025	0.0048	0.0032

A.2 Extra data for sensitivity study on sorption isotherm

The uncertainty on sorption isotherm will only be investigated for gypsum board. Since the main interest is the moisture accumulation, we assume the point at 33% RH fixed and the uncertainty is investigated by the standard deviation on the slope of the sorption isotherm as measured in the round robin experiment.

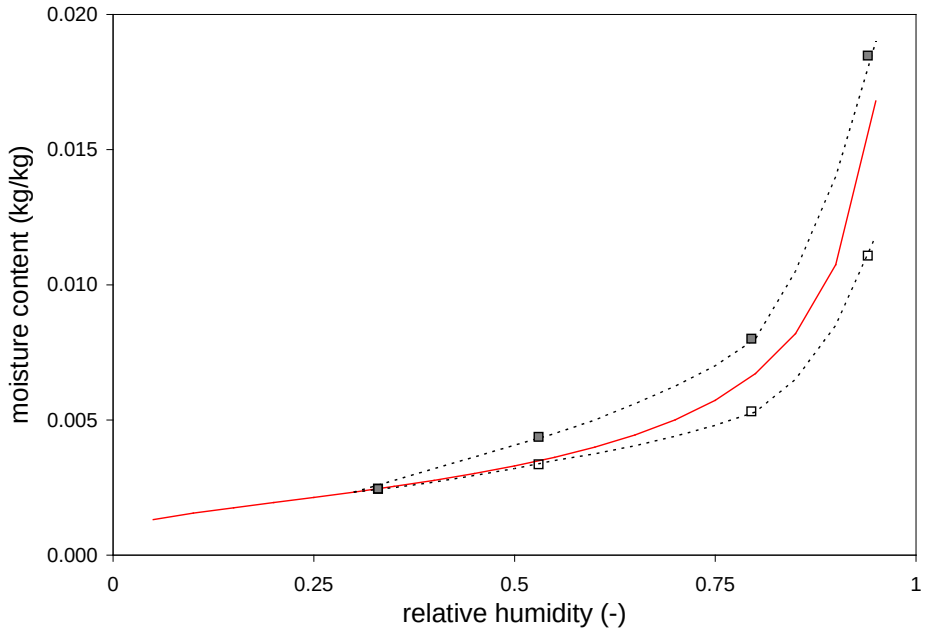

Figure A.2: Sorption isotherm and corresponding uncertainty bands of the gypsum board determined from round-robin testing.

The corresponding values are:

Table A.3: Sorption isotherm data of the gypsum board with corresponding minimum and maximum values from round-robin testing.

RH (%)	mean	minimum	maximum
30	0.002333	0.002333	0.002333
35	0.002542	0.002500	0.002766
40	0.002769	0.002700	0.003200
45	0.003019	0.002950	0.003633
50	0.003299	0.003200	0.004067
55	0.003620	0.003500	0.004500
60	0.003996	0.003750	0.005000
65	0.004447	0.004050	0.005600
70	0.005007	0.004400	0.006250
75	0.005729	0.004800	0.007000
80	0.006719	0.005300	0.008000
85	0.008195	0.006500	0.010500
90	0.010746	0.008500	0.014000
95	0.016800	0.011800	0.019000

A.3 Extra data for sensitivity study on vapour permeability

The uncertainty on the vapour permeability will be investigated for gypsum board and two types of coat. The upper and lower curves are determined from the standard deviation on the round robin results. The corresponding values are :

Table A.4: Vapour permeability data with the corresponding minimum and maximum values of the gypsum board and the acrylic and latex paints.

RH (%)	Mean	minimum	maximum
Gypsum board			
5	0.136	0.103	0.165
10	0.135	0.103	0.165
15	0.133	0.102	0.164
20	0.132	0.101	0.162
25	0.130	0.099	0.161
30	0.128	0.098	0.159
35	0.125	0.096	0.157
40	0.122	0.094	0.154
45	0.119	0.091	0.150
50	0.115	0.088	0.146
55	0.111	0.084	0.141
60	0.106	0.080	0.136
65	0.101	0.076	0.129
70	0.095	0.071	0.122
75	0.089	0.065	0.114
80	0.083	0.060	0.105
85	0.076	0.054	0.096
90	0.069	0.048	0.086
95	0.063	0.043	0.076
Acrylic coating (alone)			
5	0.304	0.239	0.369
10	0.299	0.235	0.364
15	0.293	0.229	0.357
20	0.285	0.222	0.348
25	0.276	0.213	0.337
30	0.265	0.202	0.325
35	0.251	0.187	0.310
40	0.235	0.171	0.293
45	0.217	0.152	0.273
50	0.198	0.132	0.251
55	0.176	0.111	0.228
60	0.155	0.091	0.203
65	0.133	0.073	0.179
70	0.113	0.057	0.154
75	0.094	0.044	0.131
80	0.077	0.033	0.110
85	0.062	0.025	0.091
90	0.049	0.019	0.075
95	0.039	0.014	0.061
Latex coating (alone)			
5	3.639	3.379	4.107
10	3.609	3.326	4.066
15	3.564	3.250	4.008
20	3.498	3.146	3.925

Table A.4 continued: Vapour permeability data with the corresponding minimum and maximum values of the gypsum board and the acrylic and latex paints.

RH (%)	Mean	minimum	maximum
Latex coating (alone)			
25	3.403	3.004	3.811
30	3.269	2.818	3.655
35	3.085	2.583	3.450
40	2.844	2.302	3.188
45	2.544	1.986	2.870
50	2.194	1.653	2.506
55	1.816	1.327	2.114
60	1.441	1.029	1.722
65	1.099	0.774	1.355
70	0.809	0.568	1.033
75	0.578	0.409	0.767
80	0.404	0.290	0.558
85	0.278	0.203	0.399
90	0.189	0.141	0.282
95	0.127	0.097	0.197

For CFD simulations of this experiment, the following flow profiles are required (Table A.5)

Table A.5: Flow profiles above the gypsum board measured for the laminar (a) and turbulent (b) cases.

(a) Laminar Case		(b) Turbulent Case	
y/H	V/V_{max}	y/H	V/V_{max}
0.08	0.59	0.07	0.79
0.17	0.78	0.15	0.85
0.31	0.94	0.25	0.91
0.41	0.99	0.34	0.96
0.51	1.00	0.45	1.00
0.56	0.98	0.59	1.00
0.60	0.96	0.64	0.99
0.65	0.92	0.75	0.96
0.75	0.80	0.84	0.84
0.86	0.70	0.92	0.77
0.92	0.65		

Appendix B – Tabular Data for Change Magnitudes

The following tables show the maximum measured and average simulated change in relative humidity and moisture accumulation/release for the adsorption loading (Table B.1) and desorption loading (Table B.2)

Table B.1: Tabular data for adsorption phase

Test	Experimental Change			Average Simulated Change		
	RH 12.5 mm	RH 25 mm	U (g)	RH 12.5 mm	RH 25 mm	U (g)
Test 1 – Bare gypsum bed, 24 hour ads/des phases, Re2000	39.6	38.8	8.5	37.2	34.5	8.1
Test 2 – Bare gypsum bed, **8 hour ads/des phases**, Re2000	30.4	24.9	6.0	26.3	19.0	4.7
Test 3 – Bare gypsum bed, 24 hour adsorption/desorption phases, **Re5000**	36.9	37.1	8.1	35.4	32.7	7.9
Test 4 – Acrylic coated, 24 hour ads/des phases, Re2000, **paint-surface transfer coefficient**	29.8	27.7	5.6	25.3	22.5	5.1
Test 4 – Acrylic coated, 24 hour ads/des phases, Re2000, **paint-separate porous layer**	29.8	27.7	5.6	25.0	22.1	5.1
Test 5 – Acrylic coated, 24 hour ads/des phases, Re2000, **paint-surface transfer coefficient**	11.4	5.2	0.0	6.3	5.6	0.9
Test 5 – Latex coated, 24 hour ads/des phases, Re2000, **paint-separate porous layer**	11.4	5.2	0.0	8.1	7.1	1.5

Table B.2: Tabular data for desorption phase

Test	Experimental Change			Average Simulated Change		
	RH 12.5 mm	RH 25 mm	U (g)	RH 12.5 mm	RH 25 mm	U (g)
Test 1 – Bare gypsum bed, 24 hour ads/des phases, Re2000	-38.9	-36.5	-7.1	-33.9	-28.9	-7.7
Test 2 – Bare gypsum bed, **8 hour ads/des phases**, Re2000	-24.1	-16.2	-3.6	-19.0	-7.0	-3.3
Test 3 – Bare gypsum bed, 24 hour adsorption/desorption phases, **Re5000**	-36.6	-35.2	-7.5	-32.9	-28.1	-7.4
Test 4 – Acrylic coated, 24 hour ads/des phases, Re2000, **paint-surface transfer coefficient**	-24.7	-21.8	-4.3	-20.3	-15.1	-4.2
Test 4 – Acrylic coated, 24 hour ads/des phases, Re2000, **paint-separate porous layer**	-24.7	-21.8	-4.3	-16.5	-11.2	-3.6
Test 5 – Acrylic coated, 24 hour ads/des phases, Re2000, **paint-surface transfer coefficient**	-1.8	-1.7	0.0	-1.2	-0.3	-0.2
Test 5 – Latex coated, 24 hour ads/des phases, Re2000, **paint-separate porous layer**	-1.8	-1.7	0.0	-1.1	0.0	-0.5

Table B.3 shows the measured data for Case 1, the uncoated case.

Table B.3: Measured data (relative humidity, temperature and moisture change) for Case 1, the uncoated case.

RH and Temperature					Moisture Change	
Time	RH (%)		T (ºC)		Time	U
(hours)	y=12.5mm	y=25mm	y=12.5mm	y=25mm	(hrs)	(g)
0.00	30.6	30.8	23.3	23.3	0.00	0
2.68	53.4	43.6	24.7	24.8	2.03	0.9
4.01	57.7	48.9	24.8	24.9	4.07	3.4
6.66	60.8	55.8	24.4	24.5	6.10	2.9
7.98	62.5	58.3	24.3	24.4	8.14	5.9
10.18	64.8	61.4	24.0	24.1	10.17	7.2
11.95	66.3	63.3	23.9	24.0	12.20	8.9
14.17	67.9	65.3	23.9	23.9	14.24	9
15.96	68.7	66.5	23.8	23.8	16.27	9.6
18.18	69.8	67.8	23.9	23.9	18.31	10.2
19.97	70.2	68.5	23.8	23.8	20.34	10.7
22.20	70.7	69.3	23.8	23.8	22.37	9.2
24.04	70.2	69.6	23.6	23.8	23.95	8.5
26.26	51.0	60.1	22.8	22.8	25.98	5.4
28.04	44.7	53.0	22.4	22.4	28.02	4.1
30.27	40.7	46.6	22.3	22.3	30.05	4.5
32.03	40.0	44.1	22.3	22.3	32.09	3.3
34.22	37.8	41.6	22.4	22.3	34.12	3.2
35.97	36.6	40.0	22.4	22.4	36.15	1.7
38.16	35.3	38.4	22.5	22.5	38.19	0.2
39.92	34.4	37.1	22.5	22.5	40.22	-0.8
42.11	33.3	35.8	22.6	22.6	42.26	-1.1
44.33	31.7	34.5	22.6	22.6	44.29	-0.8
46.13	31.6	33.6	22.8	22.7	46.32	2
47.91	31.4	33.1	23.0	23.0	47.95	8.5

Table B.4 shows the measured data for the acrylic coated gypsum bed.

Table B.4: Measured data (relative humidity, temperature and moisture change) for Case 4, the acrylic coated case.

RH and Temperature					Moisture Change	
Time	RH (%)		T (ºC)		Time	U
(hours)	y=12.5mm	y=25mm	y=12.5mm	y=25mm	(hours)	(g)
0.00	34.7	34.8	24.1	24.1	0.00	0
2.33	41.0	37.5	24.2	24.2	2.12	-0.4
4.11	44.8	40.7	24.1	24.1	4.15	1
6.34	48.6	44.3	23.9	24.0	6.19	1.7
8.12	51.0	47.1	23.8	23.8	8.22	2.6
9.95	53.6	49.9	23.7	23.7	10.26	3.4
12.21	56.4	53.2	23.6	23.7	12.29	4.1
13.99	58.2	55.3	23.7	23.7	14.32	3.6
16.22	60.1	57.6	23.7	23.8	16.36	3.6
18.01	61.1	59.0	23.7	23.8	18.39	3.8
20.24	62.4	60.3	23.6	23.7	20.43	5.3
22.02	63.4	61.5	23.6	23.6	21.95	5.2
24.25	64.5	62.7	23.5	23.7	23.98	5.6
26.04	59.2	61.2	23.5	23.6	26.02	5.7
28.28	55.0	57.8	23.4	23.5	28.05	4.6
30.06	52.1	54.9	23.4	23.5	30.09	5.3
32.30	48.9	51.6	23.2	23.3	32.12	5.3
34.14	46.9	49.2	23.1	23.2	34.15	5.3
35.94	45.5	47.5	23.1	23.2	36.19	3.7
38.17	44.1	45.7	23.2	23.3	38.22	2.2
39.96	43.1	44.6	23.3	23.4	40.26	1.3
42.18	42.0	43.3	23.3	23.5	42.29	0.8
43.97	41.2	42.3	23.3	23.4	44.33	2.4
46.20	40.3	41.3	23.1	23.3	46.36	1.5
47.98	39.8	40.7	23.1	23.2	47.89	1.3

Table B.5 shows the measured data for the latex coated gypsum bed.

Table B.5: Measured data (relative humidity, temperature and moisture change) for Case 5, the latex coated case.

RH and Temperature					Moisture Change	
Time	RH (%)		T (ºC)		Time	U
(hours)	y=12.5mm	y=25mm	y=12.5mm	y=25mm	(hours)	(g)
0.00	31.5	37.5	24.2	24.1	0.00	0
2.23	33.3	34.0	23.9	23.9	2.38	1.4
4.01	34.5	34.2	23.8	23.7	3.91	1.3
6.24	35.5	34.9	23.6	23.6	5.94	1.9
8.03	36.3	35.7	23.5	23.5	7.98	3
10.26	37.3	36.9	23.6	23.5	10.01	4.2
12.04	38.2	37.8	23.6	23.5	12.05	2.7
14.28	39.3	38.8	23.8	23.7	14.08	2.3
16.06	40.0	39.6	23.8	23.7	16.11	2.4
17.84	40.8	40.4	23.8	23.8	18.15	2.9
20.07	41.6	41.3	23.9	23.8	20.18	4.2
22.31	42.3	42.1	23.8	23.7	22.22	4.1
24.10	42.9	42.7	23.7	23.6	24.25	4.9
26.33	42.9	43.1	23.8	23.7	26.28	7
28.11	42.8	43.0	23.8	23.7	28.32	7.4
30.34	42.8	42.7	23.8	23.7	29.84	8.1
32.12	42.6	42.6	23.8	23.7	32.38	8.4
33.91	42.5	42.5	23.9	23.8	33.91	9.7
36.15	42.3	42.3	23.9	23.8	35.94	8.6
37.93	42.1	42.1	23.9	23.8	37.98	8.7
40.16	41.9	41.8	23.9	23.8	40.01	8.7
41.95	41.7	41.7	23.9	23.8	42.05	8.3
44.17	41.4	41.4	23.9	23.7	44.08	9.8
46.18	41.3	41.2	23.8	23.6	46.11	9.4
47.97	41.1	41.0	23.8	23.7	47.64	8.3